MŰEGYETEM 1782

Budapest University of Technology and Economics
Faculty of Civil Engineering
Department of Construction Materials and Technologies

Influence of Supplementary Cementitious Materials on the Properties of High Strength Cement Paste at Elevated Temperatures

PhD Thesis

Nabil Abdelmelek

Supervisor:
Associate Professor **Éva Lublóy**

Budapest, 2021

DECLARATION OF AUTHENTICITY

I declare that the contents and the work described at this thesis were performed at the Budapest University of Technology and Economics, Faculty of Civil Engineering. I hereby certify that all materials presented in this thesis are either my work or acknowledged wherever adapted from other sources.

Dedicated to

My beloved parents
My brother and sisters
To the soul of my cousin
'Moufida'

Acknowledgments

بِسْمِ ٱللَّهِ ٱلرَّحْمَٰنِ ٱلرَّحِيمِ

رَبِّ أَوْزِعْنِي أَنْ أَشْكُرَ نِعْمَتَكَ الَّتِي أَنْعَمْتَ عَلَيَّ وَعَلَى وَالِدَيَّ وَأَنْ أَعْمَلَ صَالِحًا تَرْضَاهُ وَأَدْخِلْنِي بِرَحْمَتِكَ فِي عِبَادِكَ الصَّالِحِينَ

In the Name of Allah, Most Gracious, Most Merciful

"My Lord! grant me that I should be grateful for Your favour which You have bestowed on me and on my parents, and that I should do good such as You are pleased with, and include me, by Your mercy, in the ranks of Your righteous servants" (The Qur'an, An-Naml 19)

I would like to express my deepest appreciation to my supervisor Dr. Éva Lublóy for her continuous guidance and support throughout the study.

I would like to extend my sincere gratitude to Prof. Dr. György L. Balázs and his wife Dr. Katalin Kopecskó for their help and support during my PhD period.

Many thanks for the current Head of Department of Construction Materials and Technologies at the BME, Dr. Dunai László and the Former Head of Department, Dr. György Mihály Stocker.

I would like to extend my appreciation to the doctors, friends, and colleagues: Dr. Salem Nehme, Dr. Gálos Miklós Péter, Dr. Tamás Károly Simon, Dr. Rita Nemes, Dr. Fenyvesi Olivér, Dr. Danish Farooq, Dr. Sólyom Sándor, Dr. Viktor Hlavička, Dr. Ahmed M. Seyam, András Jakab, Biró András, Szijártó Anna, Sánta Ildiko, and Bakai Krisztina for their supports and sharing expertise.

I got a lot of recommendations, advices, and help from my special friend Dr. Naser S. Alimrani, thank you very much for everything and such unforgettable memories.

I am very grateful to my wife Nada, thank you so much for being with me in my joys and sorrows.

Eventually, I am very grateful for the Algerian and Hungarian Governments to provide me with the "Algerian" and "Stipendium Hungaricum" scholarships.

TABLE OF CONTENTS

LIST OF ABBREVIATIONS

ACI	American Concrete Institute
CT	Computed Tomography
FA	Fly Ash
HPC	High-Performance Concrete
HSC	High-Strength Concrete
HSCP	High-Strength Cement Paste
ITZ	Interfacial Transition Zone
MK	Metakaolin
NSC	Normal-Strength Concrete
OPC	Ordinary Portland Cement
PCA	Portland Cement Association
SCM	Supplementary Cementitious Materials
SEM	Scanning Electron Microscope
SF	Silica Fume
TG/DTG/DTA	Thermogravimetry/Derivative Thermogravimetry/Differential Thermal Analysis
RRBS	Relative Residual Bending Strength
RRCS	Relative Residual Compressive Strength
w/b	Water to Binder Ratio
w/c	Water to Cement Ratio
XRD	X-Ray Diffraction

ABSTRACT

The scientific research described in this thesis has been carried out to gain further knowledge on the use of supplementary cementitious materials (SCM) related to the properties of high-strength concrete (HSC) at ambient and elevated temperatures. The current work is mainly directed to the performance of the hardened cement paste which is the weakest part of concrete during fire exposure. The high strength cement paste (HSCP) has been produced by the incorporation of three types of SCM as partial replacements of the ordinary cement. The main parameters of the current study are (i) fineness of cement, (ii) type of SCM with different replacement ratios, (iii) water to binder ratio (w/b), and (iv) maximum level of temperature.

Two fineness of cement were used CEM I 42.5 N and CEM I 52.5 N. SCM were metakaolin (MK), silica fume (SF), and fly ash (FA) used in the replacement ratios of 0%, 3%, 6%, 9%, 12%, and 15% of the cement by mass. Three w/b ratios have been tested as well, i.e., 0.30, 0.35, and 0.40. Finally, all mixes have been tested under 8 different levels of temperatures, i.e., 20, 50, 150, 300, 400, 500, 800, and 900 °C. All previous mixes were tested at the age of 90 days at the cold state testing. Tests include compressive strength and bending strength tests. Besides, chemical, physical, and durability properties were investigated. The current study could be considered as a development of sustainable and heat resistance structural material of HSCP developed based on different green produced materials. The findings of this study are expected to enrich the field of concrete technology, particularly contributing to cover the role of SCM in affecting the macro and microstructure of sustainable HSCP.

The results have proved that using HSCP containing SCM is a preferable choice for the future developments of concrete, in which results showed an excellent heat resistance at all levels of maximum temperatures. Finally, the current study has been mainly carried out at mixtures made of cement paste, with a limited number of concrete mixtures, therefore the researchers recommend further tests in the future using concrete mixtures. In addition, analytical models are also recommended for future studies.

CHAPTER 1: INTRODUCTION

This chapter outlines the research issue by highlighting and discussing the subject area background, objectives, materials, and experiments.

1.1 Challenges

Conservation and protection of the environment have become a serious issue in the global world context *(Suhendro, 2014)*. Since 1992 in the Rio Summit, the introduction of sustainable and economic development concept has not been a worthless idea *(Agenda, June 1992)*. It was an inflection point of the recognition of the massive growth of population that have been observed in the last century, and the progressive assessment of the coming rapid urbanization of developing countries. Therefore, research on sustainable technologies has been the interest in the early 21st century. Due to its diverse benefits, concrete is the most common widely material used in the construction industry, producing approximately 20 billion tons of raw materials every year *(Fredonia, 2011)*. Cement production, which is an essential part of concrete production, has primarily been contributing to the increase in the world cement demand to over 3.6 billion tons annually in 2011 *(European Cement Association, 2011)*. The latter amount is expected to be doubled in 2050 *(Scrivener, 2012)*.

Concrete as a material is mainly formed of cement, aggregate, and water. The industry of cement requires large quantities of natural resources resulting in huge quantities of CO_2 emissions, induced over different phases of production of cement. Furthermore, cement processing, such as mining, and transport operations increases carbon emission and energy consumption. On the other hand, the annual global productions of supplementary cementitious materials (SCM) like metakaolin (MK), silica fume (SF), fly ash (FA) is significantly increased. For instance, amounts of waste FA and slag are approximately 1 billion tons and 360 million tons, respectively *(Reynold, 2009; Juenger and Siddique, 2015)*. Including these large amounts of the waste of SCM as substitutions for cement could be the way of decreasing the global rising of cement demand and its environmental impacts. In addition, under the boom of population pressure and limitation of land, the need for high-rise buildings, tunnels, and underground construction is increased every year. Thus, researchers started to develop further enhancements including the use of high-strength concrete (HSC), which is characterized by numerous economically, short- and long-term serviceability and durability benefits. However, some disadvantages of using HSC have emerged regarding resistance to fire *(Chan et al., 1999a)*. Recent fire cases and laboratory studies showed disastrous deterioration of HSC after exposure to elevated temperatures. In addition, researchers agree that HSC is more prone to spalling *(Ma et al., 2015)*. Some of the tragic cases of fire are widely recognized accidents such as of Channel Tunnel in 1996, Mont Blanc Tunnel in 1999, St. Gotthard tunnel in 2001, and Liverpool car park in 2017 (**Figure 1.1**) *(Hager, 2013; Rajora and Yadav, 2018; Fehérvári and Nehme, 2009a)*.

The challenge of incorporating SCM into concrete mixtures to produce HSC with enhanced properties against fire is of a significant importance for the benefit of the environment, economy, and different engineering applications.

Figure 1.1 *Example of fire case in the St. Gotthard tunnel showing extensive damages in the "Zona Rossa" (Bettelini et al., 2004; Martin et al., 2005)*

1.2 Research significance and objectives

The concept of adoption of the waste materials in construction is a quantum leap for not merely cleaning the environment but also introducing them into construction, thereby further contributing to improving the properties of concrete. Therefore, the sustainability of engineering products is not a choice anymore but a demand. HSC based on SCM is a new generation of concrete that is based on the concepts of high-performance concrete (HPC) and fire-resistant concrete. An eco-friendly version of this concrete can be developed by the replacement of specific amounts of cement with amounts of SCM, where sustainable and economic value could be added. The significance of incorporating SCM into concrete mixtures to produce HSC with enhanced properties against fire is of a great importance for the benefit of the environment, economy, and different engineering applications.

The behaviour of HSC based on SCM at elevated temperature has shown different thermal and mechanical properties compared to the ordinary HSC. To evaluate the fire resistance of HSC based on SCM, there is a need to characterize the physical, chemical, and mechanical properties of the constituents including the SCM. One of the major properties that are affected in HSC is related to spalling. To obtain beneficial effects of SCM regarding spalling as well as stabilizing the hardened cement paste from different harmful chemical composition, comprehensive experimental investigations have been carried out by testing several parameters, i.e., different types and amounts of SCM, different ratios of water to binder (w/b), different types of cement fineness, and different levels of elevated temperature. Therefore, the main objective of the study is to investigate the properties of the high strength cement paste (HSCP) using different types and amounts of SCM at elevated temperatures. In order to fulfil the main objective, the current study aims to address the following sub-objectives:

- Defining the optimum replacement of using MK in HSCP after exposure to elevated temperatures.
- Defining the optimum replacement of using SF in HSCP after exposure to elevated temperatures.
- Defining the optimum replacement of using FA in HSCP after exposure to elevated temperatures.
- Determining the effect of changing w/b ratio on the optimum replacements of using SCM in HSCP after exposure to elevated temperatures.
- Determining the effect of changing the fineness of cement on the optimum replacements of using SCM in cement paste after exposure to elevated temperatures.

Several laboratory experiments were conducted on the produced HSCP. In addition, different properties that were directly interconnected with the macro and micro-structure of the pastes were also investigated using several tests and techniques.

CHAPTER 2: LITERATURE REVIEW

This chapter provides an overview of HSC including definitions, limitations, possibilities, different properties, and the ability to introduce supplementary cementitious materials in the production of HSC to produce thermally stable HSC.

2.1 High strength concrete (HSC)

The production of HSC has been one of the incentives research for engineers and researchers in terms of enhancing the performance of concrete *(Kawai, 2005)*. HSC is a state-of-the-art material that meanwhile can be produced by most concrete plants. Moreover, applications of HSC are widely increased in civil engineering fields because of its several advantages. For instance, the mechanical and durability properties of HSC are more enhanced than that of normal-strength concrete (NSC). From an economical perspective, the higher costs of material for the production of HSC can be compensated by many other uncountable benefits. Moreover, the architectural advantage of HSC allows the use of smaller size columns in high-rise buildings resulting in more usable space, shear walls, foundations, and early removal of formwork. Furthermore, HSC could be used in bridges application, marine, offshore structures, nuclear power plants, and places of extreme and adverse climatic conditions *(PCA Concrete Technology, 1980; Vinayagam, 2012)*. Other advantages such as long serviceability and high durability by reducing the risk of corrosion of steel and the attack of aggressive chemicals due to low permeability are also gained by using HSC. All previous beneficial advantages, coupled with the ease of production, have increased the demand for HSC in structural applications *(Phan, 1996; Aitcin, 1998; Tangchirapat et al., 2009; Vinayagam, 2012)*.

The critical question is to what compressive strength grade of HSC has to attain. In fact, there is no consensus regarding specific strength grades to separate HSC from NSC. Historically, the definition of HSC depended on its continuous development and application over the years. The American Concrete Institute (ACI) ACI 393R-92 in 1950 defined the compressive strength value of 34 MPa or greater to be considered as HSC. The reason for this relatively low limit was because HSC was not widely available at that time, thus most engineers and designers had limited choices. Later, ACI 363 updated the definition of HSC, in which, concrete with a compressive strength value of 41 MPa or greater was considered as HSC *(American Concrete Institute, 2005)*. Nowadays, ACI 363R-9200 gives a description for HSC in the updated draft with a specified compressive strength of 55 MPa or greater to be considered as high strength *(Caldarone, 2008)*. The later definition of HSC will be adopted in this thesis. From another hand, the *fib* model code for concrete structure in 2010 considered concrete with a characteristic compressive strength more than 50 MPa as HSC *(Model Code, 2010)*.

2.2 Material aspects of HSC

Similar to NSC, HSC consists of cement, coarse and fine aggregate, and water. However, minerals and chemical admixtures are highly important in the case of HSC, in which the characteristics and ratios of its ingredients highly influence the performance in both fresh and hardened states.

2.2.1 Cement

Cement is the most consumed material in the world after water. Where in 2011, 3.6 billion tons of cement were produced worldwide *(European Cement Association, 2011)*, and expected to increase to 5.8 billion tons by 2050 *(Scrivener, 2012)*. The commonly used cement type is the OPC that is utilized either pure binder or by SCM combinations. The used basic constituent materials in the production of cement are lime (CaO), silica (SiO_2), alumina (Al_2O_3), and ferrite oxide (Fe_2O_3) *(Bazant and Kaplan, 1996)*. The cement production process consumes high energy, i.e., from 1700 MJ to 1800 MJ, per ton of clinker to produce cement, in addition to using fossil fuels with high amounts of electricity *(Taylor, 1997)*. Therefore, the industry of cement is considered the second-largest producer of carbon dioxide gases *(Malhotra and Mehta, 2005)*. The total content of cementitious material for the production of HSC is relatively higher than that of NSC *(Krishna et al., 2014)*.

2.2.2 Water Content

The hydration of cement starts with the presence of water. The formation of cement strength requires water to bind the particles of aggregate together. Typically, HSC is featured by using a low w/b ratio, yet producing HSC requires ranges from 0.20 to 0.45 in addition to the presence of high content of binder *(Kosmatka et al., 2002b)*.

2.2.3 Aggregate

Since the aggregate is an important material occupying the largest volume of concrete, i.e., 80%, the quality and characteristic properties of aggregate have a significant contribution *(Duggal, 2003)*. Properties of aggregate including amount, size, shape, and texture of particles have an important role in the properties of HSC at both states, fresh and hardened *(Chen and Liu, 2004; Neville and Brooks, 2010)*. The aggregate should be durable and compatible in terms of stiffness and strength with cement paste. The grading of sand and coarse aggregate has to be fit and uniform in terms of packing purpose. Generally, a smaller maximum size coarse aggregate is used in the case of HSC compared to NSC. Finally, the breaking of concrete could commonly occur as a result of the breaking-off of hardened paste in NSC, or due to breaking-off of the aggregate in case of HSC.

2.2.4 Chemical Admixtures

The suitable admixtures are found to be influential and the key factor for producing HSC. Water reducing admixtures and superplasticizers are the most commonly used chemical admixtures in the concrete *(Rashid and Mansur, 2009)*. The superplasticizers' advantages include: (1) production of high workable concrete for easy placement, and (2) production of HSC with normal workability but have lower water content *(Ramachandran and Malhotra, 1996)*. *Sobolev (2004)* investigated the compressive strength of HSC concluding that increasing the dosages of superplasticizer from 1.3% to 3% of total binder led to a reduction of water to cement (w/c) ratio from 0.31 to 0.26 at a constant slump, improving the concrete compressive strength from 86 to 97 MPa.

2.3 Supplementary cementitious materials

In recent years, global interest in the development and evolution of sustainability has been achieved emphasizing the necessity of producing eco-friendly materials including reducing the content of OPC *(Ismail et al., 2011; Abdulmatin et al., 2018)*. SCM could be considered as a possible solution to reduce cement production by substituting it with different types and amounts of SCM. The common types of SCM are FA, MK, SF, and ground granulated blast-furnace slag (GGBS) which are widely used in HSC production. Basically, these materials are formed from minerals dominated by silica (e.g., SF, perlite, powder of quartz), alumino-silicates (e.g., MK, activated clays), or ternary composition SiO_2-Al_2O_3-CaO (e.g., FA and slags). The chemical compositions, degree of crystallinity, and fineness of SCM have an important role in the hardened property of concrete. Furthermore, the pozzolanic reaction of SCM with the $Ca(OH)_2$ resulted from the hydration product of cement increases additional strength. Besides the provided strength by these materials, SCM is used for filling the skeleton of concrete, thus enriching macro/micro-structure, and resulting in reducing the permeability *(Sata et al., 2007)*. As a result of including these SCM into cement, the world average percentage of clinker in cement is reduced from 85% to 77%. Further, a decrease to reach 71% is projected in the future *(Schneider et al., 2011)*. SCM could be blended with cement or be added to ready-mixed concrete *(Kosmatka and Wilson, 2011)*. **Figure 2.1** shows the different types of SCM powders.

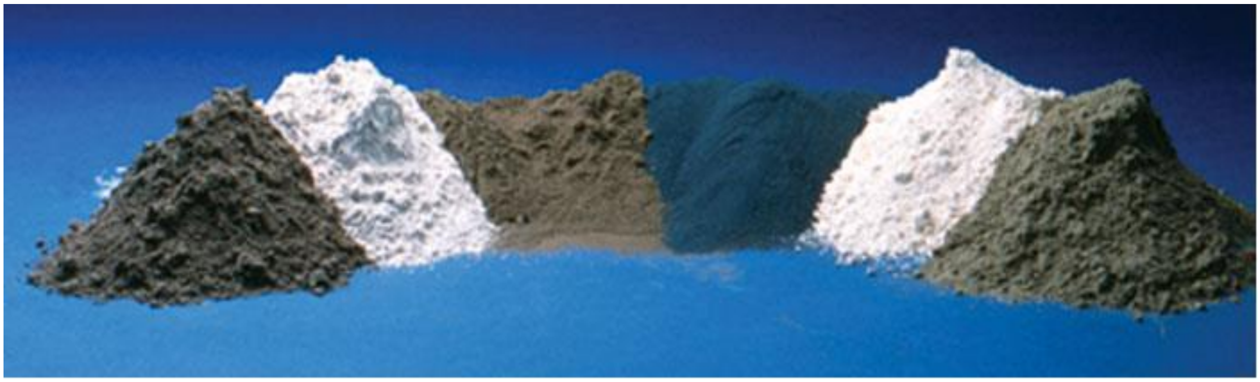

Figure 2.1 *Different types of SCM powders (Portland Cement Association (PCA), 2019)*

2.3.1 Metakaolin

Metakaolin is a primary material with attractive white colour, mostly amorphous aluminium silicate, made by calcination of natural kaolin at a typical temperature range of 600 °C to 800 °C. The mode of calcination is a process which remarkably influences the shape of particles, fineness, and reaction of MK *(Cassagnabere et al., 2013)*. With respect to the mechanical properties, different results are reported from different studies. *Dinakar et al. (2013)* have investigated the effect of MK as a binder on the mechanical properties of high strength concrete using w/b of 0.3. They tested cement replacements with MK of 5, 10 and 15%. Results showed that a 10% replacement was the optimum dosage. However, results from other studies *(Khatib, 2008)* showed that the optimum dosage of incorporating MK, in terms of compressive strength, was 20%

replacement using the same w/b, i.e., 0.3. From another perspective, it was reported that pozzolanic cement paste containing 5% of MK dosage gives higher compressive strength values than other MK replacements *(El-Diadamony et al., 2018)*. Justifying that 5% MK acts as a nucleating agent which increases the hydration rate of OPC.

2.3.2 Silica Fume

Silica fume SF is a by-product material of silicon metal production and ferrosilicon alloys in smelters that produced in electric furnaces. These types of metals are widely available around the world and used in many industrial applications containing steel and aluminium production, production of silicones, and computer chip fabrication. The condensed SF has a high content of amorphous silicon dioxide (SiO_2) (more than 90%), and very fine spherical particles with a typical average diameter of 0.1 to 0.2 µm *(ACI Committee 234, 2006)*. Therefore, different features have influenced SF to be suitable material for HSC in recent years *(Sata et al., 2007)*. *Sobolev (2004)* studied the development of compressive strength of HSC containing SF. Results of the compressive strength tests showed that the maximum value was obtained at 15% of SF (achieving 91 MPa). *Wong and Razak (2005)* have investigated the compressive strength of concrete incorporating SF (0%, 5%, 10%, 15% replacements from cement mass) using w/b ratios of 0.27, 0.30 and 0.33. The results showed that after 90 days of curing, the average strength improvement of using 10% of SF was the maximum value achieving 17% of increase compared to reference mixes for the three w/b ratios, whereas results of 0.27 showed relatively better results than results of w/b ratios of 0.30 and 0.33. *Hooton (1993)* studied the compressive strength of HSC containing 0, 10, 15, and 20% of SF at the ages of 91 days. Results showed that a mixture of 10% of SF exhibited higher compressive strength values. Different studies investigated the inclusion effect of using SF in different replacements of 0%, 5%, 10%, 15%, 20% and 25% to cement mass in terms of bending strength of HSC at 0.26, 0.30, 0.34, 0.38 and 0.42 of w/b ratios (*Bhanja and Sengupta, 2005).* Results reported that SF influences bending strength, where the enhancement is achieved even at very high replacements of SF. In conclusion, the results indicate that the optimum replacement of SF to cement has been varied from 15% to 25% with the variation of w/b ratio.

2.3.3 Fly Ash

Fly ash or flue-ash is a by-product material and one of the formed residues ash in the combustion of coal. FA consists of fine spherical glassy particles and hollow inside *(Senapati et al., 2014)*. American Society for Testing and Materials (ASTM) *(ASTM, 2003; ASTM - C618-8a, 2009)* classified FA into two classes: “C” and “F”. Class F is mainly made by burning anthracite or bituminous coal were the results of the combination of SiO_2, Al_2O_3 and Fe_2O_3 content is exceeding 70%. Class F as a normal pozzolan is a material consisting of silicate glass, modified with iron and aluminium *(RILEM 73-SBC Committee, 1988)* with the content of CaO less than 10%. Class C is prepared by burning lignite or sub-bituminous coal that contains the combination of the aforementioned chemicals in between 50% and 70%. Class C of FA is of a high content of calcium that undergoes to high reaction with the water even without the addition of lime *(Parsa et al., 1996)*. *Elahi et al. (2010)* studied the inclusion of FA on HSC using

0%, 20%, and 40% replacements from cement mass. Results showed that the development of compressive strength of the concrete at all FA replacements was consistently lower than the control mix at all ages. Concluding that FA mixtures did not only exhibit a lower strength compared to the control mixture but also the increase in FA content did further reduction in the strength. This outcome may be attributed to the very slow pozzolanic reaction of FA.

2.4 Advantages of using SCM

The basic material compositions of the HSC with and without SCM are quite similar. They consist of binders, aggregates, water, and admixtures. However, to achieve a better performance of the HSC, the inclusion of SCM is the right way, where the amount of CSH is increased simultaneously with decreasing the content of $Ca(OH)_2$ and $CaCO_3$. This leads to cause a significant increase in bond in the interfacial transition zone (ITZ) between aggregate and cement paste *(Kuroda et al., 2000)*. **Figure 2.2** shows the typical differences between the ordinary HSC, and HSC contains SCM. HSC using SCM have advantages more than the ordinary concrete does; these advantages can be grouped into three categories, as discussed in the following sub-sections.

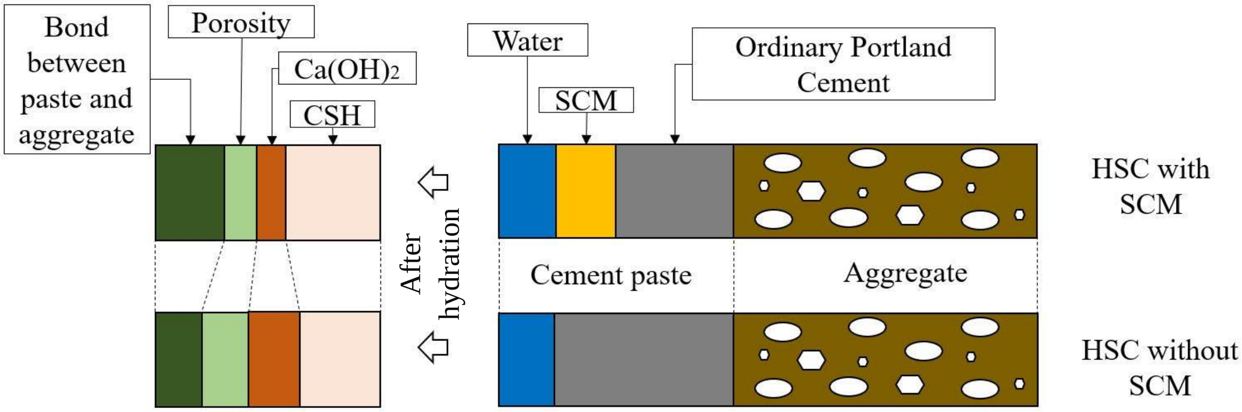

Figure 2.2 *Example of the main variation of HSC in the presence of SCM*

2.4.1 Constructional value

The constructional richness added due to the presence of SCM is enormous at both states, fresh and hardened. For the fresh properties of concrete, SCM are used to increase the workability in the form of self-compacting concrete own compaction facilitates and simplifies the implementation process of complex design structural elements and cast of complicated architectural forms, particularly in case of a small section containing large amounts of reinforcement *(El Mir and Nehme, 2017)*. From another hand, different mechanical properties are influenced on the hardened concrete, i.e., high early compressive strength, high tensile strength, high bending strength, high modulus of elasticity, increased toughness, improved the bond strength, improved durability due to very low permeability to the intrusion of chloride and water, increased abrasion resistance, high resistance to chemical attack from acids, resistance to chlorides intrusion, nitrates, and sulphates *(Sabir et al., 2001; Siddique, 2011; Merida and Kharchi, 2015; Alcamand et al., 2018)*.

The mechanism of the SCM is carried out through the filler effect. Filler effect is characterized by the physical effect of the fine particles that able to fill the pore microstructure of the concrete. Besides, there is a chemical contribution of the SCM to fill and enhance the microstructure of the cement paste *(Gutteridge and Dalziel, 1990; Cyr et al., 2005; Rossen et al., 2015)*. The filler effect has two mechanisms, at the physical presence of SCM that affect the clinker phases reaction:

(i) The first mechanism is related to the clinker dilution effect, where the replacement of ground clinker by other SCM means that more space is relatively available for the formation of hydrates from the hydration. Thus, the degree of reaction from the clinker component becomes significantly higher than the case of unsubstituted material. For instance, *Berodier and Scrivener (2014)* found that pastes from OPC have a hydration degree around 80% compared to 90% of pastes from blends (30% quartz or FA), at 28-days and the same conditions.

(ii) The second mechanism is the heterogeneous nucleation of C-S-H on the filler surface where there is a clear dependence on the surface provided by the particles of SCM. *Berodier and Scrivener (2014)* showed that this impact is relatively minor if the particle size distribution of SCM similar to that of Portland cement. Thus, the effect is major in case of materials containing fine particles like SF or MK, that has a significant acceleration influence on the clinker hydration *(Halse et al., 1984; Gutteridge and Dalziel, 1990; Rossen, 2014)*.

2.4.2 Economic value

Concrete containing SCM to produce self-compacting concrete helps in decreasing the number of needed laborers for the placement of concrete, thus reducing the construction costs. Furthermore, using these types of concrete save large concrete quantities by reducing sections of structural elements *(Safiuddin, 2008)*. Finally, some of these materials allow for a quickened formwork reuse and saving time such as accelerating the strength development at the early ages of concrete, for example, it can be obtained by adopting rice husk ash (RHA), SF, and FA to cement *(Li et al., 2004)*.

2.4.3 Environmental value

Concrete could consume large amounts of SCM, which are considered as waste materials. Thereby, saving the environment from excessive waste materials in addition to the low impact of cement production and disposal places. Additionally, by using SCM no further clinkering process is involved, leading to a significant reduction in CO_2 emissions. Knowing that clinkering process consumes much more energy than the energy used during mixing, transporting, and placing of concrete *(Lothenbach et al., 2011)*.

2.5 Applications of SCM

The current widespread use of SCM as a binder in the construction industry finds its roots by the ancient Greeks dates back to at least 500-400 BC in the form of volcanic pumice and ashes as a functional supplement. Several famous Roman buildings such as the Pantheon were constructed with the aid of pozzolan mortars showing excellent and durable binder materials properties of the buildings. The reason behind it is the preservation conditions, whereas the result is in an exceptional lifetime. As a result of the previous success, continuous applications have been extended in different structural fields and for different purposes, i.e., highway bridges, marine structures, parking decks, bridge deck overlays, SCM shotcrete for rock stabilization use, mine tunnel linings, rehabilitation, and other products needing repairing *(Siddique, 2011; Snellings et al., 2012)*. Several applications that used SCM were widely notable, such as the tallest tower in the world 'Burj Khalifa' that consumed approximately 250000 cubic meters of HPC, particularly using blended cement with FA *(Abdelrazaq, 2012; Baker and Pawlikowski, 2015)*.

Figure 2.3 shows different structural applications by using different types of SCM. Walls for residential buildings using FA, pavements using slag, high rise tawers using FA, and dams using calcined shale are presented in **Figure 2.3** **a**, **b**, **c**, and **d**, respectively.

a) b) c) b)

Figure 2.3 *Different applications of different types of SCM: a) walls for residential buildings, b) pavements, c) high-rise towers, and d) dams (Kosmatka et al., 2002a)*

2.6 Behaviour of HSC at elevated temperatures

Concrete is generally considered to be an excellent fireproofing material due to its high specific heat and low thermal conductivity, thus widely used in buildings and other civil engineering infrastructures where ensuring fire safety is of primary considerations. Nevertheless, recent fire cases have shown catastrophic failure and extensive damage particularly in HSC, which could not have the same capacity of fire resistance like the NSC *(Kodur, 2000; Khaliq, 2012)*. In consequence, HSC shows inferior thermal performance resulting in a serious threat for HSC applications in several engineering structures in addition to the risk of the human safety *(Chan et al., 1999a; Peng et al., 2006)*. Therefore, researchers are encouraged to identify, evaluate, and enhance the behaviour of HSC at elevated temperatures *(Shah et al., 2019)*. From another hand, the behaviour of HSC is different in terms of strength loss and explosive spalling compared to NSC, in which HSC is more vulnerable to explosive spalling than NSC due to its low porosity *(Shah et al., 2019)*.

HSC is typically produced through the inclusion of SCM and other chemical admixtures. These binders add specific properties to HSC, i.e., high strength grade and dense microstructure in the hardened state. Thus, the properties of HSC after being exposed to elevated temperatures can be different from that of normal concrete *(Khaliq, 2012)*. Fire engenders heat which affects the mechanical, microstructural, and thermal behaviour of HSC. Understanding the performance of the heated HSC as a material and assessing their elevated temperature properties is required and important in order to provide enough data for the fire response. Therefore, it can be finding an optimized approach for better fire performance in future *(fib, 2007)*. However, there is limited information and data of HSC made of different SCM after exposure to elevated temperatures. The following sections present further properties of HSC exposed to elevated temperatures.

2.6.1 Physical and chemical changes

2.6.1.1 Colour changes

The change of colour caused by exposure to elevated temperatures is considered the first simple and reliable inspections for HSC or concrete generally. The change of colour of the heated concrete is due to the gradually removed water, dehydration of the paste and other transformations occurred within the aggregate. This colouration is caused by the oxidation of mineral components. As temperature rises, certain colours correspond to a specific temperature range. Thus, it is possible to develop from the experiences the use of colour to determine which temperature level a specific element of concrete has been exposed to. Consequently, the residual mechanical properties of the element at different parts of the structure could be assessed from the colour ranges *(Lau and Anson, 2006)*. It is generally agreed *(Short et al., 2001*; *Colombo and Felicetti, 2007)* that concrete containing siliceous aggregates when heated between 300 °C and 600 °C will show the red colour; between 600 °C and 900 °C would turn to a whitish-grey colour; and between 900 °C and 1000 °C, a buff colour is present as shown in **Figure 2.4** *(Hager, 2013)*.

2.6.1.2 Crack Behaviour

The observation of concrete cracking levels that the results of rapid heating are quite different from those of slow heating. In case of slow heating at a rate of 0.50 °C/min, HSC below 600 °C suffered no obvious cracking even if it possesses high moisture content, while the rapid heating such as firing may cause considerable detrimental internal cracking. Microcracks cause corresponds to the development of difference in thermal expansion coefficients between components and by decomposition of $Ca(OH)_2$, such cracks are more observed in HSC *(Noumowe et al. 1996)*.

From another hand, the performance of hardened cement paste is different during and after cooling. Changes that happen during heating exposure are to a certain degree irreversible. After cooling, performance is dominated by the moisture absorption from the surrounding environment. However, the released CaO during heating from the dehydration of $Ca(OH)_2$ as well as from the decarbonation of $CaCO_3$ rehydrates with surrounding water after cooling producing $Ca(OH)_2$. This results in increasing of volume of 44% and significantly affecting paste, thus forming cracks *(fib, 2007)*.

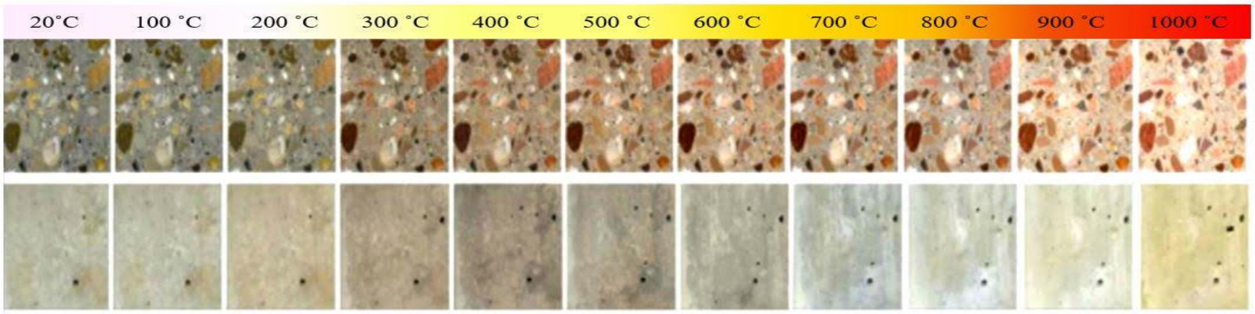

Figure 2.4 *Colour change of heated HSC (Hager, 2013)*

2.6.1.3 Porosity

The entrapped air bubbles formed in the fresh state during casting engenders to cavities or minor holes known as pores *(Duggal, 2003)*. The total porosity, distribution, and structure of pore are important features and key parameter that influence the permeability. Generally, porosity is related to cement paste which increases non-linearly with temperature corresponds the progressive changes of the gel structure (CSH) as well as the enlargement of pores by the pressures *(fib, 2007)*. The key parameters that govern the porosity are saturation level, compaction, then after the temperature parameters *(Duggal, 2003; Lau and Anson, 2006)*. However, various sizes of pores do not necessarily change and increase in the same proportion, thus, some could decrease with rising in temperature *(Rostasy et al., 1980; Piasta, 1984)*.

The porosity of HSC is expected to be lower compared to the NSC. This could be referred to the low w/b ratio as well as the packing effect of SCM, and the pozzolanic reaction of SCM with cement hydration production. *Khan (2003)* reported that the inclusion of SF from 0% to 15% as partial cement replacement resulting in a more significant decrease in porosity. In addition to that, the reduction in the porosity was greater when SF was at up to 10% replacement level. *Poon et al. (2006)* investigated the influence of SF with the replacement of 5% and 10% and MK with 5%, 10%, and 20% to cement mass on the porosity of HSC mixtures using mercury intrusion porosimetry (MIP). Results showed that the decrease in porosity with age is due to the addition of SF and MK. *Cwirzen and Penttala (2005)* studied the durability of HSC containing different replacements of SF to cement mass with 0%, 3%, 7% for w/b ratios of 0.3, 0.35 and 0.42. Results from the MIP investigation showed that the concrete having a w/b ratio of 0.3 showed a decrease in capillary porosity with SF. However, for 0.35 and 0.42 w/b ratios, capillary and total porosities are exhibited to be quite similar.

The low porosity in case of HSC is considered as the leading reason for the more severe strength deterioration after exposure elevated temperatures. Accordingly, the porosity of the concrete varies with the level of saturation and with a maximum temperature of exposure. Where the type of cooling varies, a significant change in the porosity of HSC is observed *(Luo et al., 2000)*. Some studies developed a model to predict a relationship between the porosity and strength of concrete after exposure to elevated temperatures using different cooling regimes *(Luo et al., 2000)*. **Figure 2.5** presents the relationship model for porosity and the strength of concrete.

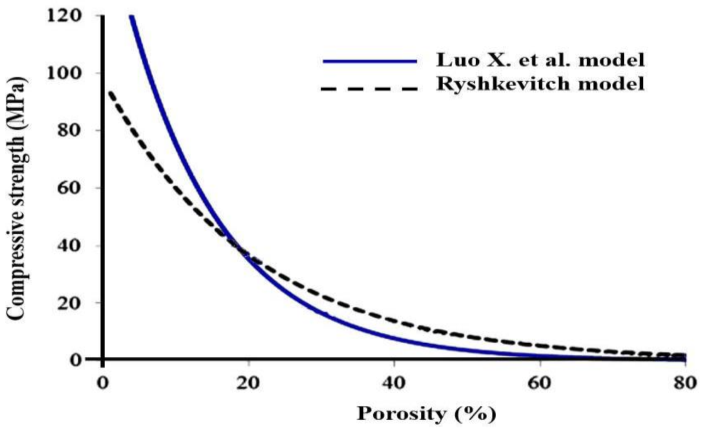

***Figure 2.5** Relation between compressive strength and porosity (Luo et al., 2000)*

2.6.1.4 Permeability

Permeability of HSC is very low at ambient temperature; with the increase of temperature the permeability of concretes increases drastically *(Poon et al., 2001b; Poon et al., 2003)*. *Noumowe et al. (2009)* reported the loss of impermeability (2000–10,700%) suggesting the reason to be caused by internal cracking and pore structure coarsening at elevated temperatures. *Janotka and Bagel (2003)* presented the permeability coefficient based on the measured pore sizes which are suitable for the evaluation of concrete quality when exposed to temperature.

2.6.1.5 Loss of mass

The distribution of temperature is dependent on the thermal properties of concrete at elevated temperature. The thermal properties that affect the behaviour of concrete at elevated temperatures are thermal expansion and loss of mass that influence the development of internal thermal stresses *(Khaliq, 2012)*. The loss of mass of concrete due to temperature is generally increased with the increase of temperature, reaching a maximum rate of loss in the first stage of heating (from 20 °C to 300 °C, or from 150 °C to 300 °C), which is mainly correspond to the evaporation of the physically bonded water *(Hager, 2004; Memon et al., 2019)*. During this temperature phase, the hardened cement paste is subjected to two successive and opposite physical changes whereas a slight expansion occurred up to 100 °C, then followed by significant shrinkage after 100 °C. At the chemical level, the loss of chemically combined water of CSH and $Ca(OH)_2$ results in a non-linear decrease in weight above 100 °C *(Hager, 2004; fib, 2007)*.

The nature of loss of mass is related to the constituents of concrete, their proportions, and the alteration occurred in the level of chemical and physical properties of the produced concrete *(Khoury, 2000)*. Thereby, the degree of loss of mass changes in case of HSC compared to NSC due to the low amount of physically absorbed water. Moreover, the loss of mass of HSC containing SCM is not similar to HSC without SCM. The loss of mass due to temperature elevation is usually measured by the method of Thermo-Gravimetric Analyser (TGA) technique *(ASTM E1868, 2010)*.

2.6.2 Mechanical properties

Fire is a serious hazard that threatens the safety of concrete structures. This is due to the loss of bearing capacity of concrete caused by the formation of macrocracks and microcracks on the body of concrete. The effect of heat on the mechanical properties of HSC has been studied since the 1970s *(Abrams, 1971; Shirley, 1987; Sanjayan and Stocks, 1991; Saito, 1992; Kumagai, 1992; Hansen, 1995; Hammer, 1995; Furumura, 1995; Felicetti, 1996; Bangi, and Horiguchi, 2011)*. The change of mechanical properties is related to several factors, i.e., rate of heating, duration of exposure, temperature levels, type of aggregate, specimen shape and size, specimen age, and moisture content *(Sudarshan and Vyas, 2019)*. Finally, several mechanical properties are of essential interest in the design of fire resistance including compressive strength, bending strength, elastic modulus, and stress-strain response in compression. These properties are discussed in detail in the following sections.

2.6.2.1 Compressive strength

The compressive strength property is widely considered as a pillar of the design rules for concrete structures. Generally, the concrete compressive strength depends on the w/b ratio, binder-to-aggregate ratio, compaction degree, type of cement, and the type of the used SCM. However, the w/b represented the first parameter in controlling the concrete compressive strength evolution. Some research revealed a distinct difference in the strength properties of HSC and NSC at elevated temperatures *(Aslani and Bastami, 2011)*, showing that the loss of strength of HSC varied differently from NSC during all temperature levels *(Phan, 1996)*. Therefore, data on the strength properties of new types of HSC contain a different type of SCM as a function of temperature is of an urgent need for the evaluation of fire response *(Khaliq, 2012)*. The differences between HSC and NSC have been determined into two main areas: (1) the relative loss of strength in the intermediate temperature range of 100 °C to 400 °C, and (2) the occurrence of explosive spalling in HSC at similar intermediate temperatures. In terms of strength loss, studies have shown that, for intermediate temperatures between 100 °C and 400 °C, the compressive strength of HSC could be decreased by close to 40% of the strength of ambient-temperature – a reduction of approximately 20% to 30% more than in NSC subjected to the same temperatures *(Phan and Carino, 1998; Phan and Carino, 2001; Phan and Lawson, 2001; Phan and Carino, 2002)*.

2.6.2.2 Bending strength

The bending strength is an important property of concrete and particularly sensitive to temperature. The bending strength significantly decreases by increasing temperature more than compressive strength does. Bending strength is very susceptible to the micro and macro cracks making the bending failure to be considered as one of the most common failure types for horizontal members *(Sudarshan and Vyas, 2019)*. However, the effect of elevated temperature on concretes with low w/c ratio is less than the effect on concrete with high w/b with respect to bending strength. The origin of this difference is attributed to the acceleration, of the hydration of poorly hydrated concretes at elevated temperatures *(Hager, 2004)*.

2.6.3 Spalling

Spalling of concrete is considered as one of the consequences of the most harmful phenomenon. Spalling is defined as explosive or non-explosive breaking-off of layers of concrete, which is mainly dependent on the pressure of vapour on the pores. This pressure is being in a function of temperature, heating rate and time, moisture content, the size of the pore, the size and shape of the specimen, aggregate size and type, and the type and amount of SCM *(Bazant and Kaplan, 1996; Khoury, 2000; Kodur, 2000; Lau and Anson 2006; fib, 2008; Khaliq, 2012)*. Pore pressure and dense microstructure of the hardened paste which does not allow moisture to escape from the heated concrete are the dominant factors of the occurrence of spalling. The movement of inner moisture of HSC at elevated temperature engenders a dramatic increase in vapour pressure. The low permeability of HSC provides pressure often reaching the saturation *(Bazant and Kaplan, 1996)*. The combined activity of pore pressure; compression forces in the uncovered surface zone induced by thermal stresses, the external loading, and inner cracking resulting from the occurrence of spalling *(Kodur, 2000)* as shown in **Figure 2.6**.

Generally speaking, HSC characteristics increase the probability of spalling *(Taylor, 1997)*. Thus, it is necessary to better cover and understand the fundamental mechanisms for concrete spalling *(Kodur, 2000)*. Moreover, HSC appears to be more prone to spalling at elevated temperatures than NSC *(Sanjayan and Stocks, 1993)*. For HSC, the spalling is expected to begin when the temperature is reached to approximately 600 °C *(Lau and Anson, 2006; Sideris et al., 2009)*. This has mainly two effects: (1) a physical effect because of the reduced Van der Waals' forces as water is expanded upon heating (Van der Waals forces resulted by the movement of cement gel layers close to each other), (2) a chemical effect through which detrimental transformations occurred under hydrothermal conditions *(Kulkarni et al., 2011)*.

Spalling can be classified into four categories: (i) Surface spalling (ii) Explosive spalling (iii) Aggregate spalling (iv) Corner/sloughing-off spalling. The first three take place during the first 20–30 minutes of a fire and are affected by the rate of heating, while the fourth happens after 30–60 minutes of fire and is affected by the maximum temperature *(Khoury, 2000)*. Although many categories of spalling are defined by researchers, explosive spalling is the most serious from all categories *(Sanjayan and Stocks 1993)*. In the other hand, *Ozawa et al., (2012)* have found that spalling of HSC takes place above 200 °C, where, the build-up of vapour pressure and explosive spalling occur at 44 min and 47 min, respectively.

Finally, the spalling tendency of HSC under fire circumstances is a reason for inhibiting its application in buildings, bridges, and tunnels, as several considerations of safety are raised *(Sideries et al. 2009)*.

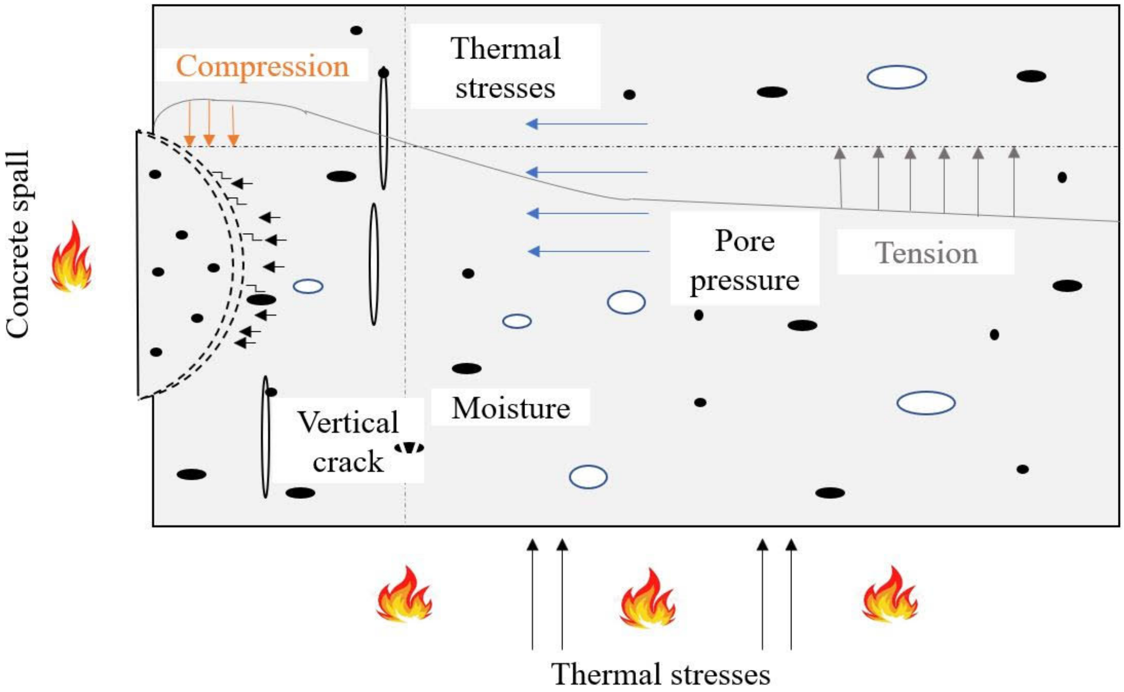

Figure 2.6 *Explosive spalling as influenced by pore pressures and thermal stresses*

2.6.4 Microstructure

The composition and structure of cement paste has an important influence on the properties of concrete exposed to elevated temperatures, such as the hydration mechanism, hydrates nature and other formed compounds, a physical structure particularly its pores distribution, and the states of water within the pores *(Bazant and Kaplan, 1996)*. After mixing the raw materials of concrete, the formation of large amounts of ettringite and hexagonal crystals of $Ca(OH)_2$ results in a further porous framework between the interface of aggregate-cement matrix and the other bulk matrix. By continuing the progress of hydration, the porosity starts to decrease *(Liao et al., 2004; Lootens and Bentz., 2016)*.

In fire applications, the practical use and testing of mechanical and thermal properties alone could be insufficient. Therefore, the design of concrete against fire is of great importance by understanding the microstructural performance of the concrete material during and after the fire, including the hydral condition that is very important. The microstructure changes of concrete due to elevated temperatures result in corresponding alterations in its properties. A direct link between the Physico-chemical changes of the heated concrete at the microstructural level and the thermo-hydro-mechanical performance of the material of concrete at the larger phenomenological level has not been easy to establish. This could be due to the level of complexity of the science involved *(Bazant and Kaplan, 1996; Fernandes et al., 2017)*.

Finally, changes of the microstructure of the heated pastes have been studied by many methods i.e., neutron diffraction, TGA, X-Ray Diffraction (XRD), Scanning Electron Microscope (SEM), Computed Tomography (CT), and MIP test that allow a further understanding of the heated hardened paste *(Wang et al., 2005)*. Thereafter, it is possible to monitor the major features of different phases and their growing and decaying such as portlandite, ettringite, Tobermorite gel, as well as the loss of free and bounded water *(Castellote et al., 2004)*.

2.6.5 Thermal properties of cement paste

The design of hardened cement paste varies on the basis of components and proportions *(fib, 2007; Fehérvári. and Nehme, 2008)*. With the addition of water, the paste develops in continuous stages which are related upon not only the involved constituents but also upon the procedures and temperature curing. In addition, there are other controlling parameters of the behaviour at elevated temperature i.e., the ratio of CaO/SiO_2, the amount of $Ca(OH)_2$ formed, the amount of CSH and CASH. The purpose is to highlight that the formation of different cement pastes can behave differently in fire *(Khoury et al., 2002)*. According to these end products, it would be interesting to follow the physical and chemical changes as the heated hardened cement paste from the first time.

Cement paste is a very unstable part of concrete during heating due to a lot of reactions. It is generally accepted that up to 80 °C the hydration products of OPC remain chemically unaltered. Changes within this temperature range can be attributed only to the physical effects, i.e., porosity, changes in Van Der Waals cohesive forces, crack pattern, surface energy, or to accelerate the hydration. Then above about 80 °C, the performance of cement paste microstructure starts to diverge. Temperature strongly affects the changes in cement paste, a schematic diagram is presented in **Figure 2.7** showing the components dissociation of hardened cement paste and their rehydration upon cooling *(fib, 2007)*. Then, by increasing of temperatures the chemical changes continue in non-linear conversion to reach 70% and 100% at 500 °C and 800 °C, respectively *(Harmathy, 1970)*. The dehydration of the $Ca(OH)_2$ into CaO and H_2O remain a prominent feature at elevated temperature, the decomposition rate is zero at about 400 °C, reaching the peak at about 500 °C, and reaching zero rates again at 600 °C. The liberated CaO that is formed expansively and detrimentally reacts with the surrounding moisture upon cooling, this phenomenon causes subsequent destruction of the bonds of paste structure showing severe damage. Studies of hardened Portland cement paste using Differential Thermal Analysis (DTA) indicates that the transformations in cement paste are largely endothermic (**Figure 2.7**) *(Khoury, 1992; fib, 2007)*. Other paste components experience transformations at given temperature ranges measured by DTA which indicates endo and exothermic reactions, and TGA which measures simultaneously the loss of mass *(fib, 2008; Lublóy et al., 2016)*.

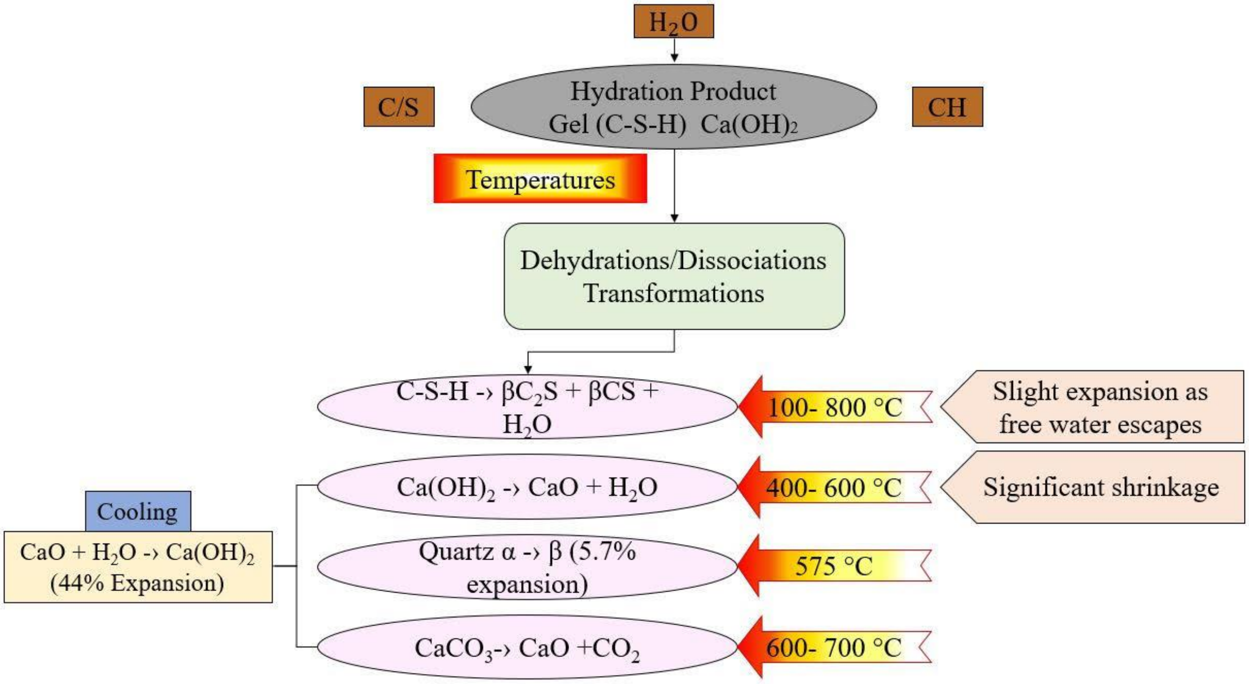

Figure 2.7 *The influence of temperature and moisture upon the chemical transformation of hydration products (Khoury, 1995)*

2.6.6 Thermal properties of aggregate

The key role that the aggregate plays is important and should be considered from the outset of the mix design. The properties of the aggregate either the physical or the chemical property show changes after subjected to elevated temperature, that is varied with the type of aggregate. The right selection of aggregate is, therefore, an important parameter in determining the thermal properties and the thermal stability of the heated concrete *(Hager, 2013)*.

Nilsen and Bieanic (2003) reported that the type of aggregate has a significant influence on the thermal properties of HSC. Concrete prepared by gravel aggregate is degraded faster than concrete prepared of basalt aggregate. *Robert and Colina (2009)* indicated that HSC made by siliceous aggregate has lower residual compressive strength performance than HSC of silico calcareous and calcareous aggregate. The coefficient of linear thermal expansion for siliceous aggregate considered to dilate slightly more than the calcareous aggregate. This is attributed to the calcine-carbon dioxide released from the calcareous aggregate and calcium oxide were remained during fire exposure. In the other hand, The HSC contains carbonate aggregate increases fire resistance *(Kodur and Sultan, 2003)*. *Khoury (2000)* suggested that the mechanical properties deterioration of concrete can be minimized by judicious design of concrete mixture, with the choice of the appropriate aggregate could being the most important factor. Granite is expected to be thermal stability up to 600 °C, while the properties of basalt aggregate exhibited to be thermally stable up to 800 °C *(Khoury, 1985)*. From the spalling perspective, *Bastami et al. (2011)* studied the performance of HSC at elevated temperatures, results showed that the aggregate type has a significant effect at elevated temperatures. Furthermore, increasing the ratio of fine aggregate (sand) to the total aggregate increases the residual strength and showing a significant contribution. Concluding that a slight influence of fine and coarse aggregates on the degree of spalling was noticed.

Finally, the extent is found to be much greater in the case of lightweight aggregate. This is mainly due to the more content of free moisture in the lightweight aggregate, which induces higher vapour pressure during the fire *(Kodur and Phan, 2007)*.

2.6.7 Bond zone

The characteristics of the ITZ of the particles of aggregate and cement paste have a significant role in the adhesion property of concrete *(Siddique, 2011)*. In which, the bond zone of aggregate-cement paste has been considered the weakest interlock in the concrete since it is also weaker than the cement paste. The 'bond shell' which forms around the aggregate has properties different from that of the bulk of cement paste. General speaking, these results suggest that the aggregate-cement paste bond fails on heating due to chemical transformation or as a result of thermal incompatibility between the paste and aggregate. It is considered that the different thermal strains for aggregates and hardened cement have engendered in the development of the micro-cracks. Due to the increase of temperature, the hardened cement shows expansion followed with shrinkage, while aggregate keeps expansion during the whole heating. Such incompatible strains will result in stress between the cement matrix and aggregates, forming micro-cracks in the ITZ *(Fu et al., 2004)*. For this concept, SCM enriches the thickness of ITZ phase of concrete and decrease on the degree of the $Ca(OH)_2$ crystals. Hence the mechanical properties and durability are improved. Eventually, this improvement is not only corresponding to the pozzolanic reaction in the interface, but also connected to the microstructure modification, and the decrease in the porosity within the packing effect *(Siddique, 2011)*.

2.6.8 Thermal properties of blended Cement

The first information that draws the attention of blended cement is the low ratio of CaO/SiO_2. In which, results in a low content of $Ca(OH)_2$ and ensures more beneficial hydrothermal reaction. Researchers concluded that the adoption of slag results in best behaviour at elevated temperatures followed by FA and then SF *(Khoury et al., 1990; Sarshar and Khoury, 1993)*. In the other hand, some of the SCM show relatively low performance at elevated temperatures due to the spalling problem. Generally, the nature of the changes is upon the mineralogical composition of the cement and the fineness of the particles *(Verbeck and Copeland, 1972)*. **Table 2.1** summarizes different studies on SCM usage on the residual mechanical properties of concrete after exposure to elevated temperatures, including compressive strength, bending strength, splitting tensile strength, and modulus of elasticity.

Table 2.1 *Summary of the previous studies carried out on different types of SCM at elevated temperatures*

#SCM	***Type of specimen***	***Replacement (%)***	***Test temperatures (°C)***	***Mechanical properties tested***	
Slag	*Concrete*	*0, 10, 30, 50*	*20, 150, 300, 400, 500, 600, 700*	*C, E*	*(Li et al., 2012)*
	Concrete	*0, 20, 40, 60*	*20, 100, 200, 350*	*C, T, E*	*(Siddique and Kaur, 2012)*
	Concrete with granite	*0, 30, 40*	*20, 200, 400, 600, 800*	*C*	*(Poon et al 2001b)*
	Paste	*0, 5, 10, 20, 50, 80*	*20, 105, 200, 440, 580, 800, 1050*	*C, E*	*(Wang, 2008)*
	Concrete with limestone	*0, 30*	*20, 100, 300, 450, 600*	*C*	*(Karakurt and Topcu, 2012)*
	Pumice mortar	*0, 20, 40, 60, 80*	*20, 300, 600, 900*	*C, B*	*(Aydin, 2008)*
	Paste	*0, 35, 50, 65*	*20, 100, 200, 300, 400, 500, 600, 700, 800*	*C*	*(Mendes et al., 2008)*
	Mortar	*0, 20, 50, 80*	*20, 150, 300, 600, 900*	*C, T*	*(Delhomme et al., 2012)*
	Concrete	*0, 20, 40, 60*	*20, 100, 200, 350*	*C*	*(Siddique and Kaur, 2012)*
	Concrete with limestone	*0, 30, 40, 50*	*20, 400*	*T*	*(Gao et al., 2012b)*
	Concrete	*0, 30, 40, 50*	*20, 400*	*B*	*(Gao et al., 2012a)*
SF	*Concrete with limestone*	*0, 10*	*20, 100, 200, 300, 450*	*C, E*	*(Phan et al., (2001)*
	Lightweight concrete	*0, 5, 10*	*20, 100, 400, 800, 1000*	*C*	*(Sancak et al., 2008)*
	Concrete with limestone	*0, 10*	*20, 100, 200, 300, 600*	*C*	*(Ghandehari et al., 2010)*
	Concrete with limestone	*0, 10*	*20, 100, 200, 300, 600*	*T*	*(Behnood and Ghandehari, 2009)*
	Mortar	*0, 2.5, 5, 7.5*	*20, 400, 700*	*C, B*	*(Ibrahim et al., 2012)*
	Concrete with granite	*0, 5, 10*	*20, 200, 400, 600, 800*	*C*	*(Poon et al., 2001b)*
	Paste	*0, 5, 10, 15, 20*	*20, 250, 450, 600*	*C*	*(Heikal et al., 2013)*

	Mortar	*0, 5, 10, 15, 20*	*20, 150, 300, 450, 600, 750*	*C*	*(Yazici et al., 2012*
	Concrete with limestone	*0, 6, 10*	*20, 100, 200, 300, 600*	*C*	*(Behnood et al., 2008)*
FA	*Concrete with granite*	*0, 25, 55*	*20, 250, 450, 650, 800*	*C*	*(Xu et al., 2001)*
	Concrete with limestone	*0, 10, 30*	*20, 100, 300, 600, 750*	*C, E*	*(Savva et al., 2005)*
	Concrete	*0, 30*	*20, 100, 200, 400, 600*	*C, E*	*(Fu et al., 2005)*
	Mortar	*0, 25, 35, 45*	*20, 400, 700*	*C, B*	*(Ibrahim et al., 2012)*
	Concrete with granite	*0, 20, 30, 40*	*20, 200, 400, 600, 800*	*C*	*(Poon et al., 2001b)*
	Pumice mortar	*0, 20, 40, 60*	*20, 300, 600, 900*	*C, B*	*(Aydin and Baradan, 2007)*
	Lightweight concrete	*0, 10, 20, 30*	*20, 200, 400, 800*	*C, T*	*(Tanyildizi and Coskun, 2008)*
	Concrete with limestone	*0, 30*	*20, 100, 300, 450, 600*	*C*	*(Karakurt and Topcu, 2012)*
	Mortar	*0, 5, 10, 15, 20*	*20, 150, 300, 450, 600, 750*	*C*	*(Yazici et al., 2012)*
	Concrete with granite	*0, 25, 55*	*20, 200, 400, 600, 800*	*T*	*(Xu et al., 2003)*

Note: **C**, compressive strength; **E**, modulus of elasticity; **T**, splitting tensile strength; **B**, Bending strength.

The compressive strength of pure hardened cement paste (100% OPC) and blended paste with 50% of slag after the exposure to temperatures up to 800 °C is presented in **Figure 2.8**. Using slag significantly enhances the heat resistance of hardened cement paste after 400 °C, which is mainly by the consumption of the $Ca(OH)_2$. *Khoury (1992)* described the $Ca(OH)_2$ as the Achilles' heel of concrete in elevated temperatures cases.

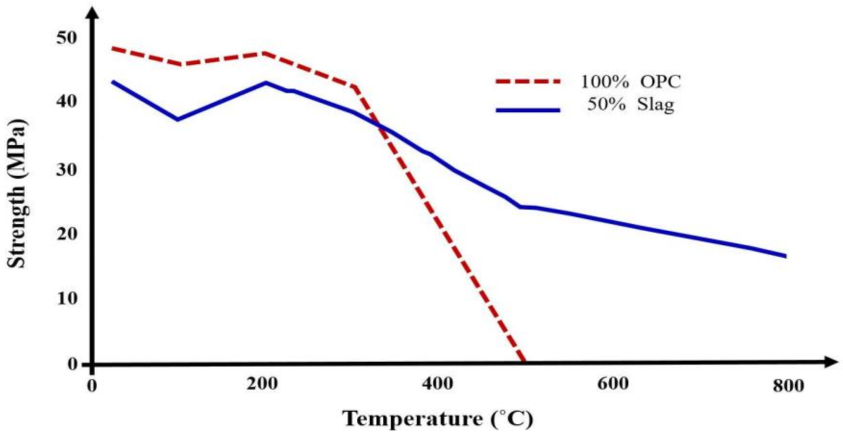

Figure 2.8 *Compressive strength of OPC and 50% slag paste at different temperatures (Mendes et al., 2012)*

2.6.8.1 Behaviour of HSC containing MK at elevated temperatures

The first usages of MK in cement production were in 1962 in Jupia Dam, Brazil where around 250,000 metric tonnes of MK have been used *(Saad et al., 1982)*. The main component of SCM is the active amorphous SiO_2 in which MK generally contains 50%–55% SiO_2 in addition to the high content of Al_2O_3 40%–45% *(Poon et al., 2001b)*. Advantages of using MK are many, it enhances the concrete properties through its filler effect, pozzolanic activity with $Ca(OH)_2$ and its contribution for accelerating the hydration of OPC *(Poon et al., 2003)*. Studies reported that 10%–15% replacement of cement with MK reduced the $Ca(OH)_2$ content in concrete by 70% at 28 days testing age *(Kostuch et al., 2000; Wild and Khatib, 1997; Poon et al., 2003).*

Several researchers studied the behaviour of MK at elevated temperature. *Morsy et al. (2009)* evaluated the performance of mortars with and without MK exposed to elevated temperatures up to 800 °C, using cement replacements from 5% to 30% of MK. However, by investigating the performance of MK exposed to elevated temperatures, results are relatively different. Some studies concluded that MK improves the compressive strength before and after exposure to elevated temperature, leading to the optimum replacement of MK to be 20% *(Poon et al., 2003)*. In which concrete with high replacement of MK (above 20%) suffered a high loss in strength at elevated temperatures as well as showing severe degradation on the durability. From another hand, *Rashad et al. (2017)* have studied the compressive strength of hardened cement paste incorporated with MK subjected to elevated temperatures. The results showed that the compressive strength increased with increasing the replacement amount of MK to cement. *Wang et al. (2019)* carried out an experimental study to assess the difference between hardened cement paste with 0% and 10% of MK at ambient and elevated temperature exposure. They concluded that 10% of MK enhances the thermal resistance, showing less shrinkage and significantly densify the microstructure. *Poon et al. (2004)*, have studied the compressive performance of fibre-reinforced high-performance concrete with and without the inclusion of MK at elevated temperatures. The frequency of spalling increases with the high content of MK, due to its high dense pore-structure. Yet, the use of 5% of MK to cement in concrete shows better performance at elevated temperatures *(Noumowe et al. 2009)*.

2.6.8.2 Behaviour of HSC containing SF at elevated temperatures

First studies of SF performance in concrete were started since the 1950s *(ACI Committee 363, 1994)*. *Cohen et al. (1990)* reported that for a 15% SF by cement mass replacement, there are approximately 2 million particles of SF for each grain of Portland cement mixture. Thus, it is no surprise that SF has a pronounced effect on cement paste properties. The advantages of SF to the concrete are also observed at elevated temperatures. Several studies have been conducted to evaluate the performance of HSC containing SF after exposure to elevated temperatures *(Hertz, 1984; Hertz, 1992; Khoury, 1993; Sarshar and Poon et al., 2001b; Phan and Carino, 2002; Alimrani et al, 2017)*. *Behnood and Ziari (2008)* have studied the effect of different amounts of SF and w/b ratio on the residual compressive strength of HSC after exposure to elevated temperatures. They concluded that the dosage of SF had no significant effect on the relative residual compressive strength at 100 °C and 200 °C, whereas the amount of SF had considerable influences on the residual compressive strength above 300 °C like the response at 600 °C. The optimum amount of SF and w/b ratio was found to be 6% and 0.35, respectively. *Ahmad et al. (2020)* studied the performance of mortar by using different replacement of SF (0%, 5%, and 10% to cement weight) at elevated temperatures. SF showed an effective contribution, and all mixtures containing SF more stable at elevated temperatures than the mixture of pure OPC. *Heikal et al. (2013)* studied the hardened cement paste with SF up to 20%, the used replacement step was 5%. They concluded that the compressive strength of the mixtures containing 10%, 15% of SF has a higher resistance to fire. *Gómez-Zamorano and Escalante-García (2010)* have reported that the pozzolanic reaction was highly accelerated by increases in temperature. *Jia et al. (1986)* concluded that replacing cement with 2% to 5% of SF produced a dense structure with a consequent increase in fracture toughness and microhardness of concrete.

On the other hand, *Poon et al. (2001b)* investigated the behaviour of HSC using different SF replacements to cement with 0%, 5%, and 10% at w/b ratio of 0.3 after elevated temperature showing that the performance is poor especially above 10% replacement of SF to cement. With respect to spalling, *Phan and Carino (2002)* investigated the mechanical properties of HSC exposed to elevated temperatures up to 600 °C. The experimental parameters were SF replacements (0% and 10%) and w/b ratio (0.22, 0.33, and 0.57). Results indicate that the loss in residual strength was affected by the w/b ratio, in which, there was an increase in spalling as the w/b ratio decreased. Furthermore, there was no clear evidence that the presence of SF by itself affects the tendency for explosive spalling. The advantages of SF are restricted by the occurrence of spalling that happens suddenly due to two main factors correspond to heat pressure and dense pore structure. *Sarshar and Khoury, (1993)* found that the residual strength of the concrete has SF showed poor performance than the concrete made of pure OPC. Fire behaviour of HSC with SF at various moisture content, results shows that the moisture content has a dominant influence on the occurrence of spalling *(Hertz, 1992; Sanjayan and Stocks, 1993; Chan et al., 1999b; Phan et al., 2001)*. Inclusion of more than 5% to 10% of SF creates a high risk of explosive spalling *(Hertz, 1992; Sarshar and Khoury, 1993; Poon et al., 2003)*. Eurocode provided the maximum amount of SF less than 6% by cement weight *(EN 1992-1-2, 2014)*.

2.6.8.3 Behaviour of HSC containing FA at elevated temperatures

The performance of concretes made by FA at elevated temperature has been widely studied. Generally, HSC containing FA shows better behaviour in residual mechanical and fracture properties after the exposure to elevated temperatures than the concrete based OPC *(Tang and Lo, 2009)*. The increase in strength is observed up to 200 °C for concrete contains FA is due to the Tobermorite formation (a product of lime and FA at high pressure and temperature), reporting to be stronger than the CSH gel of two to three times *(Poon et al., 2003)*. *Sarshar and Khoury (1993)* tested hardened cement paste with and without FA subjected to a series of different temperatures up to 650°C. A mixture containing 30% of FA as cement replacement showing a relative residual compressive strength of 88% and 73% at 450°C and 600°C, respectively, which is about the double of the residual strength obtained by pure hardened cement pastes. *Nadeem et al. (2014)* studied the durability of concrete containing FA with replacement level of 20%, 40% and 60% to cement weight at post-fire exposure. Concrete containing 20% FA showed lowest sorptivity and was regarded as having better residual performance.

2.6.8.4 Behaviour of GGBS concrete at elevated temperatures

The GGBS concrete showed the best behaviour followed by FA and condensed SF concretes as reported by *Seleem, et al. (2011)*. Inclusion of 40% of GGBS in HSC is found to be the optimum replacement to retain maximum strength and better durability after exposure to elevated temperatures *(Poon et al., 2001a)*. GGBS results have appeared better performance attributed to the reduced amount of $Ca(OH)_2$. Finally, using GGBS is beneficial to save residual compressive and bending strengths of HSC after the exposure to fire compared to SF *(Xiao and Falkner, 2006)*.

2.6.9 Rate of heating

The concrete explosion is susceptible to a very slow rate of heating of only 10 °C /min, where the heating rate of 10-20 °C/min is the normal range for the fire-exposed concrete surface as reported by *Hertz (1992)*. Similar observations have been reported by *Yan et al. (2007)*. While the heating rate follows a standard fire exposure test BS 476 curve *(BS476, 1987)*, the higher thermal gradient due to high rate of heating could early engender micro-cracks, thereafter, allowing the pore pressure to move and resulting in low maximum pore pressure *(Phan, 2008; Belkacem et al., 2008)*. Finally, HSC is vulnerable to explosive spalling even the rate of heating rate is relatively slow (≤ 5 °C/min). This is attributed to the fact that HSC containing fewer pores, in which, the thermal conductivity is higher compared to the ordinary concrete *(Husem, 2006)*.

2.6.10 Type of cooling

The way of cooling significantly affects the physical and mechanical properties of HSC, thus the influence of cooling regimes on the mechanical properties of concrete is of great importance. Thermal shock resulted by water cooling or quenching has made a serious deterioration in the mechanical strength than of cooling within the furnace *(Luo et al., 2000; Chan et al., 2000; Husem 2006)*. In case of quenching of concrete specimens, internal cracks occur due to the development of stresses where temperature differences between the core and the surface of a specimen *(Chan et al., 2000; Luo et al., 2000)*. Spraying water for 30 min duration or more is in consistency with quenching in water which has the same influence *(Peng et al., 2008)*. From the aggregate perspective, the fire resistance of aggregate is generally high yet, having a non-uniform elevation on temperature have an influence on aggregate. Using water spray in cooling the heated aggregate causes the internal pressure within the aggregates. Finally, for results of concrete under quick regimes, HSC containing SCM shows a better performance than the ordinary HSC *(Tang and Lo, 2009)*.

CHAPTER 3: EXPERIMENTAL STUDIES

Chapter 3 presents the materials and the methods used for achieving the goal of the PhD work. Besides, steps of experimental work and the procedures conducted for realizing every experimental part are explained.

3.1 Materials

Types and properties of all the used materials are described in details at the current section.

3.1.1 Cement

Types of cement used in this study program were OPC of CEM I 42.5 N and CEM I 52.5 N. These types were produced by Duna-Dráva Company (Duna-Dráva Cement, Heidelberg Cement Group), with strength classes (42.5 N and 52.5 N) that complied with the requirements of the standards of *MSZ EN 196-2 (2013)* and *MSZ EN 525-12 (2014)*. The chemical composition and physical characteristics of cement are given in **Table 3.1**. Cement particles morphology and microstructure were observed by SEM images and illustrated in **Figure 3.1**. OPC particles can be found in different shapes, angular mostly, with approximately smooth particles of the surface. However, the CEM I category 42.5 N is relatively coarser than CEM I 52.5 N as shown in **Figures 3.1 a** and **b**, respectively. This could have resulted in showing a different behaviour at ambient and elevated temperatures. In case of CEM I 52.5 N, properties are characterized by higher specific surface area and higher absorption capacity than CEM I 42.5 N where it generally shows higher strength grade. It is worth to mention that if OPC is fully hydrated, it produces $Ca(OH)_2$ of about 28% of its own weight. Finally, both types of cement have similar chemical compositions and show high content of CaO (**Figures 3.1 c**).

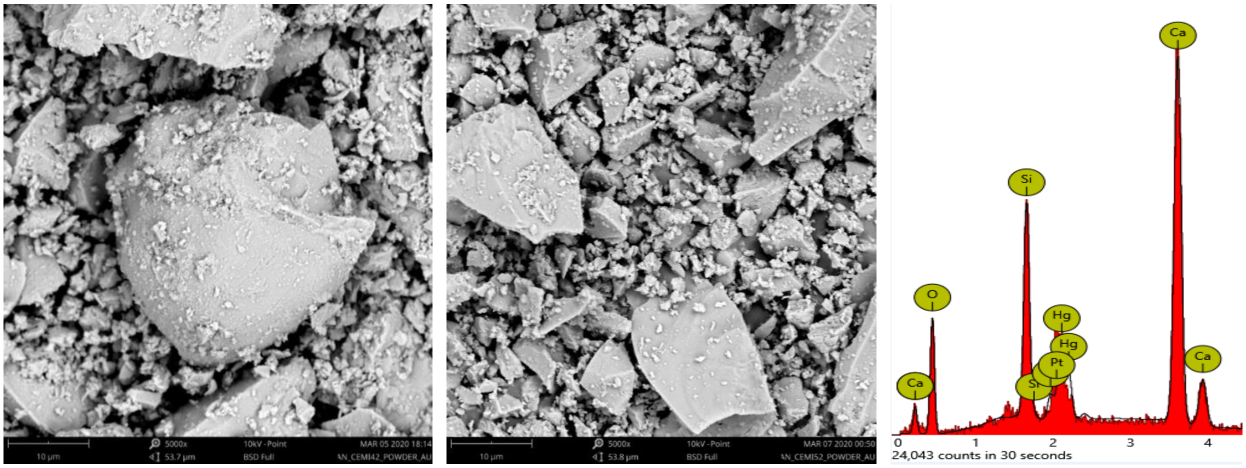

a) b) c)

Figure 3.1 *Different properties of cement powders: a) CEM I 42.5 N microstructure morphology, b) CEM I 52.5 N microstructure morphology, c) Chemical compositions by SEM (CEM I)*

3.1.2 Supplementary cementitious materials

The goal of using SCM is to improve concrete performance. A comprehensive work was applied on HSCP by the incorporation of SCM as a partial replacement of cement. To achieve the necessary properties of the HSCP paste after exposure to elevated temperature, a considerable and specified amount of SCM is required to achieve HSCP durable and with a potential to heat resistance. The types used of SCM in the current study are MK, SF, and FA.

3.1.2.1 Metakaolin

MK is a commercially available material, used as an alumino-silicate based SCM. In Hungary, it is obtained from Newchem company, as a type of Metaver N. MK is a primary material with attractive white colour (**Figure 3.2 a**), mostly amorphous aluminium silicate, made by calcination of concentrated natural kaolin at a typical temperature range of 600 °C to 800 °C. Metaver N follows the standard requirements *(MSZ 4798, 2015)*. Typical particle distribution was studied by Laser granulometry method, due to the high surface area of the particle, 7-9% of the total volume is less than 1 µm, 50% of the volume pass through 3.4-4.5 µm sieve size, and 95% of the passing take place between sieve sizes of 12-18 µm. Moreover, the microstructure and the morphology of MK is investigated by SEM (**Figure 3.2 b)**, it is characterized by very fine particles in the range of micro and nano sizes while its physical shape is like fibres. The possibility of using MK within this characteristic could promise an improvement in the mechanical properties of paste before and after exposure to elevated temperatures. The used MK is characterized by a high content of Al_2O_3 and SiO_2 (**Figure 3.2 c**).

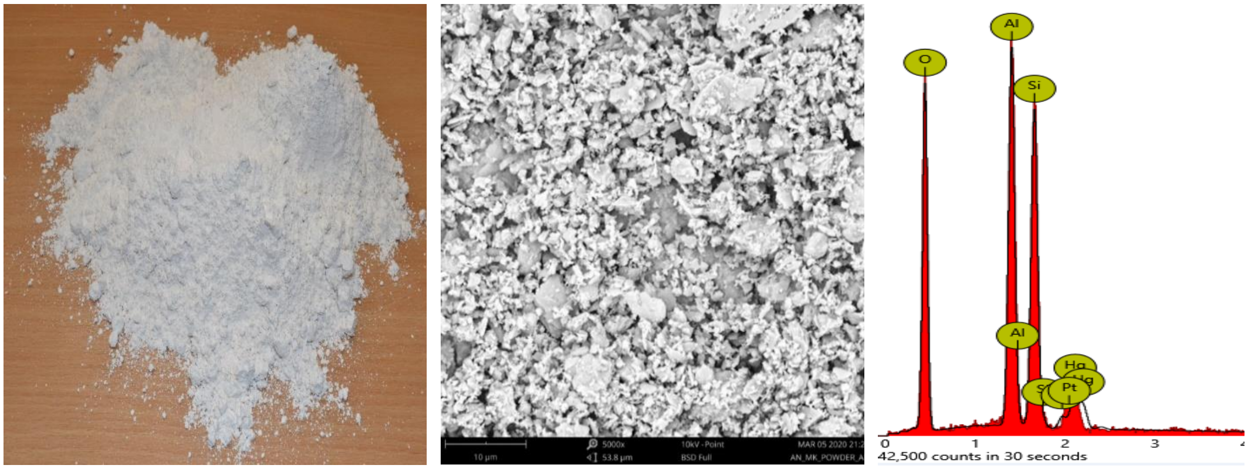

a) b) c)

***Figure 3.2** Different properties of MK: a) MK powder, b) MK microstructure morphology, c) MK chemical compositions by SEM*

3.1.2.2 Silica fume

SF is a by-product material generated from the ferrosilicon metals and silicon alloys; it is about 30% by mass of the produced silicon. The colour of the used SF is blue dark (**Figure 3.3 a**), with very fine spherical particles as shown in the (**Figure 3.3 b),** compared the size of SF particles to the OPC particles. SF is consisting of a high content of amorphous SiO_2 (**Figure 3.3 c**). The key behind the efficiency of SF is related to its extremely fine particle size (0.1 µm) as well as the reactive SiO_2. The free CaO which is available in the cement matrix is bonded with SiO_2 provided by SF. In addition to the filling effect and the pozzolanic reaction, SF can improve the pore structure and interface structure to improve the compactness of cement paste, and then increase its strength and durability *(Razak and Wong, 2005)*. The applied SF in this study (Sikafume-HR) is supplied from the company of “Sika”.

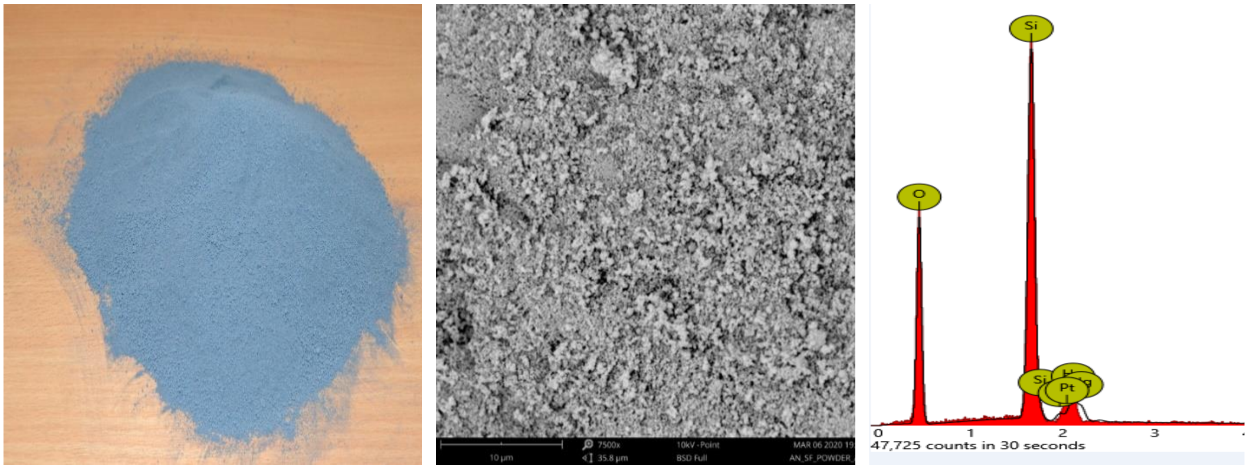

a) b) c)

Figure 3.3 *Different properties of SF: a) SF powder, b) SF microstructure morphology, c) SF chemical compositions by SEM*

3.1.2.3 Fly ash

The demand for power increases every day, and a major part of the power is supplied by the coal, which is used as fuel resulting in a large quantity of FA engendered during the process. The produced FA creates different environmental problems and takes huge disposal area. Transforming these problems into benefits by using this waste material into a suitable construction material. FA has become an attractive construction material because of its performance results which depend on its compositions and properties. The variation of its properties is related to the nature of coal, fineness of pulverization, type of furnace, and temperature exposure *(Jala and Goyal, 2006; Ismail et al., 2007)*.

Figure 3.4 shows different properties of the used FA with a grey-brown colour (**Figure 3.4 a**). The feature of FA is that composed of a variety of morphological particle types as shown **Figure 3.4 b**. The used FA is mostly characterized by a smooth glassy hollow and porous spherical grain ranging in size between 1 and 15 µm as shown in **Figure 3.4 b**. In addition to angular (the carbonaceous material), lacy, opaque as well as that some particles that have not been combusted completely *(Ahmaruzzaman, 2010)*. The used FA in the current study consists of high amounts of SiO_2 and Al_2O_3 (**Figure 3.4 c**).

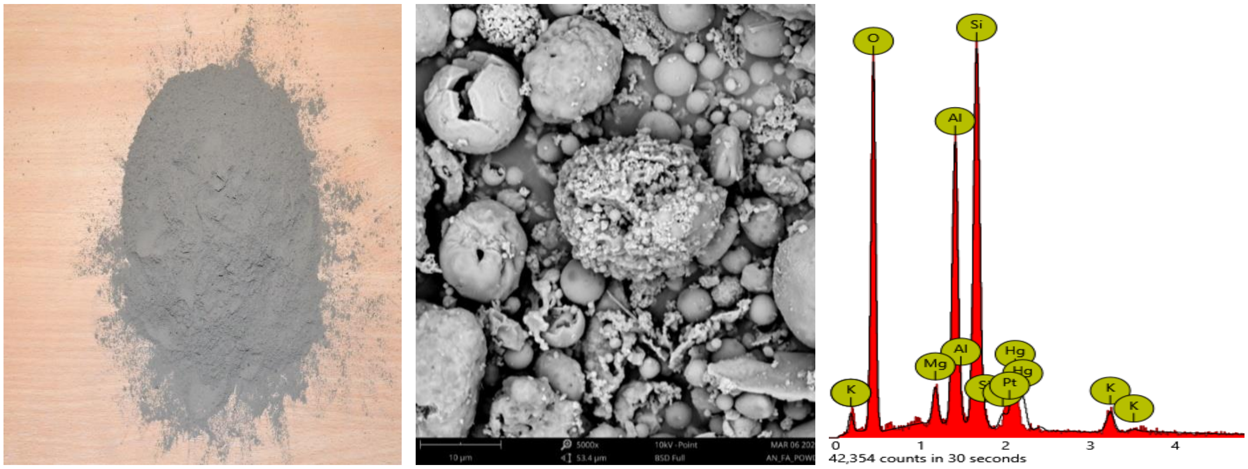

a) b) c)

Figure 3.4 *Different properties of FA: a) SF powder, b) FA microstructure morphology, c) FA chemical compositions by SEM*

3.1.2.4 Differences in the properties of the used powders

The used SF, MK and FA throughout the experimental program are mostly amorphous materials. The chemical compositions as well as measured physical properties of the used materials are presented in **Table 3.1**. The main difference between the three SCM is the shape and size of the particles, where SF is much fine with very small spherical particles, and MK is characterized by irregular flaky shape and loose porous particles. In the case of FA, the particle size is much coarser than SF and MK particles. Other observations on the acidic oxides (silica and alumina) contents were varied widely from one SCM to another, and the common feature of the three SCM is that the silica compound is the major component of their composition. It is also pointed out *(Lublóy et al., 2017)* that the low CaO/SiO_2 ratio shows higher relative residual strength after the temperature to 800 °C. The ratios of the three main oxides (SiO_2, CaO, Al_2O_3) of the four powders are presented in **Figure 3.5**, showing that the content of CaO in the three SCM powders is very low, whereas SF contains a very high SiO_2 reaching 97% of its composition. MK is characterized by a high content of Al_2O_3 around 44% and of 53% of SiO_2. The ratios of oxides in the case of FA are different from SF and MK. Thus, the performance of the three materials at elevated temperatures could have an impact on changing the results.

Table 3.1 *Chemical composition and physical properties of tested materials*

Measured property	***CEM I 52.5 N***	***CEM I 42.5 N***	***MK***	***SF***	***FA Class F***
Oxide compositions/% (by mass)					
$Si0_2$	*20.59*	*19.84*	*52-53*	*96.43*	*54.4*
Al_20_3	*5.55*	*5.38*	*43-44*	*0*	*26.5*
Fe_20_3	*3.21*	*3.22*	*< 1*	*0,073*	*4.8*

Ca0	*65.02*	*64.90*	*< 0,5*	*0,78*	*3.5*
Mg0	*1.44*	*1.38*	*< 0,4*	*0,70*	*2.5*
$S0_3$	*2.88*	*2.97*	-	*0,038*	*1.7*
K_20	*0.78*	*0.78*	*< 1*	*1,28*	*0.6*
Cl	*0.0048*	*0.0048*	-	-	-
Na_2O	-	-	*< 0,1*	-	*0.4*
TiO_2	-	-	*< 1*	-	*1.5*
Loss on ignition (%)		*3.0*	*1.59*	*2.8*	*2.3*
Density/g cm^{-3}	3.17	*3.13*	*2.6*	*2.2*	*3.13*
Specific surface area/ $cm^{+2}\ g^{-1}$	*4500*	*4000*	*24000*	*20000*	*20000*

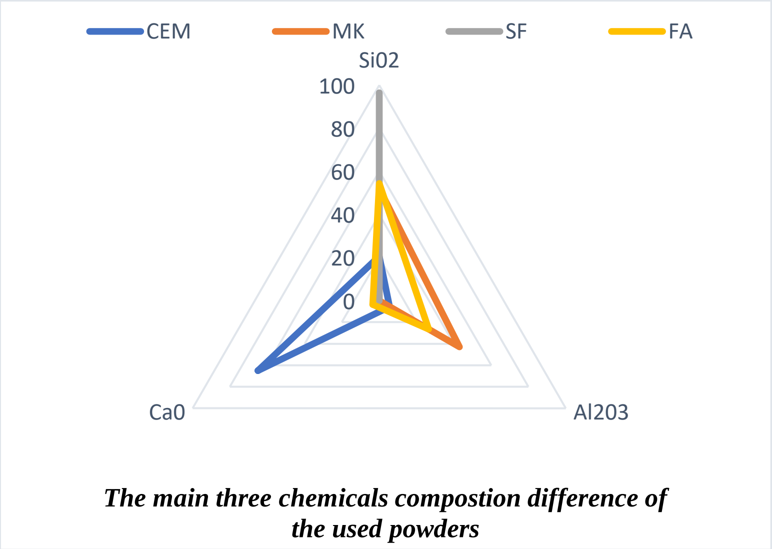

Figure 3.5 *Ratios of the three main oxides in the cement composition*

3.1.3 Aggregates

In the case of concrete mixtures, the used quartz gravel and sand with a maximum aggregate size of 16 mm meet the grading curve of the British European Standard *(BS EN 12620-2002+A1, 2008)*. The proportions of the aggregate fractions are 45% for Sand with a size of 0-4 mm, 30% for small gravel with a size of 4-8 mm, and 25% of medium gravel with a size of 8-16 mm.

3.1.4 Water

Quality of the HSCP or concrete is influenced by the quality and the quantity of water *(Neville and Brooks, 2010)*. Additionally, water content is a key parameter related to the permeability on HSC. At the current study, mixing water was tap water that complies with the requirements of the European Standards *[EN 1008 (2002)]*.

3.2 Mix design

3.2.1 Approach

High strength cement paste mixtures were designed with different parameters as presented in **Figure 3.5**. The total binder content is fixed in the whole program with an amount of 480 kg/m^3 to achieve the target properties of the hardened paste and HSC. The used binders are CEM I 42.5 N, CEM I 52.5 N, MK, SF, and FA. The method of mixing was carried out at two steps; in the first step was a dry mixing of binder (cement and SCM) for 30 seconds to ensure homogenous binder distribution. Then in the second step, the water and superplasticizer were simultaneously added and mixed with 75% of binders amount. Thereafter, the remaining amounts of binders were added during the mixing to remove Lumps and ensure water reaches binder particles.

3.2.2 Design variables

Several HSCP mixtures have been produced depending on different variables. The variables corresponding to the HSCP mixtures are (i) three w/b ratios, i.e., 0.30, 0.35, and 0.40, (ii) different types of SCM, i.e., MK, SF, and FA, (iii) different replacement amounts of SCM, i.e., 0%, 3%, 6%, 9%, 12% and 15% by cement mass, (iv) two types of cement fineness, i.e., CEM I 42.5 N and CEM I 52.5 N, and (v) different levels of temperature, i.e., 20, 50, 150, 300, 400, 500, 800, and 900 °C.

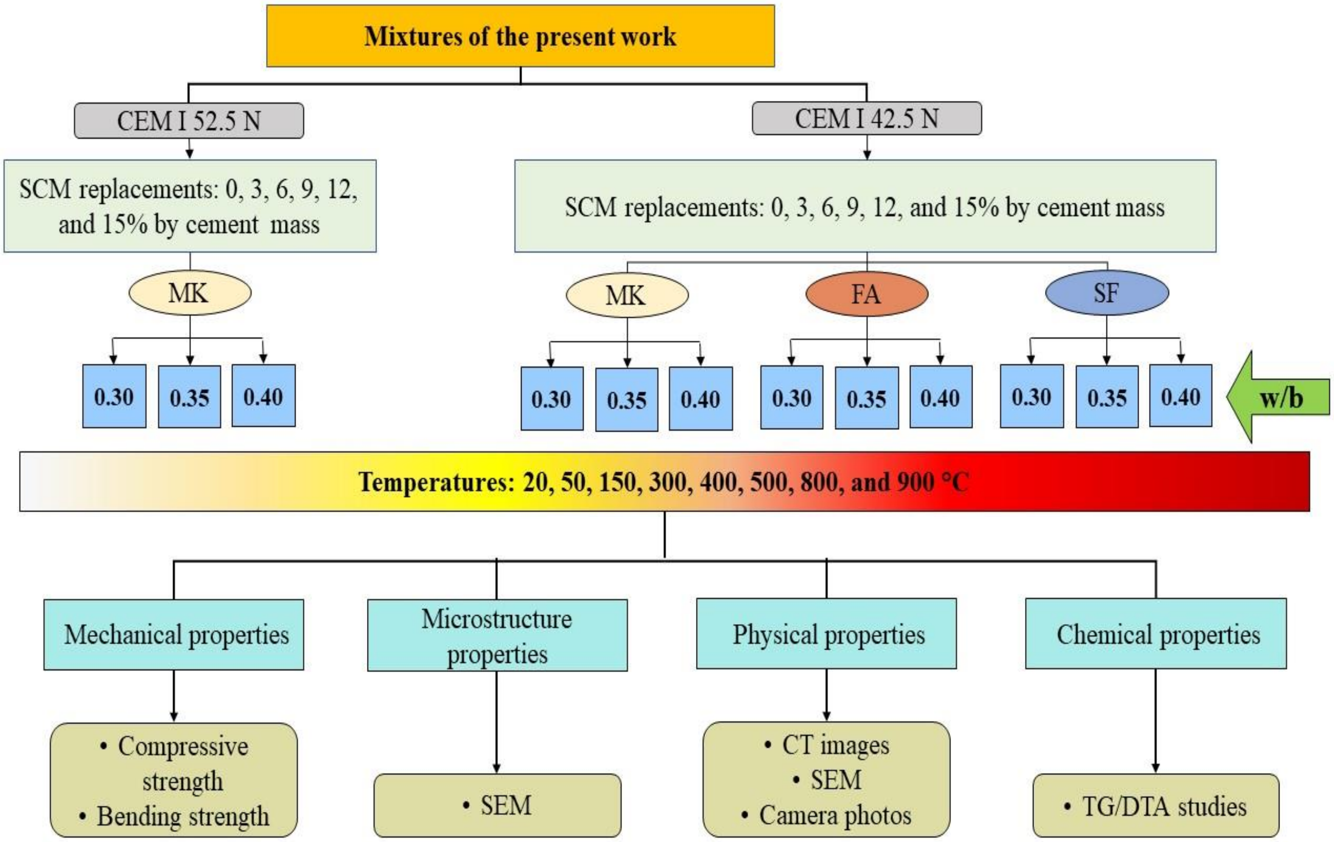

Figure 3.6 *Parameters of the mixtures for the experimental work*

A total of 66 mixtures of HSCP, including approximately 1600 cubes and 1600 prisms, were prepared, and experimentally tested. Three samples were considered for each mixture. The prepared mixtures are divided into two groups as shown in **Figure 3.6**. The first group is prepared by CEM I 42.5 N (the right branch of **Figure 3.6**) whereas mixtures in the second group were made with CEM I 52.5 N (the left branch of **Figure 3.6**). **Table 3.2** shows the proportions of the mixtures of HSCP for each type of SCM with the three w/b ratios.

3.3 Heating and testing procedures

The procedures of heating and testing have been prepared as following:

1. Mixing and casting cement paste to produce cubes and prisms.
2. Around 24 hrs after the casting, the cubes were de-moulded then placed in the water tank.
3. After 7 days of curing, the cubes and prisms were removed from the water tank then stored in the lab conditions (20 ± 2 °C and 35% relative humidity).
4. At the age of 90 days, the testing program of specimens including heating was conducted as recommended by RILEM *(RILEM Technical Committees 129-MHT, 1995)*.
5. The heating program was applied by heating specimens to the target temperature (20, 50, 150, 300, 400, 500, 800, and 900 °C,) for a duration of two hours of exposure.
6. Finally, after the heating process, the cubes were left in the lab condition for 24 hrs to be cooled down, then the load bearing tests were applied for the cold state.

***Table 3.2** Experimental matrix with detailed varied parameters*

Mixture proportions in kg/m^3								
SCM Replacements to cement	***CEM I***	***Water***	***SCM Replacements to cement***	***CEM I***	***Water***	***SCM Replacements to cement***	***CEM I***	***Water***
0 %	*480*	*144*	*0 %*	*480*	*168*	*0 %*	*480*	*192*
3 %	*465.6*	*144*	*3 %*	*465.6*	*168*	*3 %*	*465.6*	*192*
6 %	*451.2*	*144*	*6 %*	*451.2*	*168*	*6 %*	*451.2*	*192*
9 %	*436.8*	*144*	*9 %*	*436.8*	*168*	*9 %*	*436.8*	*192*
12 %	*422.4*	*144*	*12 %*	*422.4*	*168*	*12 %*	*422.4*	*192*
15 %	*408*	*144*	*15 %*	*408*	*168*	*15 %*	*408*	*192*

The heating rate of the used electric furnace was set up similar to the standard fire curve of ISO 834 for buildings, as shown in **Figure 3.7** *(ISO-834, 1975)*.

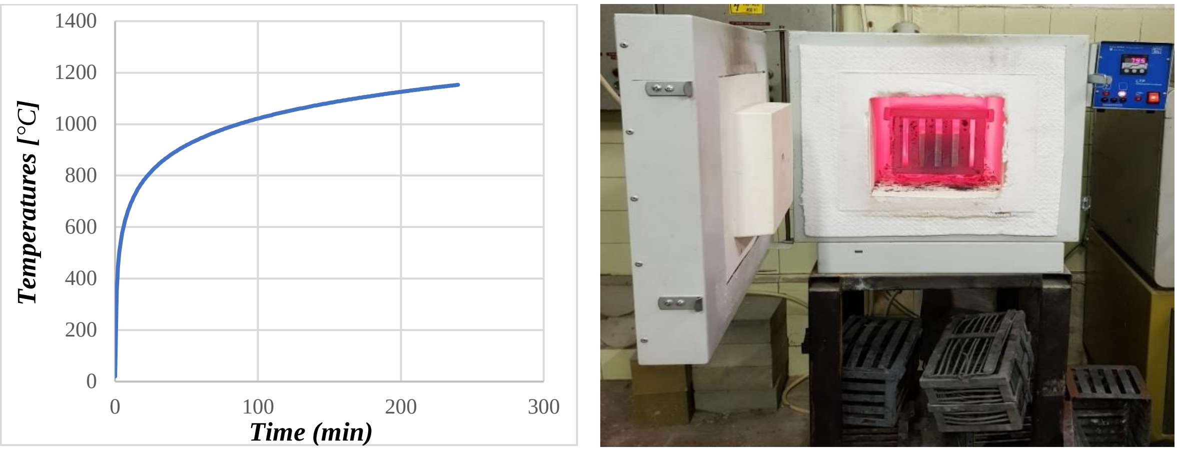

a) b)

Figure 3.7 *Heating process: a) Heating curve, and b) Electrical furnace containing a steel cage*

3.4 Mechanical properties

The tested mechanical properties are compressive strength and three-point bending strength. Tests were following the Standards *MSZ EN 12390-3 (2009)* for the compression test, and *MSZ EN 12390-5 (2009)* for the bending test. The tests were comprehensively carried out to investigate the mechanical properties of the specimen at ambient and different levels of maximum temperatures.

3.4.1 Compressive strength

Specimens (cubes) with a size of 30×30×30 mm were used for hardened cement paste investigations in compression. The test machine was ALPHA 3/3000S at a constant loading rate of 1.40 kN/s. For concrete, cubes of 150x150x150 mm have been tested by a universal closed-loop hydraulic machine with a constant rate of 11.25 kN/s.

3.4.2 Bending strength

Specimens with a size of 40×40×160 mm prisms were tested by conducting a three-point bending strength test. The test machine was ALPHA 3/3000S at a constant loading rate of 0.06 kN/s. Whereas for concrete, prisms of 70×70×250 mm have been tested by a three-point bending test.

3.5 Thermogravimetric program

TG investigation defines the ranges of various thermal decompositions of different hardened paste products and phases with simultaneous estimation of the mass loss in static condition. Moreover, changes in phases are controlled by means of TG/DTG/DTA using MOM Derivatograph-Q 1500 D TG/DTA instrument, **Figure 3.8**.

Figure 3.8 *Derivatograph Q-1500D*

During the measurements, Al_2O_3 is the reference material with a mass of 300 mg. The heating rate of samples was 10 ºC min-1 up to 1000 ºC in air atmosphere. Thermo-gravimetric samples are ground to a fine powder and measured by TG/DTA to ensure the soundness of samples from carbonation. The tested powders were taken from specimens of ambient temperatures 20 °C and selected from the core of specimens. The investigated powders are taken from the samples that showed high performance after exposure to elevated temperatures (optimum replacements of SCM), as well as the mixtures of pure OPC (reference) for the comparison. In the case of the thermo-analytical test results are determined by Winder software (Version 4.4). The TG/DTA studies were carried out when the samples have the age of 90 days.

3.6 Physical and microstructure properties

Investigating the spatial distribution and the internal pores volume of the cement paste or concrete is a key factor in understanding the transport phenomena influencing its heat resistance. Furthermore, the concrete microstructure has a remarkable effect on the other properties of concrete *(Lublóy et al., 2017).*

3.6.1 Computed Tomography (CT) study

The examination of permeability, pores, and pore size distribution of hardened cement paste can be obtained by using the CT method *(Lublóy et al., 2015; Balázs et al., 2017)*. The CT tests were carried out by a Siemens Somatom 16 device at the Diagnostic and Oncoradiology Institute of Kaposvar University in Hungary **Figure 3.9**. The thicknesses of slices were 1.5 mm and the pixel spacing was 0.225 mm. The CT slices were processed by automated algorithms in Matlab environment using predefined parameters without any user interaction *(Lublóy et al., 2019)*.

CT measurements have been carried on cylindrical specimens with a diameter of 100 mm and a height of 50 mm for the reference and SCM mixtures. The test results with CT are intended to demonstrate porosity and pore distributions through HSCS with and without SCM. The pores content was determined as the sum value of slices pores along the vertical axis of the sample.

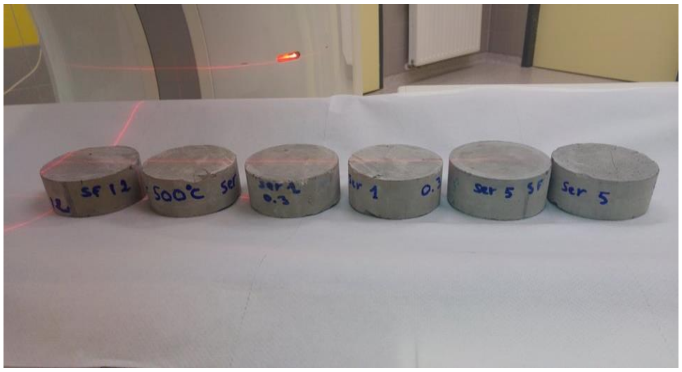

Figure 3.9 *Specimens under CT investigation*

3.6.2 Scanning electron microscope (SEM)

Scanning electron microscope investigations have helped to discover and understand the microstructure of hardened cement paste as well as the interfacial transition zone of concrete, using Phenom XL SEM (**Figure 3.10)**, in the lab of Budapest university.

SEM offers greater magnification, and resolution to the microstructural level of the modified HSCP *(Tam et al., 2020)*. The tested samples were prepared with a smooth viewing face in order to obtain a better image resolution. SEM images were taken of the reference samples and mixture containing SCM. After the compressive strength tests, the samples have taken from the core of the cross-sectional areas of the specimen, then the samples faces were coated with golden spray for 30 s in a vacuum chamber (**Figure 3.10 b**) and thereafter, the samples are investigated under SEM (**Figure 3.10 a**).

3.7 High strength concrete mixtures

In order to find a correlation between the hardened cement paste and concrete mixtures, concrete mixtures have been prepared and tested after elevated temperatures. The ITZ of aggregate and hardened cement paste in the presence of SCM is provided herein as well.

a) b)

Figure 3.10 *Phenom XL desktop SEM: a) SEM, and b) vacuum chamber*

CHAPTER 4: RESULTS OF DIFFERENT TYPES OF SCM

This chapter presents the results of the experimental plan for producing HSCP with the use of different supplementary cementitious materials in different replacements. The results are presented in three main groups depending on the type of SCM used. Each section contains the presentation, analysis, and discussion for the results of the tested properties.

The interest of enhancing the concrete performance at elevated temperatures has been raised up as a result of the extensive damages, partially or totally, especially high-rise buildings, tunnels, and many other structures *(Hoff et al., 2000)*. Additionally, SCM significantly enhances the concrete's resistance of aggressive environments exposure and fire accidents *(Chan et al., 1996; Hoff et al., 2000)*. According to the fact that binder is one of the main ingredients that affect the mechanical behaviour of concrete exposed to elevated temperatures, significant importance has attributed to the SCM as replacement material of the ordinary cement *(Xu et al., 2001; Khoury et al., 2007; Aydın, 2008; Tanyildizi et al., 2008; Wang, 2008; Morsy et al., 2010)*.

In general, the characteristics of MK, SF, and FA refer to have a good indication for the sustainable development of green and high temperature resistant concrete. The presented results were performed to obtain the optimum dosage of MK, SF, and FA replacements at a given w/b ratio in HSCP exposed to elevated temperatures. Short incremental replacements with 3% replacement were chosen to provide more accuracy to the results.

4.1 Influence of MK using CEM I 42.5 N

Different properties of HSCP mixed with MK depend mainly on many factors, such as w/b ratio, properties of MK, mixing program and procedures, initial cement content, the amount and type of plasticisers and other admixtures. The compressive strength values of HSCP specimens are graphically represented as a function of MK replacements in **Figure 4.1.**

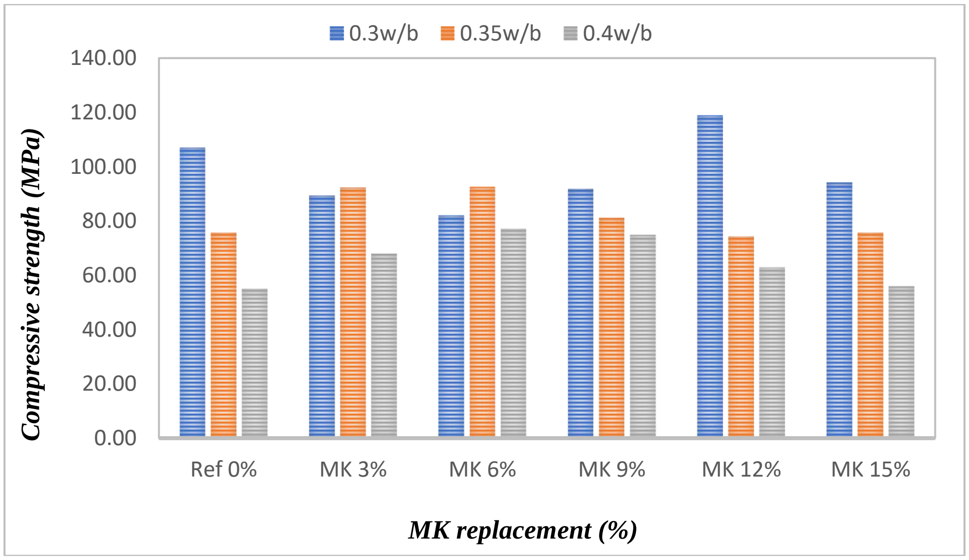

***Figure 4.1** Compressive strength of different MK replacement with respect to w/b ratio*

The results are prepared with different w/b ratio, in which for mixtures prepared by 0.3 w/b, the mixture that contains 12% of MK shows the highest compressive strength with 118.94 MPa, compared to the other MK replacements. On the other hand, the mixture of 6% of MK has the highest value for both mixes of 0.35 and 0.4 w/b ratio, as far as compressive strength is concerned. MK increases the strength of the so-called pozzolanic reaction, packing effect, and increasing the interfacial zone between cement particles *(Ramezanianpour and Jovein, 2012)*.

4.1.1 Impact of different MK replacements on surface cracking

Specimens during temperature loading undergo chemical and physical changes leading to surface cracks. Developing surface cracks as a result of the elevated temperatures is presented in **Figure 4.2**. There were no macroscopic observable changes on the cubes surface up to the maximum temperature of 400 °C. This observation is also valid for the reference specimens (0% MK). However, the number and size of cracks grow with heating up to 900 °C for the reference mixtures. The more amount of MK the smaller number of cracks. From the other hand, specimens with a low w/b ratio show fewer cracks than specimens with higher w/b ratio at the same MK levels. That is obvious after exposure to elevated temperatures i.e., 800 °C. On the contrast, specimens with low w/b are more prone to sudden spalling. After cooling down, more cracks are noticed in the surface of specimens. The reason for this phenomenon is the rehydration of CaO which could considerably increase the extent of the crack development with further changes in volume.

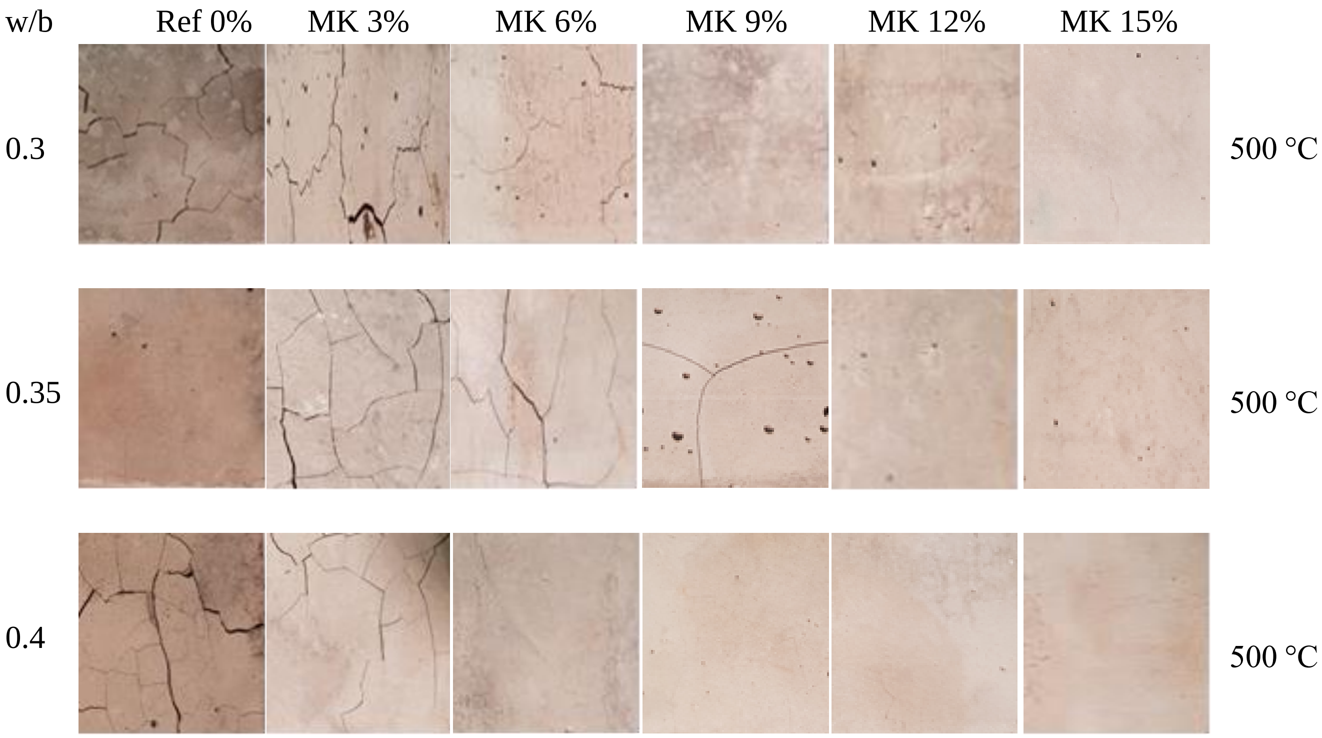

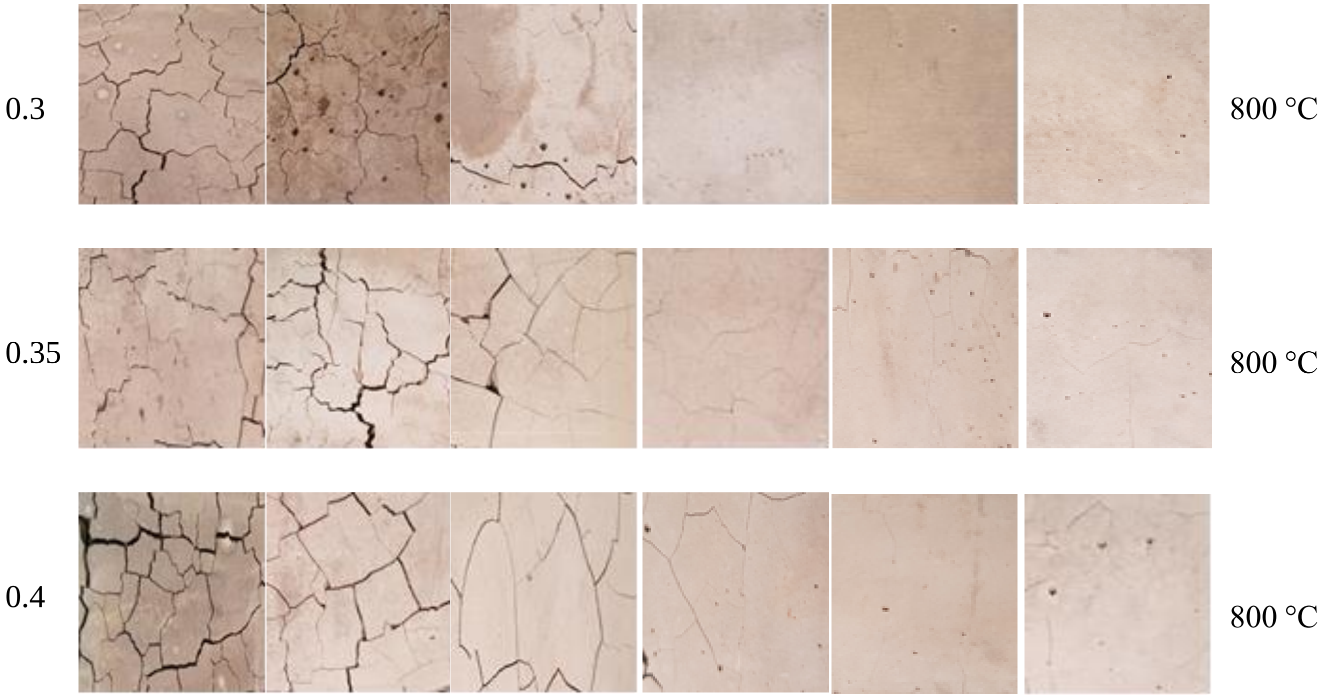

***Figure 4.2** Effect of MK dosages and w/b ratio on the development of surface cracks as a result of the elevated temperature (scale of photo x=30 mm, y=30 mm)*

4.1.2 Relative residual compressive strength (RRCS) for mixtures of different MK replacements

The residual mechanical properties of HSCP (compressive strength and bending strength) after temperature loading are presented in this section. The results of the compressive strength tests in a function of temperature are considered as the average of three measurements and given in the form of relative residual compressive strength (RRCS). The RRCS is expressed by the division of the residual strength for each single temperature degree to residual strength of the same mixture at 20 °C. Besides, heat resistance method is adopted from the previous study *(Fehérvári and Nehme, 2009b)*. This could help to clear the complexity of curves by the calculation of the area under each curve (20 °C–900 °C).

Figure 4.3 shows the development of RRCS for all mixtures with 0.3 w/b, and the tendency of RRCS with all-temperature levels is almost similar. Most of the curves begin to slightly decrease after 50 °C. Yet, some mixtures start to show sharp degrading after 400 °C (**Figure 4.3**). Moreover, MK content has a significant influence on RRCS. By comparing various types of the studied mixtures, it can be observed that the mixture that contains 9% of MK shows the highest RRCS (76%) among the other five replacements at 500 °C with a slight reduction in the relevant RRCS at 800 °C to reach 60%.

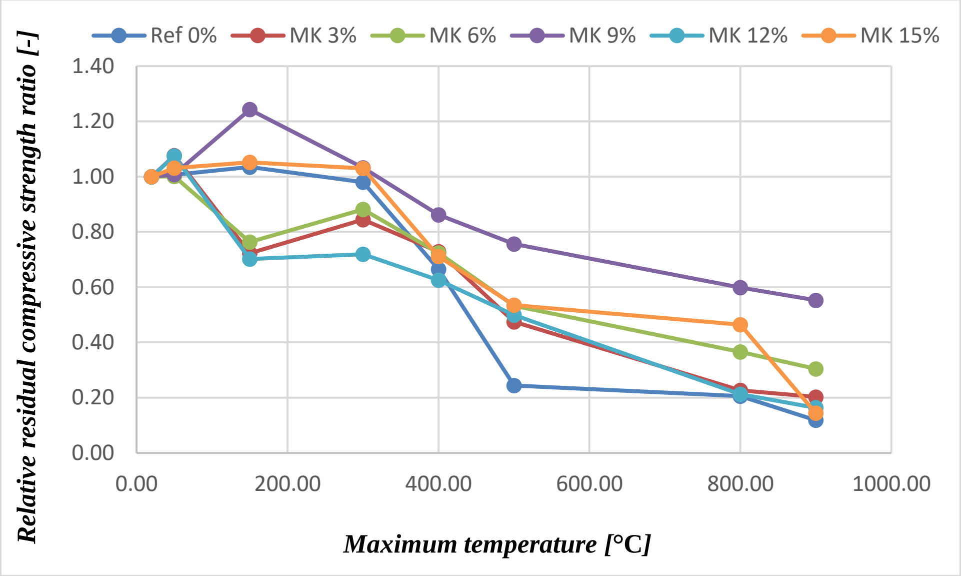

Figure 4.3 *Relative residual compressive strength of HSCP as function of temperature and MK replacements for 0.3 w/b*

In case of the reference mixture (0% of MK), specimens suffer more after 400 °C exposure, showing the lowest RRCS with 24% and 21% after exposure to 500 °C and 800 °C, respectively. whereas the RRCS of the other mixtures is increased by increasing MK content. The intensity of $Ca(OH)_2$ is decreased as MK amount increases, and this could be a part of the reason why RRCS of MK 9% is higher than the others, in which the $Ca(OH)_2$ acts as the arrow that destroys the mechanical and physical properties of hardened cement at elevated temperatures. Notwithstanding, specimens with the higher replacement of MK exhibit a considerable loss in strength after exposure to elevated temperatures. This could be due to high dense microstructure, clinker dilution effect, or heating rate *(Poon et al., 2001b; Poon et al., 2003; Hager, 2013; Nadeem et al., 2013)*. *Poon et al. (2003)* investigated the porosity by using mercury intrusion porosimetry method proposing that MK densifies the microstructure at elevated temperatures, suggesting also that the high dense microstructure as a reference to the high surface area leads to form large pore area fraction at elevated temperatures in the presence of vapour. Furthermore, the increase in pore pressure induces internal cracks.

Figure 4.4 shows the RRCS results of all mixtures prepared with 0.35 w/b ratio after elevated temperatures. The reference mixture still shows a sharp decrease in the RRCS at elevated temperatures showing an RRCS of 34% and 26% after exposure to 500 °C and 800 °C, respectively. Nevertheless, the mixture containing 12% of MK shows a noticeable improvement, in which the RRCS is 88%, and 64%, after exposure to 500 and 800 °C, respectively.

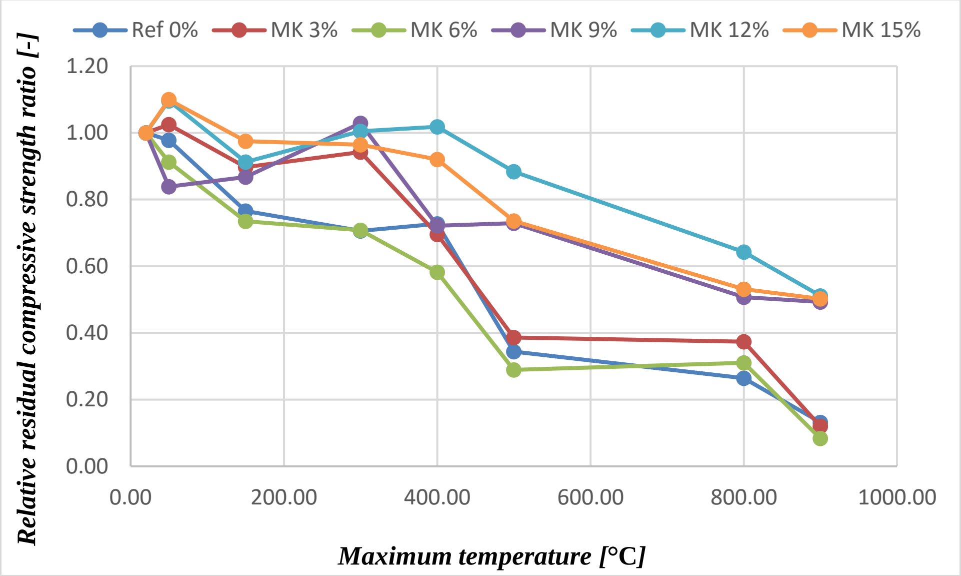

Figure 4.4 *Relative residual compressive strength of HSCP as a function of temperature and MK replacements for 0.35 w/b*

Figure 4.5 presents the results of all mixtures with 0.40 w/b after exposing to elevated temperatures. The RRCS of the reference mixture is 43% and 22% after exposure to 500 °C and 800 °C, respectively. By including MK, the mixture containing 12% of MK shows less loss in RRCS compared to the other mixtures. The average of the RRCS for the same mixtures is 64% by heating up to 500 °C and a further 54% by heating up to 800 °C.

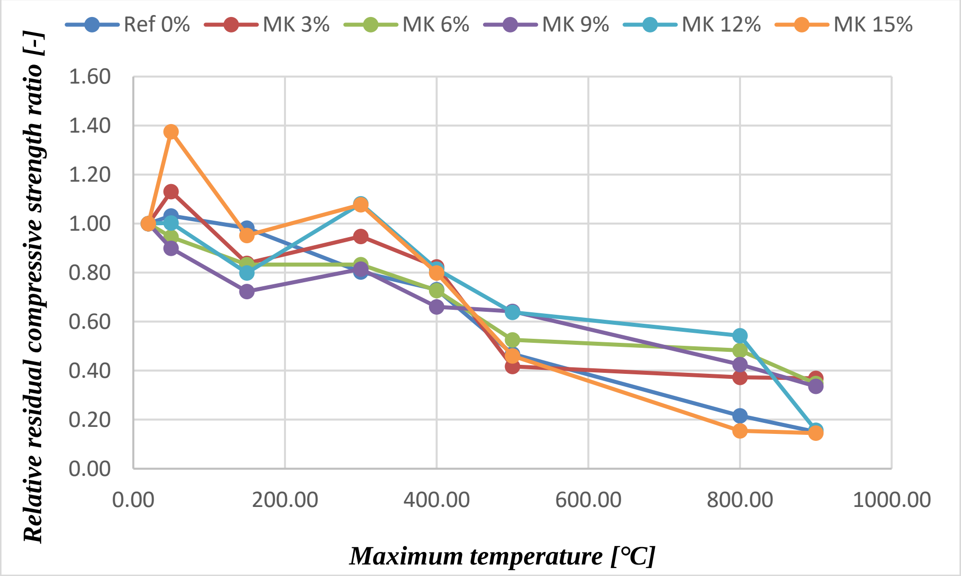

Figure 4.5 *Relative residual compressive strength of HSCP as a function of temperature and MK replacements for 0.4 w/b*

From another hand, microcracks are formed on mixtures that contain a high amount of MK, because of the fineness of MK which decreases the amount of water. The filling effect of particles leads to make a discontinuity of pores (pore-blocking effect) and densifying the microstructure, which could adversely affect the microstructure at elevated temperature by the vapour pressure effect *(Wild et al., 1996; Poon et al., 2003; Khatib and Clay, 2004; Nadeem et al., 2013)*. Inversely, the increase in the w/b ratio work opposite of MK by increasing the porosity and allowing the use of more MK amount, explaining why MK 12% was an optimum ratio for mixtures with 0.35 w/b, whereas it was shifted to 9% for mixtures with 0.3 w/b.

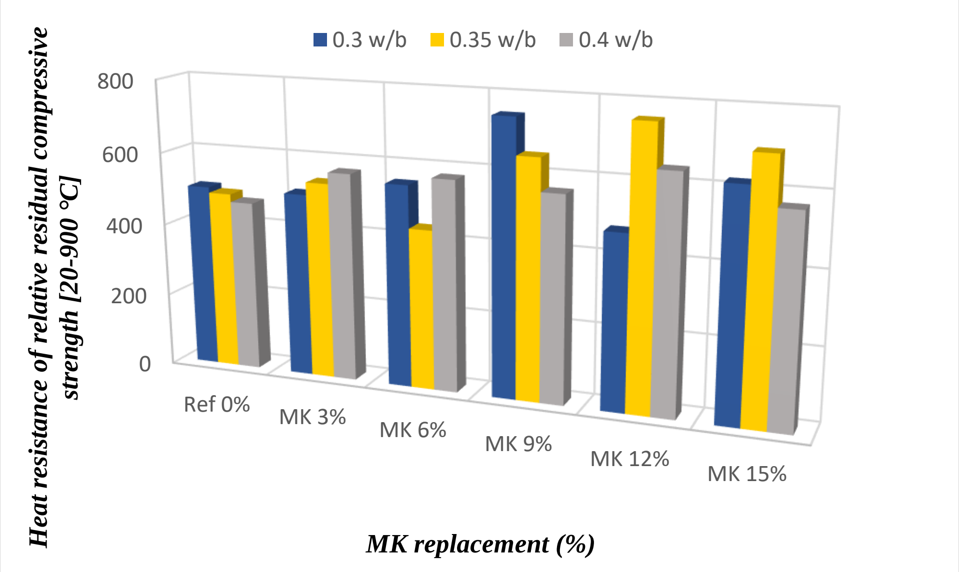

***Figure 4.6** Heat resistance results of all MK mixtures with the three w/b ratios*

Regarding the heat resistance for all MK mixtures, results are presented in **Figure 4.6.** Heat resistance is generally improved with the use of MK. The heat resistance of the mixtures containing 9%, 12%, and 12% of MK for the w/b ratio of 0.3, 0.35, and 0.4, respectively, have shown the highest heat resistance, which improved the heat resistance, compared to reference mixture, by about 152%, 155%, and 137%, respectively.

The loss of mass of the reference sample and sample containing MK have been investigated by TG/DTA analysis. Results are presented in **Figures 4.7**. During the thermo-analytical test, several heat reactions take place on hardened cement paste between temperature ranges of 20–1000 °C. As illustrated in the figure, different endothermic peaks were observed i.e., 20–200 °C, 430-540 °C, and 600-900 °C. The loss of mass appeared in the first peak is wide which could be mainly due to the evaporation of physically combined water, dehydration of ettringite ($C_3A.3CaSO_4.H_{32}$), and dehydration of mono-sulphate ($C_3A.CaSO_4.H_{12}$). The second endothermic peak (430-540 °C) corresponds to the decomposition of $Ca(OH)_2$ *(Lublóy et al., 2017)*. The third endothermic peak corresponds to the decomposition of CSH sheets and calcium–carbonate ($CaCO_3$) compounds. The amount of $Ca(OH)_2$ and the amount of $CaCO_3$ in the hardened cement paste are responsible for the deterioration of residual compressive strength *(Lublóy et al., 2016; Balázs et al., 2018)*.

Incorporation of MK increases the mass loss due to evaporation of moisture this performance could be related to the high content of physically combined water as a reference to the high specific surface area of MK. As shown in the **Figures 4.7**, the mixtures containing MK show less loss of mass due to the dehydration of $Ca(OH)_2$ between 430 °C and 540 °C, in which MK consumes $Ca(OH)_2$ crystals and produces additional strength. In the last stage of heating (third peak) the loss of mass corresponds to the decomposition of $CaCO_3$ is decreased in the case of samples containing SCM. These outcomes are, consequently, the main reasons for the better performance exhibited by mixtures containing MK after exposure to elevated temperature. Worth to mention that results of the TG/DTA are presented for the reference and optimum mixtures only.

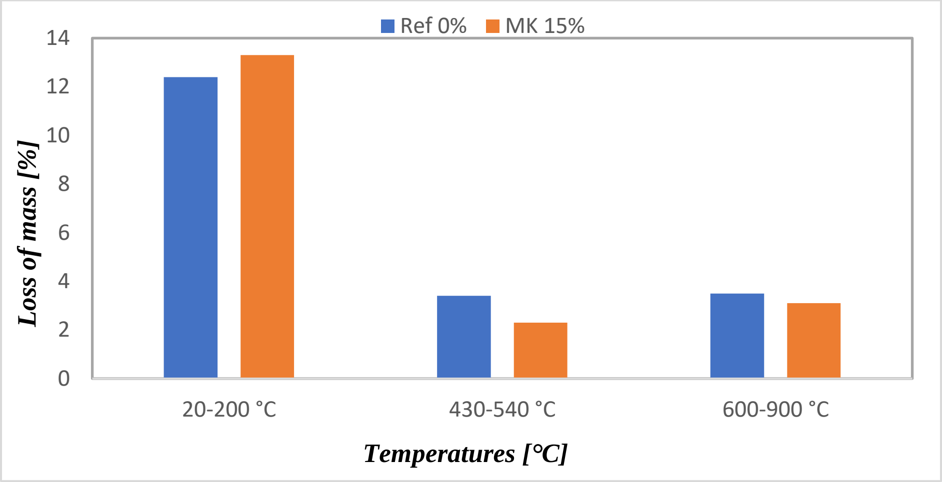

Figure 4.7 *Loss of mass of different phases of MK sample using TG/DTA*

The SEM images of the HSCP of the reference mixture and mixture containing MK at 20 °C and after exposing to 500 °C are presented in **Figure 4.8**. In case of results at 20 °C, the reference sample contains a high content of $Ca(OH)_2$ in hexagonal shapes in addition to rods of ettringite. In contrast, hardened paste contains MK showed high contents of CSH and CASH especially for MK, in addition to the presence of $Ca(OH)_2$. The physical property at ambient temperatures paste contains MK showed denser microstructure than the reference cement paste.

The presented SEM images at 500 °C, the reference mixture have shown a lot of pores and destruction in the microstructure at elevated temperatures. In case of cement paste contains MK still show denser microstructures than the reference at elevated temperatures. This is due to the higher reaction of $Ca(OH)_2$ with the pozzolanic materials that lead to the formation of more crystalline products. Thus, filling and making refinement of pores in addition to keeping the structure coherent. The major problem causing the deterioration of cement paste at elevated temperatures is the decomposition of $Ca(OH)_2$, in which its presence in the reference cement paste reaches about 28% of its weight *(Sabir et al., 2001)*. Therefore, the cement pastes blended with MK exhibited higher capacities than the reference cement paste.

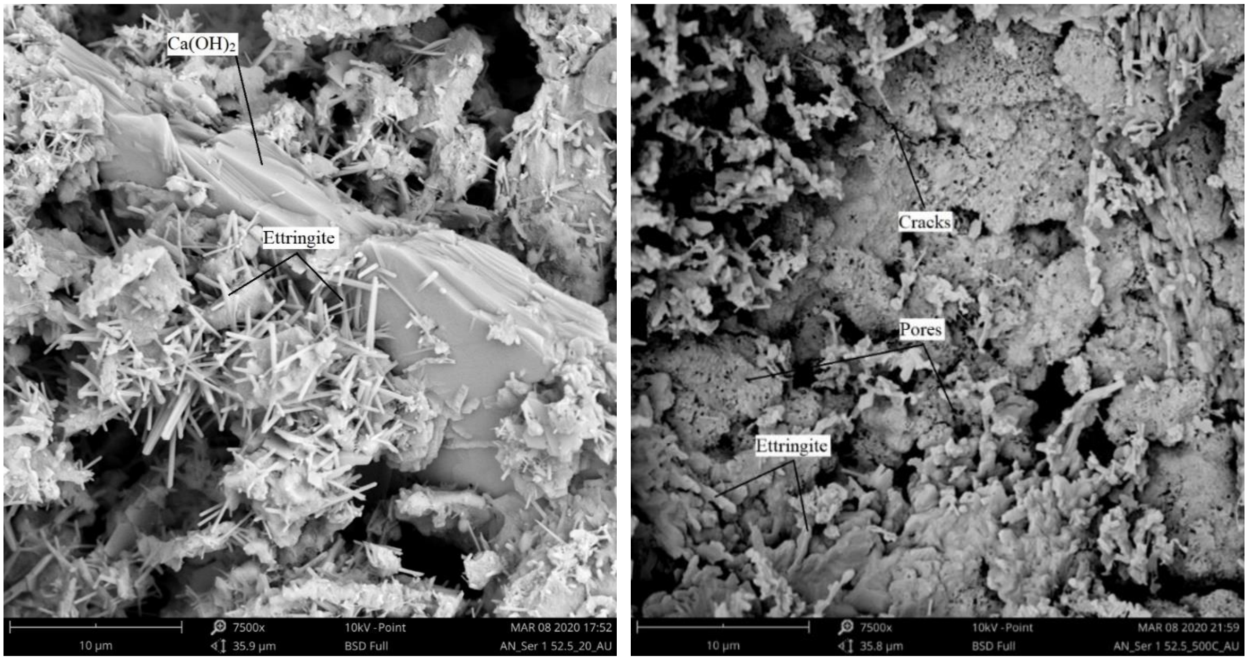

OPC cement paste ‘reference’ at 20 °C OPC cement paste ‘reference’ after exposure to 500 °C

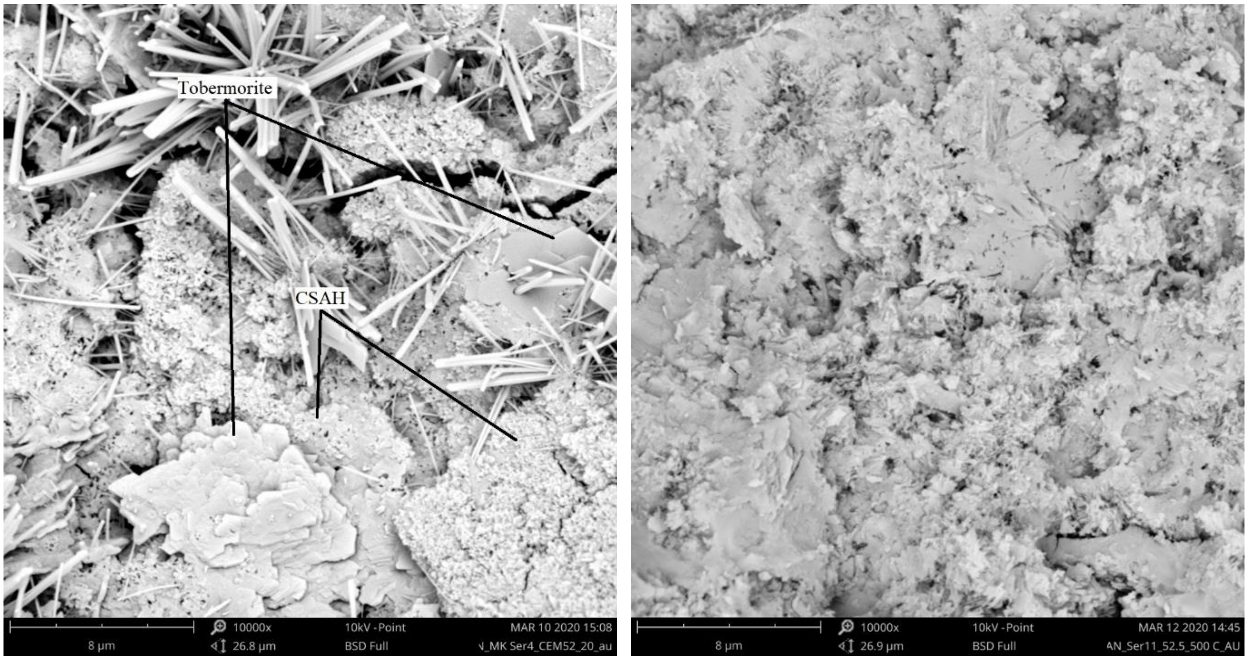

Cement paste with MK at 20 °C Cement paste with MK after exposure to 500 °C

Figure 4.8 *The SEM images of microstructures of reference mixture and mixture contains 9% of MK replacement at 20 °C and 500 °C for the optimum replacements*

4.1.2 Relative residual bending strength (RRBS) for mixtures of different MK replacements

Hardened cement paste is characterized by weak resistance to bending loads, showing typically resistance between 3 to 10 MPa. Studying the hardened cement properties are usually confined to the compressive strength. However, some studies that investigated the bending properties have considered bending property of concrete possess major weakness of hardened cement paste, due to the porous structure *(Birchall et al., 1981)*. Additionally, pozzolanic materials are an appropriate material and played important role in the properties of hardened paste such as physical filling of the pores and pozzolanic action *(Koksal et al., 2015)*.

The relative residual bending strength (RRBS) of all mixtures is decreased with increasing temperatures, especially after 300 °C regardless of the type of w/b ratio. **Figure 4.9** shows the RRBS of mixtures with 0.3 w/b ratios. The values of RRBS of all mixtures that contain MK are higher than values from the reference mixture. The reference mixture shows almost zero RRBS values at 400 °C. But using 9% and 12% replacements of cement by MK improve the RRBS in all temperature levels, showing RRBS values of 48% and 49% after exposure to 500 °C, and 43% and 49% after exposure to 800 °C, respectively. Previous studies reported that the bending strength increases by increasing MK amount between 10% and 15% replacements *(Kim et al., 2007)*.

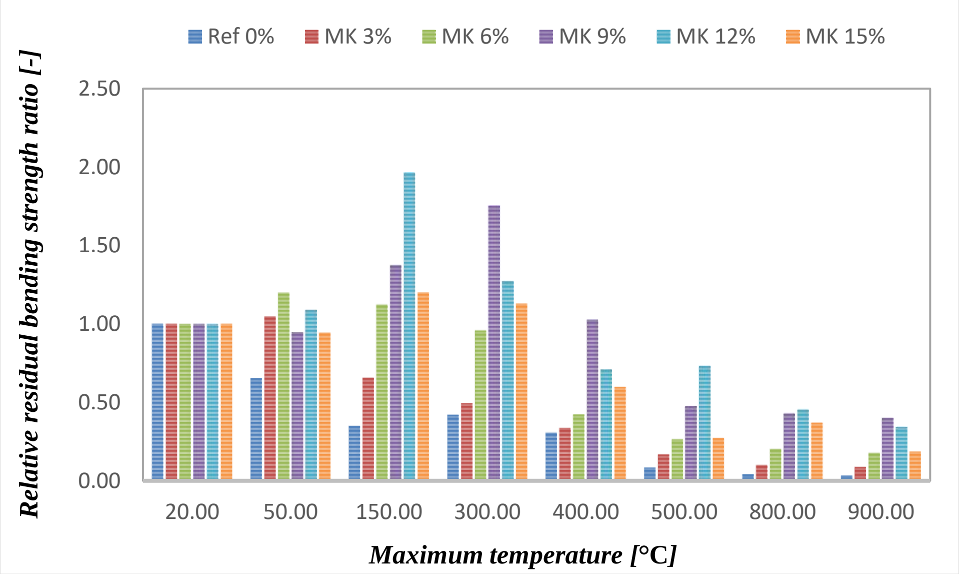

Figure 4.9 *Relative residual bending strength as a function of the temperature of mixtures incorporated with MK of 0.3 w/b*

Figures 4.10 shows the results of RRBS for all MK mixtures of 0.35 w/b ratio. After elevated temperatures, the mixture containing 12% of MK replacement shows the highest values of RRBS, similar to the trend observed for residual compressive results. However, 12% of MK could be accepted as an optimum replacement from the perspective of elevated temperature resistance, showing RRBS values of 72% and 52% after exposure to 500 °C and 800 °C, respectively.

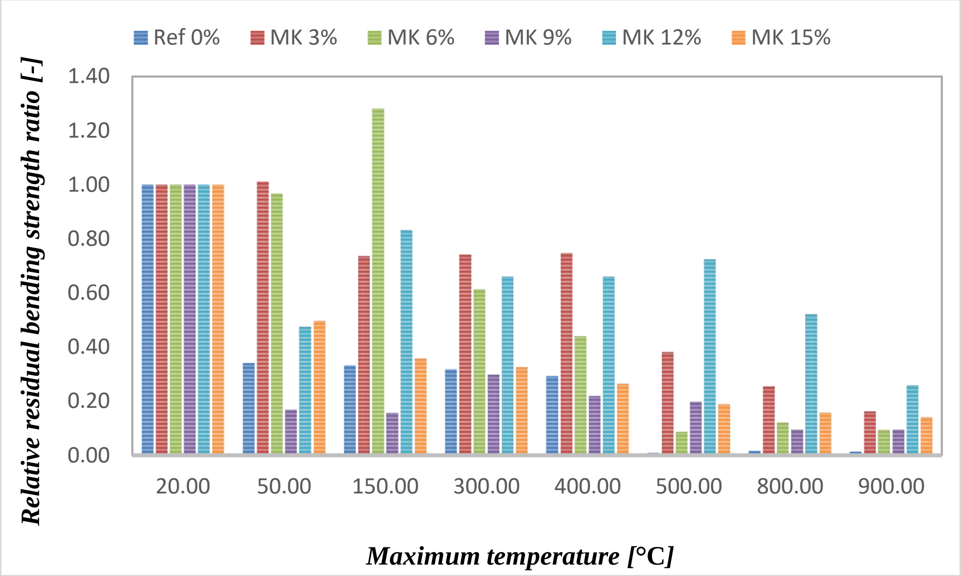

Figure 4.10 *Relative residual bending strength as a function of temperature of mixtures incorporated with MK of 0.35 w/b*

Figure 4.11 presents the RRBS for all MK mixtures of 0.4 w/b. Adoption of 12% of MK shows the highest RRBS, thus 12% of MK could be accepted as an optimum replacement from the perspective of elevated temperature resistance. However, the mixture containing 6% of MK shows relatively similar behaviour to the mixture containing 12% of MK after exposure to elevated temperatures. Therefore, from the perspective of the stability in all temperature levels and from the quantity of MK to cement replacement, 12% of MK is considered as the optimum replacement.

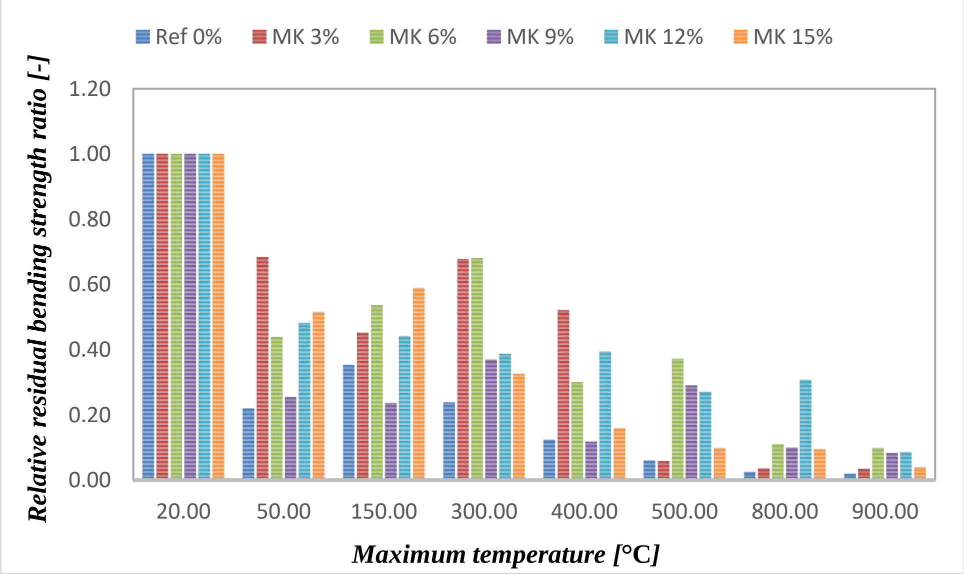

Figure 4.11 *Relative residual bending strength as function of temperature of mixtures incorporated with MK of 0.4 w/b*

Figure 4.12 presents the heat resistance of all mixtures of the three w/b ratios, using 12% of MK increases the heat resistance regardless of the type of w/b ratio. The efficiency by adding MK on the RRBS with the elevation of temperatures has been observed. In addition to the autoclaving and filling effects, presence of MK performs as fibres in the cement mixture microstructure that helping to bridge the micro-cracks in the microstructure *(Morsy et al., 2012)*. The pozzolanic reaction product, i.e., CSH compacts the structure of the matrix and fills the micro open pores thus enhancing the fire resistivity *(Heikal et al., 2013)*. Some results in the literature *(Khaliq et Khan, 2015)* reported that cement containing high Al_2O_3 content showed denser microstructure and minor fine cracks due to the presence of gibbsite (AH_3) gel covering and protecting the CASH crystals.

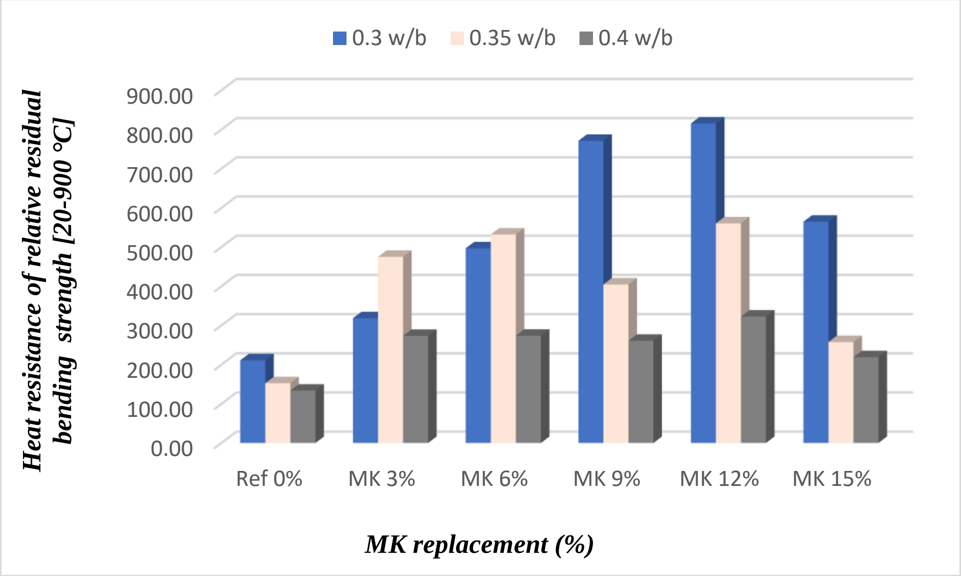

Figure 4.12 *Heat resistance results of all MK mixtures with the three w/b ratios*

4.2 Influence of SF using CEM I 42.5 N

The compressive strength of eighteen mixtures before heating is presented in **Figure 4.13**. HSCP mixtures containing the following SF replacements of 3%, 3%, and 6% for the w/b ratio of 0.30, 0.35, and 0.40, respectively, have shown the highest compressive strength values. This resulted in compressive strength values to reach 112.62 MPa, 109.86 MPa, and 91.47 MPa, respectively. This could be mainly due to the reaction of the hydration product of cement with SF caused the formation of CSH which contain a high content of SiO_2 *(Behnood and Ziari, 2008)*. As shown in **Figure 4.13**, considerable differences were observed in the compressive strength values as a result of changing w/b ratio.

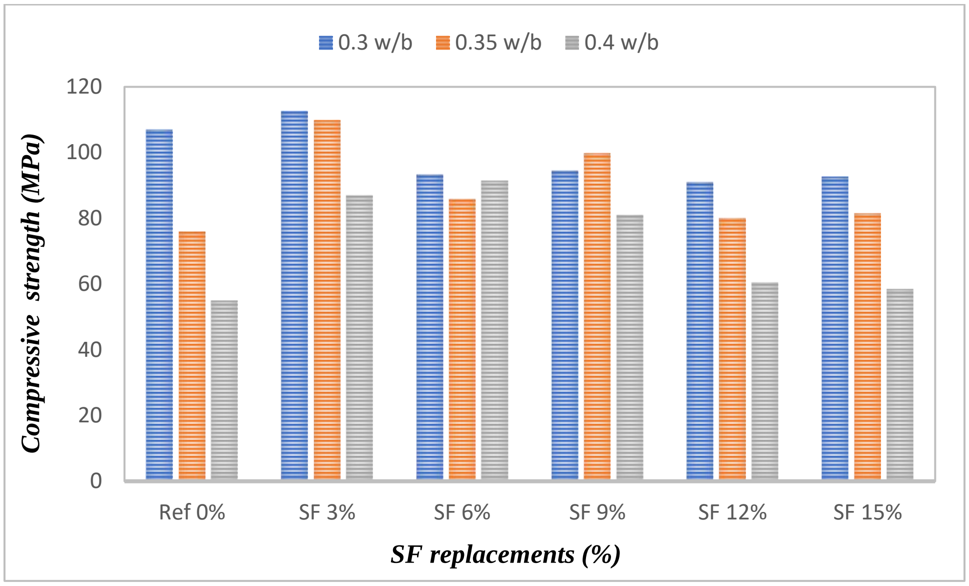

***Figure* 4.13** *Compressive strength of different SF replacement with respect to w/b ratio*

Furthermore, specimens containing the optimum SF replacement showed a higher value of compressive strength compared to the reference mixture especially those obtained in w/b ratios of 0.35 and 0.4. This could be attributed to the availability of moisture for the development of the pozzolanic reactions which is restricted at low w/b ratio. Eventually, it has been concluded that the gain of compressive strength based on SF replacements increases up to 9% replacement for all mixtures of w/b ratios of 0.35 and 0.40.

4.2.1 Relative residual compressive strength for mixtures of different SF replacements

Generally, the RRCS decreases after temperature exposure up to 150 °C because of the dehydration of cement product started from 60 °C (decomposition of ettringite). Then the residual strength increases up to 300 °C, this because of the hydration of the un-hydrated cement grains in the microstructure due to the movement of steam. Afterwards, (Above 300 °C), the residual strength decreases again *(Lubloy et al., 2016)*. **Figures 4.14, 4.15, and 4.16** show that strength improvement for SF mixtures is occurred with the increase of temperatures, particularly after 150 °C. This increase could be attributed to the fact that SF mixtures are enriched with fine particles in which the hydration of un-hydrated particles is more compared to the ordinary mixture. With an increase of temperature up to 500 °C, significant reductions occurred in the RRCS of cement paste without SF mainly due to the decomposition of portlandite ($Ca(OH)_2$) at this phase. As shown in **Figure 4.14, 4.15, and 4.16**, the RRCS values reached 24%, 34%, and 40% at 500 °C for 0.30, 0.35, and 0.40 w/b ratio, respectively.

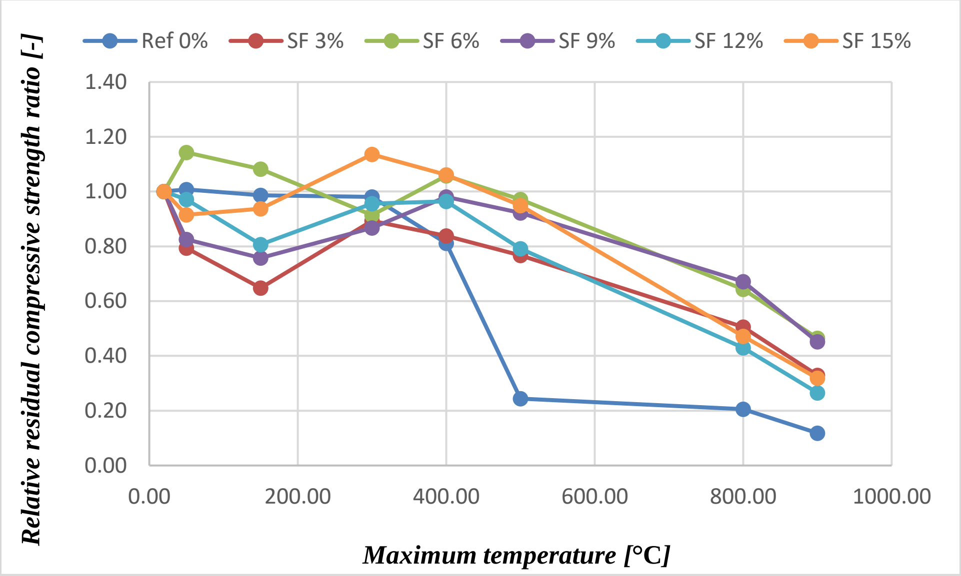

Figure 4.14 *Relative residual compressive strength for different SF replacements with 0.3 w/b at different temperatures exposures*

On the other hand, the RRCS values increase with the increase of the amount of SF. For specimens prepared by w/b ratio of 0.30, the RRCS values of specimens containing 6% and 9% of SF were 97% and 92% after heating to 500 °C of ambient-temperature strengths, respectively. Test results showed that the RRCS have decreased up to 64% and 67% for 6% and 9% replacement, respectively after heating to 800 °C as shown in **Figure 4.14**. Moreover, using more than 9% replacement of SF at elevated temperatures, results showed a decrease in the RRCS that may be due to the dense microstructure *(Poon et al., 2001b)*.

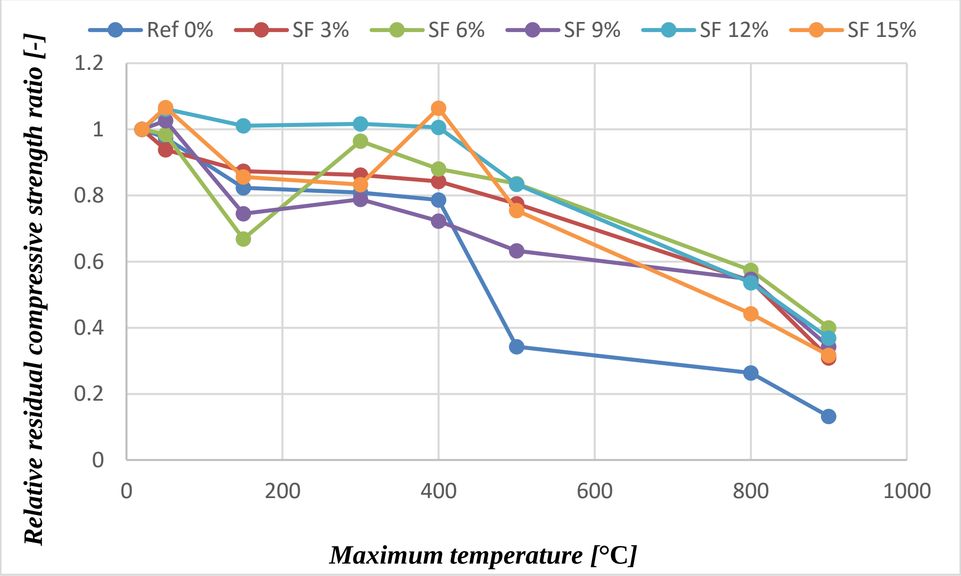

Figure 4.15 *Relative residual compressive strength for different SF replacements with 0.35 w/b at different temperatures exposures*

Results of SF made of 0.35 w/b ratio are presented in **Figure 4.15**. The RRCS of specimens contains 12% of SF were 84% and 53% after exposure to 500 °C and 800 °C, respectively. Adoption of 12% of SF has shown an enhancement on the resistance of hardened cement against elevated temperatures at changing the w/b ratio.

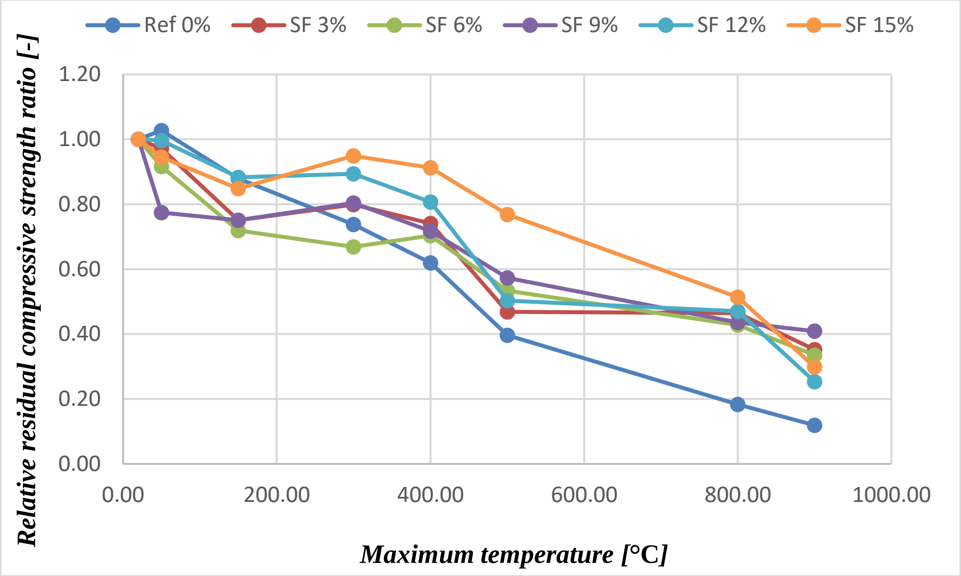

Figure 4.16 *Relative residual compressive strength for different SF replacements with 0.4 w/b at different temperatures exposures*

Figure 4.16 shows the RRCS of SF mixtures with 0.4 w/b. The mixture contains 15% of SF shows the highest value compared to other replacements. The RRCS values are 77% and 51% after exposure to 500 °C and 800 °C, respectively. Moreover, the heat resistance confirmed the better performance of the above-mentioned mixture of the three w/b ratios (6%, 12%, and 15% of SF) as shown in **Figure 4.17**. Using 6%, 12%, and 15% of SF for 0.3, 0.35, and 0.4 w/b ratios are considered as an optimum replacement as far as compressive strength is concerned.

From another hand, the results of the thermogravimetric test carried out on the reference mixture hand the mixture containing SF (SF 6%), are shown in **Figures 4.18**. Incorporation of SF increases the mass loss due to evaporation of moisture this could be related to the high specific surface area of SF particle. The loss of mass due to the dehydration of $Ca(OH)_2$ between 430 °C and 540 °C is less in case of mixtures containing SF, this because of pozzolanic reaction with $Ca(OH)_2$ crystals and producing additional strength. In the last stage of heating (third peak of 600 and 900 °C) the loss of mass due to the decomposition of $CaCO_3$ is decreased in the case of using SF. Therefore, the use of SF is producing an alteration in the level of chemical compositions, thereupon enhancing the behaviour of HSCP after exposure to elevated temperatures.

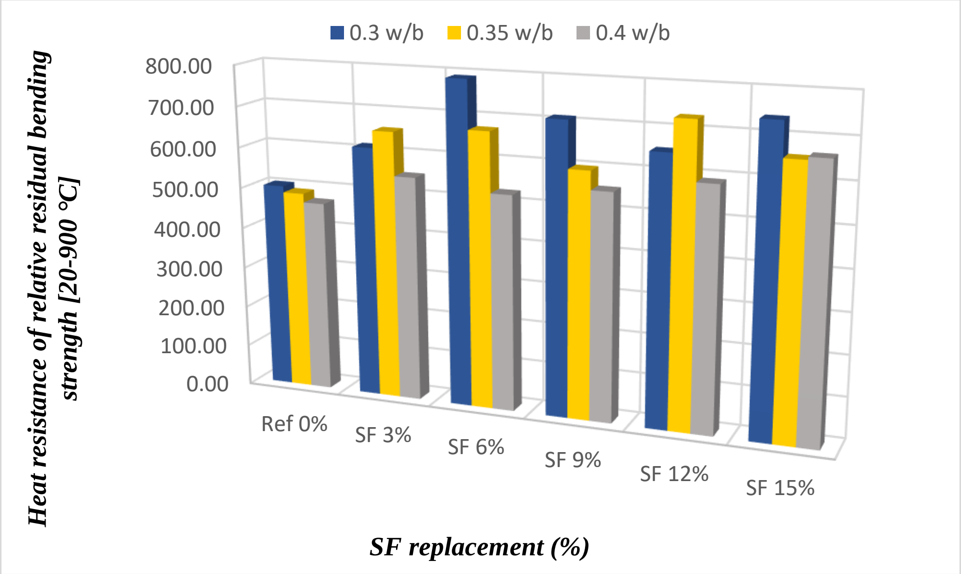

Figure 4.17 *Heat resistance results of all SF mixtures with the three w/b ratios*

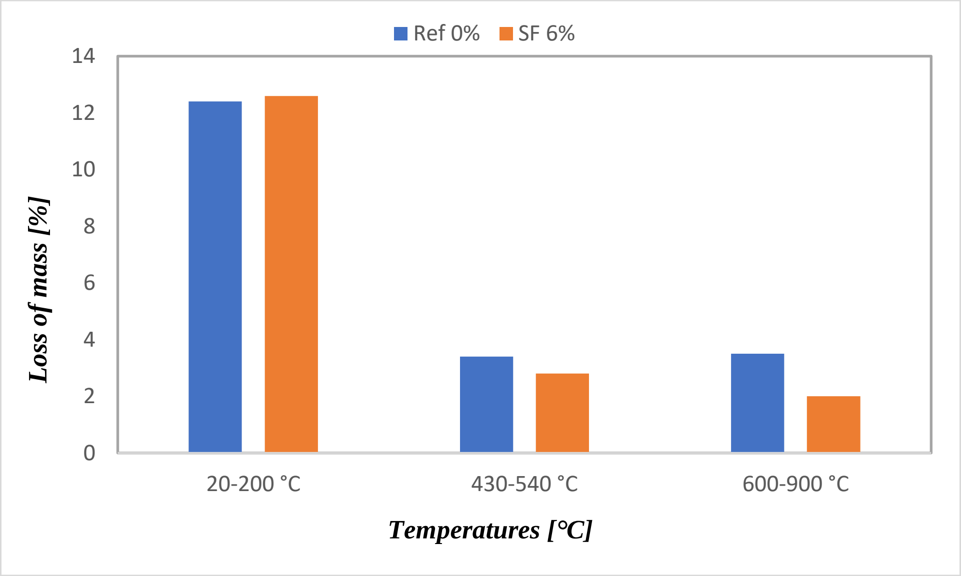

Figure 4.18 *Loss of mass of different phases of SF using TG/DTA*

The SEM images of the samples containing SF at 20 °C and after exposure to 500 °C, are presented in **Figure 4.19**. In case of results at 20 °C, using SF shows high contents of CSH and decreasing the hexagonal shapes of $Ca(OH)_2$ and showing denser microstructure than the reference cement paste (**Figure 4.8**). By increasing the temperature to 500 °C, the sample containing SF has shown coherent microstructure comparing to the reference sample that showed destruction and cracking due to ettringite and $Ca(OH)_2$. The enhancement added by SF is corresponding to the fineness of particles and could be the high content of SiO_2.

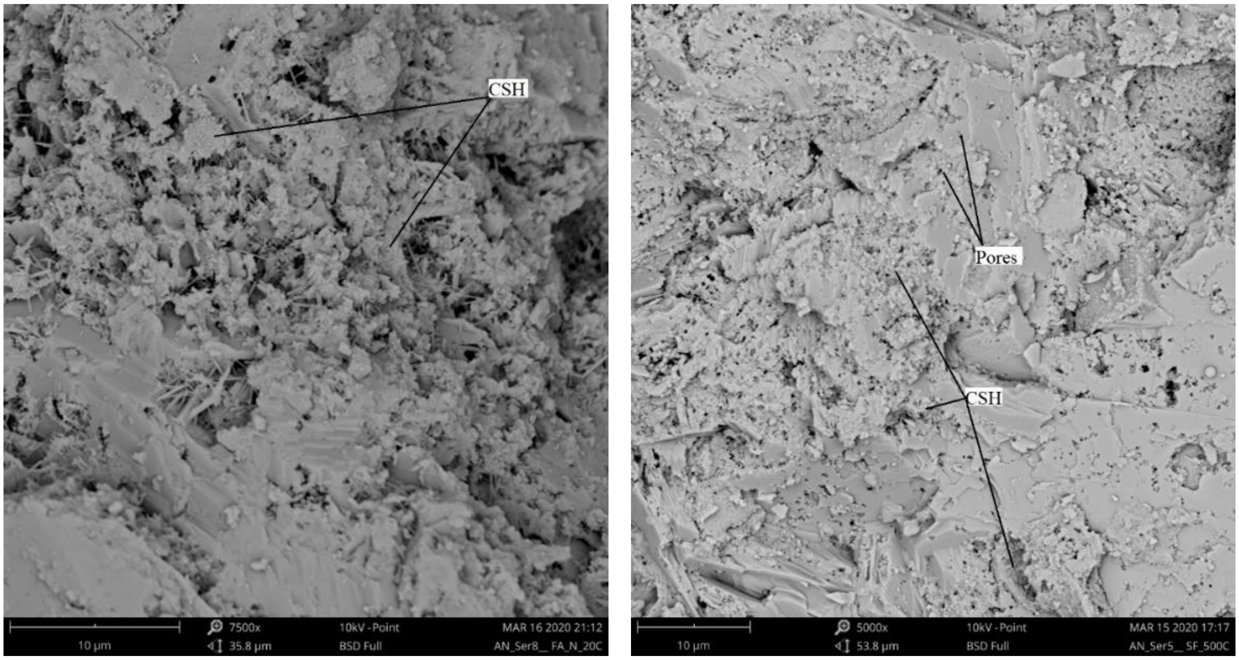

Cement paste with SF at 20 °C Cement paste with SF after exposure to 500 °C

Figure 4.19 *The SEM images of microstructures of optimum replacement of SF (6%) at 20 °C and* after exposure to *500 °C for 0.3 w/b ratio*

The porosity content and pore distribution were determined using CT. This method has high accuracy levels and could be used as an alternative method for other standard laboratory tests *(Lublóy el al., 2015)*. **Figure 4.20** illustrates the obtained results of pore distribution of the reference HSCP mixture at 20 °C, and the mixtures containing 6% of SF (at both levels of temperatures 20 and 500 °C), of at 20 °C. The pattern clearly shows a decrease in the amount of the pores at a sample containing SF. These results confirm the packing effect added to the hardened paste microstructure by SF. The total volume of the pores is also calculated in this study, in which the total volumes of the hardened cement pastes containing 6% of SF is 3.5% compared to the reference hardened cement paste that has a volume of pores about 5.93%.

By elevating temperature, the variety of the macro and microstructure changes is also investigated. The CT tests of SF sample is conducted to evaluate the improvement or alteration in the hardened cement paste body added by SF. Nevertheless, the CT analysis could not be conducted to the reference hardened cement paste after elevated temperatures because of a lot of disintegration that appeared within the body of the sample. The reason behind this could be due to the decomposition of $Ca(OH)_2$ and its rehydration with H_2O, resulting in several cracks and pores. By comparing results of the heated mixtures to the results obtained at 20 °C, the porosity volume has increased by around 5% due to temperature elevation. Yet, the sample still coherent compared to the disintegrated reference sample (0% of SF).

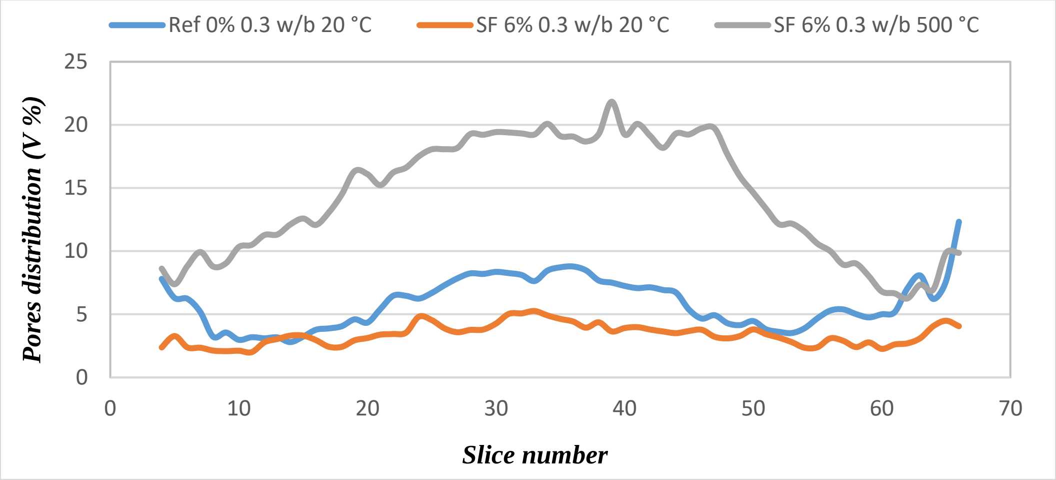

Figure 4.20 *The CT pores results of the reference mixture at 20 °C, and mixtures containing SF of 6% at 20 and 500 °C*

4.2.2 Relative residual bending strength for mixtures of different SF replacements

The variation in RRBS for different SF replacements of 0.3 w/b ratio are shown in **Figure 4.21**. The RRBS of hardened cement pastes is increased in the presence of SF replacements in all levels of temperature. The only exceptions are observed for the mixtures containing 12% and 15% which suffered after exposure to 500 °C. From the other hand, the reference mixture showed a significant degradation after 400 °C exposure. The RRBS of blended paste after exposure to 500 °C are 8%, 42%, 38%, 40%, 53% and 53% for mixtures contain 0%, 3%, 6%, 9%, 12%, and 15% of SF content, respectively. The increase in the RRBS could be due to the activating of hydration, which works as heat curing treatments, in addition to the physical filler of SF which contribute as fibre in paste structure. Furthermore, with the increase of temperatures up to 900 °C, the RRBS is decreased due to the dense microstructure and formation of micro-cracks in case of the high content of SF. Consequently, the spalling has been reported for the mixtures containing 12% and 15% of SF for temperatures above 800 °C. Moreover, the RRBS of other replacements of SF (3%, 6%, and 9%) slightly decrease with the increase of SF replacements after exposure to 500 °C, reaching the highest RRBS of 36% for the low replacement of 3% of SF after exposure to 800 °C. For the cement paste without SF, results showed a sharp loss of strength after exposure to 400 °C that RRBS reached 8% and 4% after exposure to 500 °C and 800 °C, respectively. The decrease in the RRBS from 450 °C to 550 °C is basically a common problem due to dihydroxylation of $Ca(OH)_2$, whereas above 600 °C is mostly attributed to the decomposition of $CaCO_3$ *(Morsy et al., 2012)*.

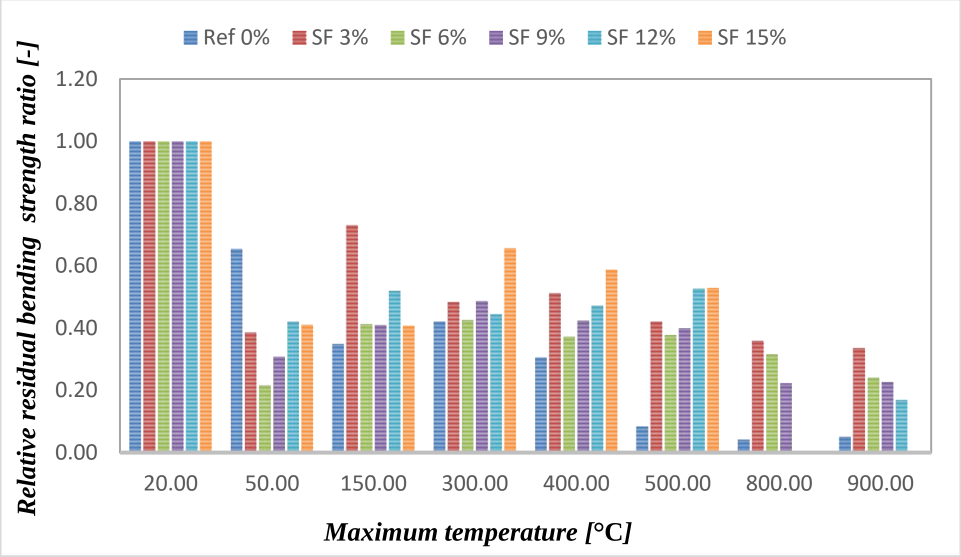

Figure 4.21 *Relative residual bending strength for different SF replacements with 0.3 w/b at different temperatures exposures*

The results of mixtures containing different SF replacements prepared by 0.35 w/b ratio are shown in **Figure 4.22**. Generally, using SF has shown a significant improvement after elevated temperatures exposure. The mixtures containing 3% and 6% replacements of SF have obtained the highest RRBS by 73% and 62% after exposure to 500 °C, and to reach 65% and 59% after exposure to 800 °C, respectively. Finally, spalling has been reported at 800 °C and 900 °C for replacement of 15% of the SF.

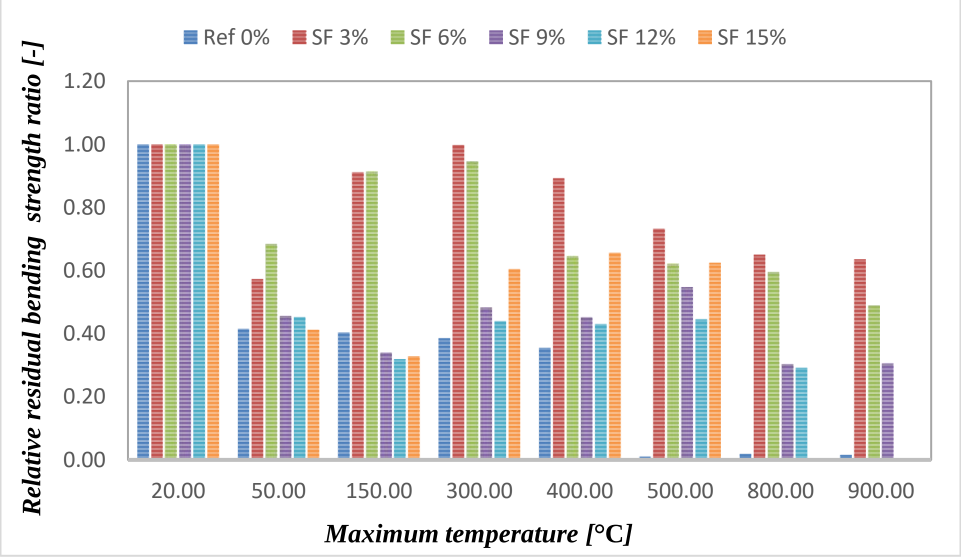

Figure 4.22 *Relative residual bending strength for different SF replacements with 0.35 w/b at different temperatures exposures*

Figure 4.23 shows the RRBS of SF mixtures with 0.4 w/b. The inclusion of SF increases the RRBS after the exposure to elevated temperatures, particularly above temperature 400 °C. Replacing cement by 3%, 6%, and 9% of SF exhibited the highest RRBS values with 89%, 86% and 82% after exposure to 500 °C. Then, it reaches 63%, 60%, and 60% after exposure to 800 °C, respectively. No spalling for all mixtures prepared by 0.4 w/b ratio has been reported.

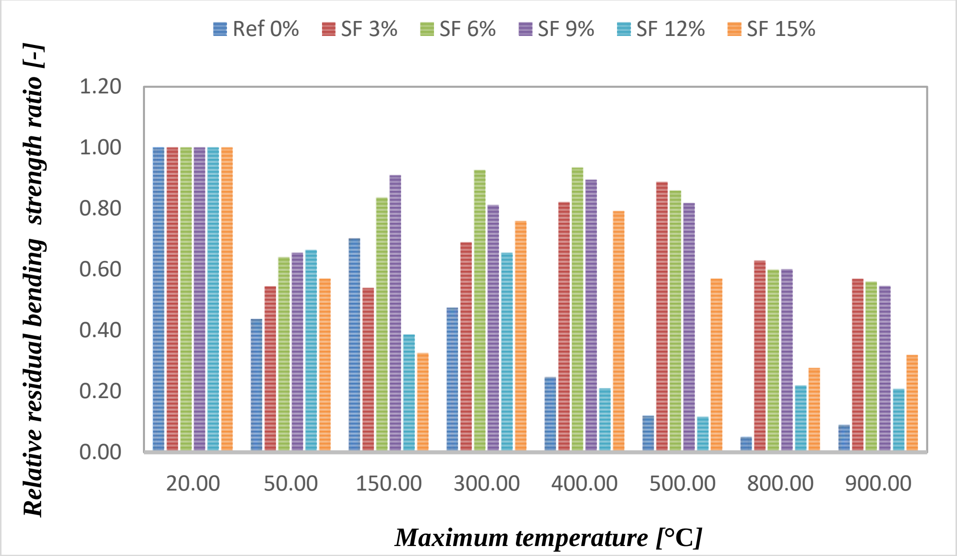

Figure 4.23 *Relative residual bending strength for different SF replacements with 0.4 w/b at different temperatures exposures*

Heat resistance was calculated and plotted in **Figure 4.24.** Mixtures containing 3%, 3%, and 6% of SF for the 0.3, 0.35, and 0.4 w/b ratio, respectively showed the highest heat resistance compared to the correspondence mixtures.

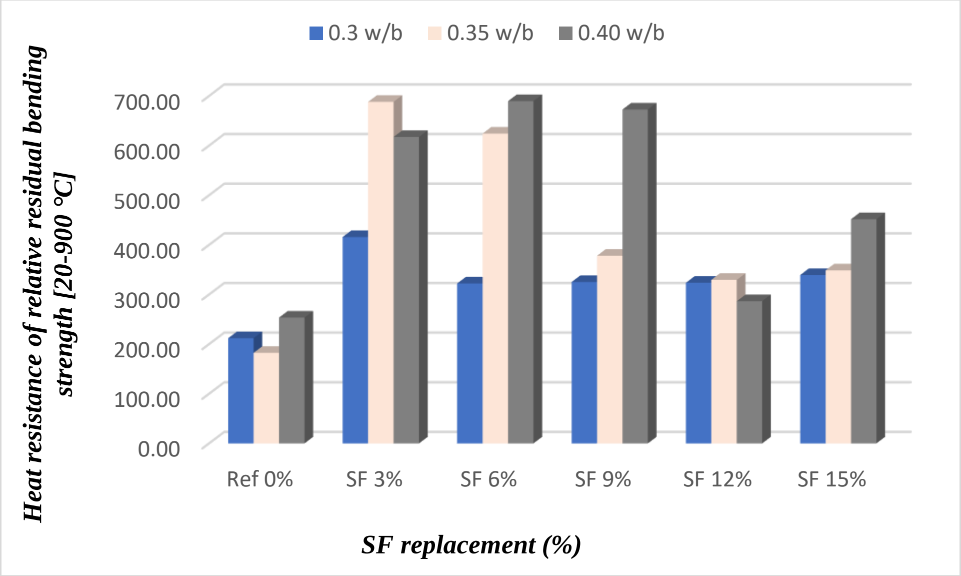

Figure 4.24 *Heat resistance of SF mixtures with the three w/b*

4.3 Influence of FA using CEM I 42.5 N

The compressive strength values for all mixtures related to FA are presented in **Figure 4.25**. It can be seen that there is an increase in strength for all mixtures containing FA.

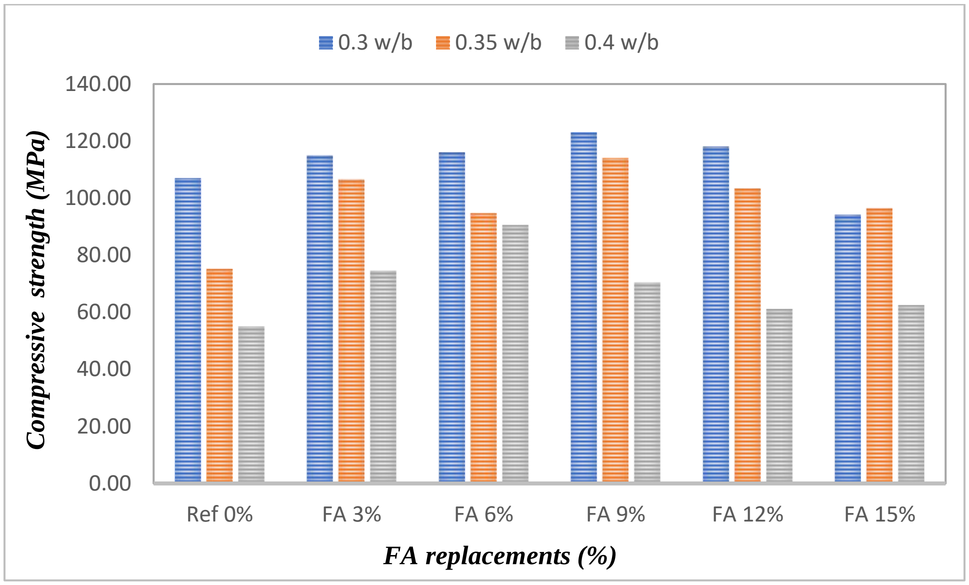

Figure 4.25 *Compressive strength of different FA replacement with respect to w/b ratio*

Compressive strength values are varied between 55 and 123 MPa with the variation of w/b ratio and FA replacements. Mixtures with replacements of 9%, 9%, and 6% for the w/b ratio 0.3, 0.35, and 0.4, respectively, are the optimum replacements as far as compressive strength is concerned. Showing values of 123, 114, and 91 MPa are, respectively.

4.3.1 Relative residual compressive strength for mixtures of different FA replacements

The RRCS results of all mixtures prepared with 0.3 w/b ratio after elevated temperatures are presented in **Figure 4.26**. Generally, the RRCS increase with the increase of FA incorporation. Furthermore, the inclusion of 15% of FA revealed the highest RRCS at all temperature levels, in which it improved the strength by 71% and 36% compared to the reference mixture (Ref 0%) after exposure to 500 °C and 800 °C, respectively. Worth to mention that the FA particles are spherical, hollow, and porous that help to show high heat resistance.

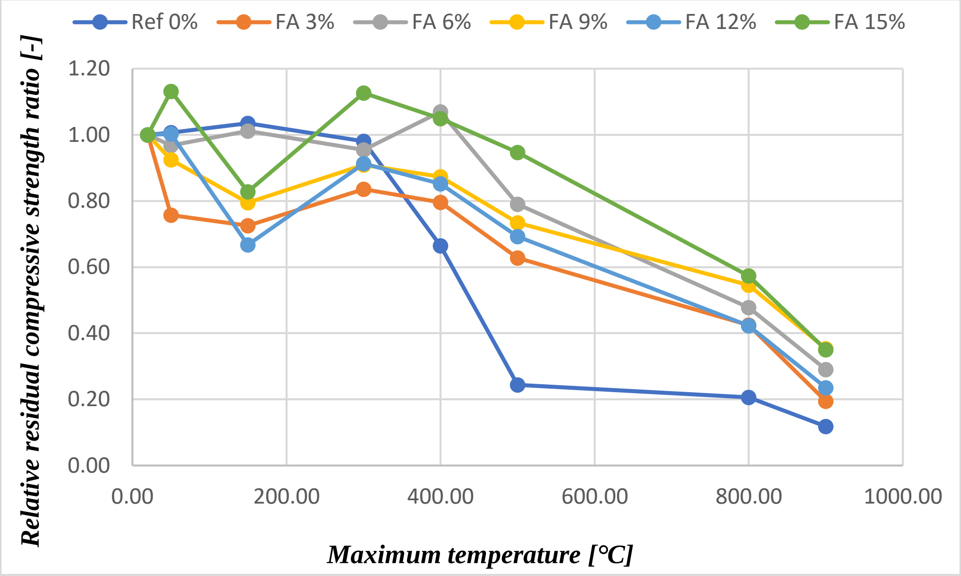

Figure 4.26 *Relative residual compressive strength as a function of temperature of FA mixtures of 0.3 w/b ratio*

The development of FA replacements on the HSCP prepared by 0.35 w/b ratio is presented in **Figure 4.27**. Using FA enhances the behaviour of hardened cement paste after exposure to elevated temperatures, where all mixtures containing FA have shown higher values than the reference mixture. The mixture containing 15% of FA has maintained the highest RRCS with a value of 67% and 46% after exposure to 500 °C and 800 °C, respectively.

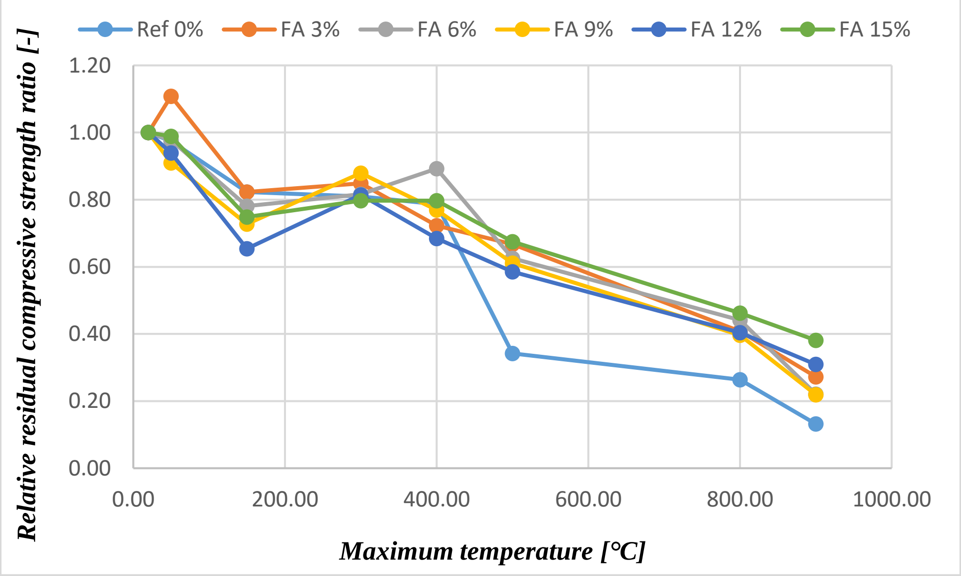

Figure 4.27 *Relative residual compressive strength as a function of temperature of FA mixtures of 0.35 w/b ratio*

Figure 4.28 presents the RRCS results of all mixtures prepared by 0.4 w/b ratio. The inclusion of FA in the HSCP has generally improved the RRCS after exposure to elevated temperatures. The mixture containing 15% of FA has maintained the highest RRBS, showing 69% and 51% of RRCS after exposure to 500 °C and 800 °C, respectively. The reference mixture has shown a high loss of RRCS at elevated temperatures.

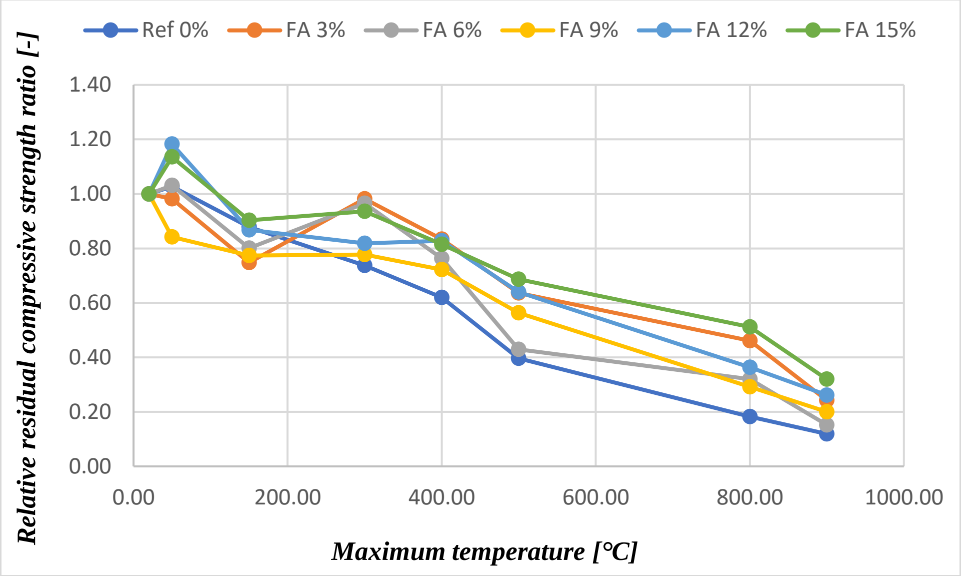

***Figure 4.28** Relative residual compressive strength as a function of temperature of FA mixtures of 0.4 w/b ratio*

The development of the additional resistance provided by the inclusion of FA is due to the filler effect of FA particle which enhancing the hydration of cement as well. The RRCS in case of FA mixtures could reach the double after exposure to elevated temperatures compared to the reference.

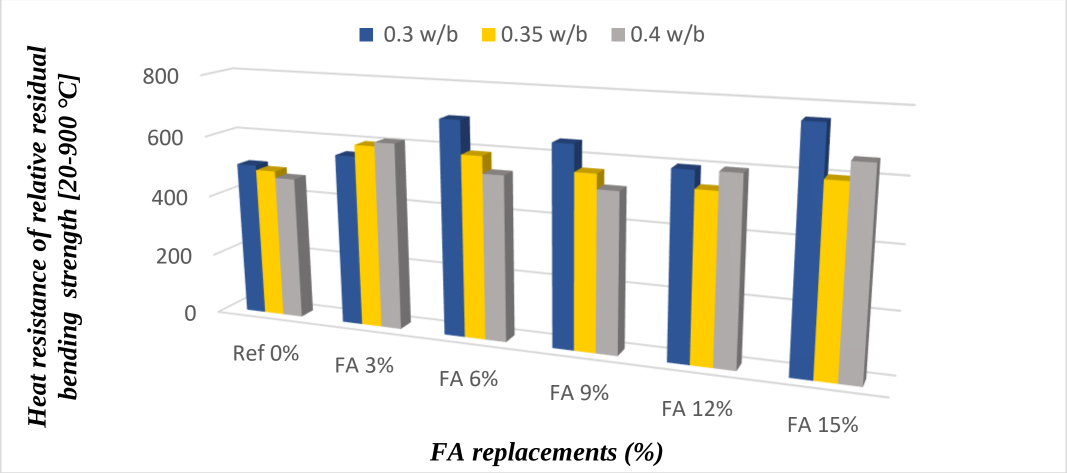

***Figure 4.29** Heat resistance of relative residual FA mixtures of the three w/b*

Finally, all the mixtures containing FA have higher heat resistance than the reference. Yet, the heat resistance has reached the maximum value by 15% of FA, regardless the type of w/b ratio, with an extra increase may reach to the maximum increase with 153% from the reference value (**Figure 4.29**). The loss of mass results of the reference sample and sample containing 15% of FA are presented in **Figure 4.30**. Interpretations of the loss of mass are similar to the previous results of MK and SF.

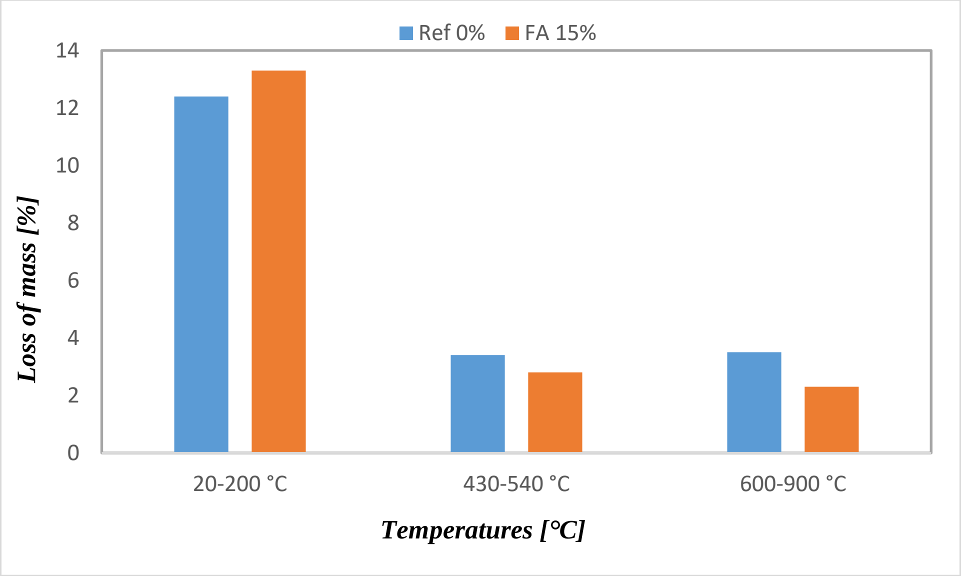

Figure 4.30 *Loss of mass of different FA phases using TG/DTA*

The SEM images of the HSCP containing FA at 20 °C and after the exposure to 500 °C, are presented in **Figure 4.31**. In case of results at 20 °C, hardened cement paste contains a high content of CSH in the form of small needles, comparing with the reference mixture (0%) have shown a high amount of $Ca(OH)_2$ in hexagonal shapes in addition to rods of ettringite (**Figure 4.8**). The physical property at ambient temperatures, the sample contains FA showed denser microstructure than the reference sample. The results of SEM images after exposure to 500 °C have shown a lot of pores and destruction in the microstructure of the reference hardened cement paste (0%) after exposure to elevated temperatures. On the other hand, the sample contains 15% of FA show dense and coherent microstructures, and the hollow shape of FA particles provides micro-channels within the hardened cement microstructure thus, improving heat resistance (**Figure 4.31)**.

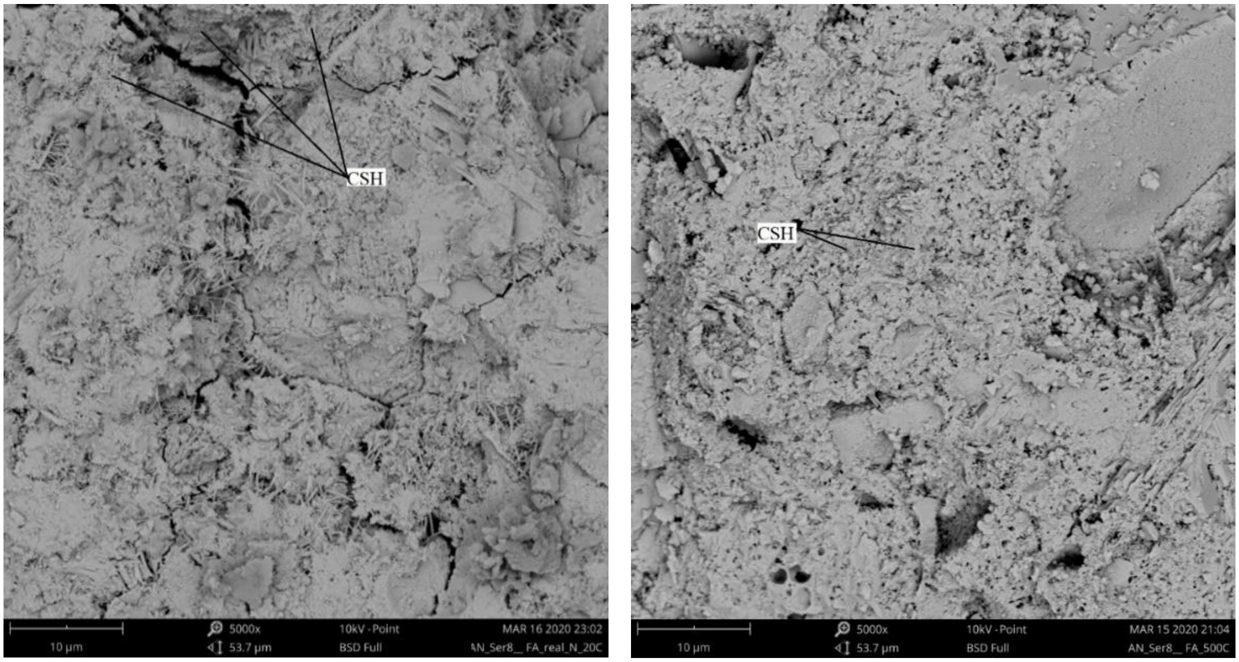

Cement paste with FA at 20 °C

Cement paste with FA after exposure to 500 °C

Figure 4.31 *The SEM images of microstructures of optimum replacement of FA (15%) at 20 °C and after exposure to 500 °C for 0.3 w/b ratio*

The porosity content and pore distribution were determined by CT for the reference sample (0%), and sample containing 15% of FA (optimum replacement) at 20 °C, in addition to sample containing 15% of FA after the exposure to 500 °C for 0.3 w/b ratio, the results are presented in **Figure 4.32**. The pattern clearly shows a decrease in the amount of the pores of samples containing FA. These results confirm the packing effect added to the hardened paste microstructure. The total volume of the pores is also calculated in this study, in which the total porosity of the hardened cement pastes containing 15% of FA is 4% per volume compared to the reference sample that has a volume of porosity about 5.93%.

After elevating temperatures, the variety of the macro and microstructure changes of samples with 15% of FA is investigated, showing a denser structure than the same samples at 20 °C (**Figure 4.32**). The distribution of pore through the cross-section of the sample is highly homogeneous, resulting in 3.0% per volume of the pore content for specimens after exposure to 500 °C. Comparing to the reference samples (0%), the samples of FA are more coherent and denser than the reference samples (0%). In which a lot of disintegration on the hardened cement paste structure due to the decomposition of $Ca(OH)_2$ and then its rehydration with H_2O.

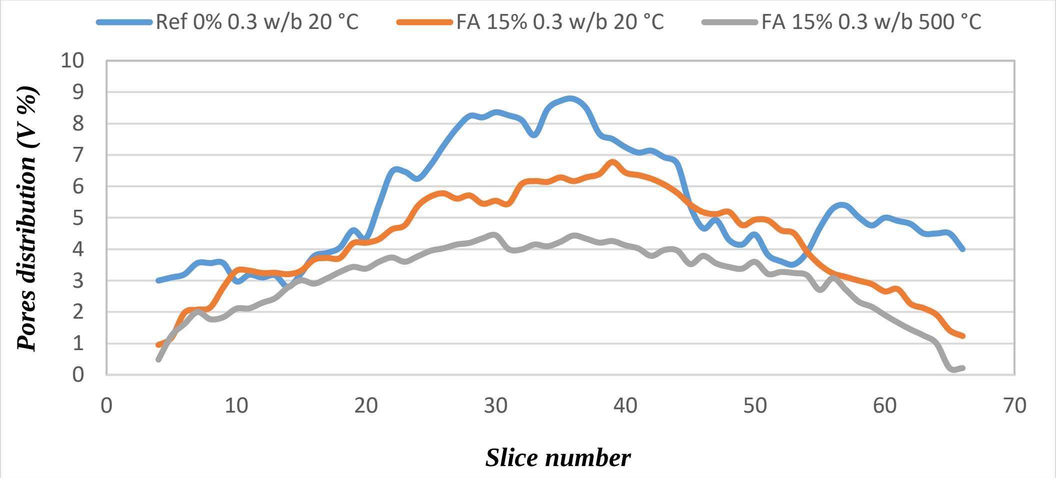

Figure 4.32 *The CT pores results of the reference mixture at 20 °C, and mixtures containing FA of 15% at 20 and 500 °C*

4.3.2 Relative residual bending strength for mixtures of different FA replacements

The RRBS results of all mixtures prepared with 0.3 w/b ratio after exposure to elevated temperatures are presented in **Figure 4.33**. Results showed that all mixtures containing FA have higher values of RRBS than the mixtures do not have FA. The mixture containing 15% of FA is considered the optimum replacement as far as RRBS is concerned. The optimum replacement achieves the highest RRBS with 61% and 47% after exposure to 500 °C and 800 °C, respectively.

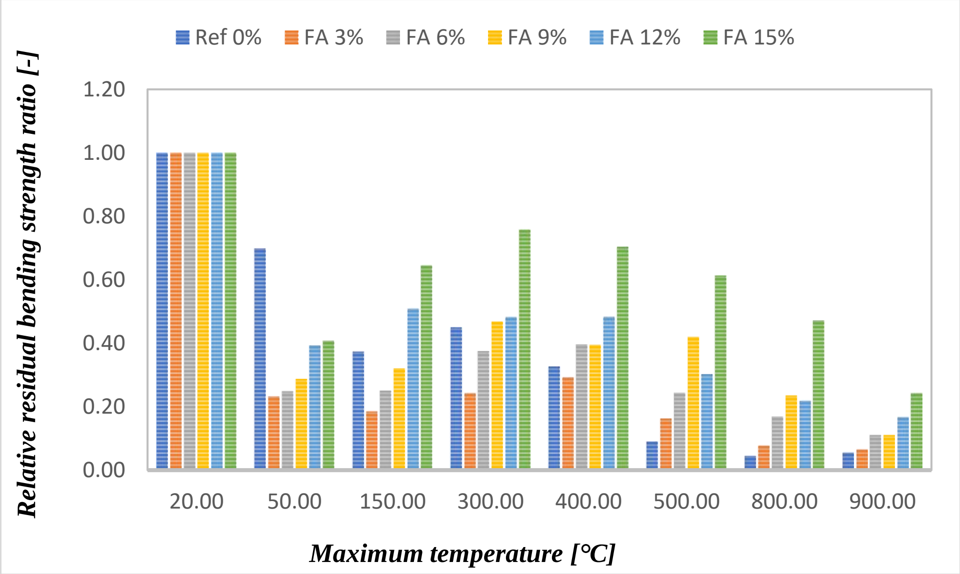

Figure 4.33 *Relative residual bending strength of different replacement of FA of 0.3 w/b ratio after exposure to elevated temperatures*

The results of the RRBS for all mixtures with 0.35 and 0.4 w/b ratio of FA are shown in **Figures 4.34** and **4.35**, respectively. As replacements of the FA increase, the RRBS of all specimens gradually increase. The reaction of FA with compounds liberated during the hydration of cement helps in the formation of bonds among particles in the transition zone, which lead to further increase in strength *(Targan et al., 2003)*.

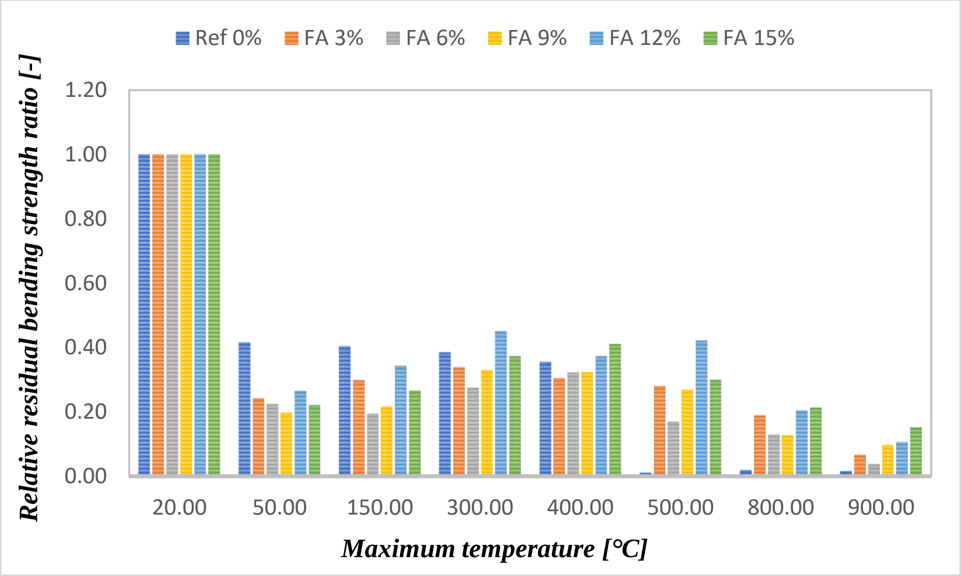

Figure 4.34 *Relative residual bending strength of different replacement of FA of 0.35 w/b ratio after exposure to elevated temperatures*

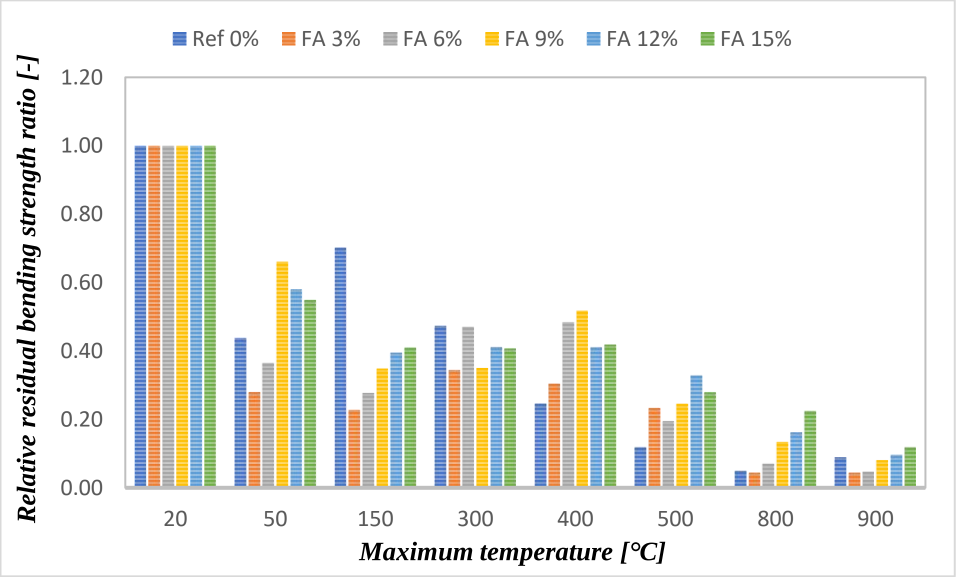

Figure 4.35 *Relative residual bending strength of different replacement of FA of 0.4 w/b ratio after exposure to elevated temperatures*

The heat resistance was calculated and illustrated in **Figure 4.36**. The maximum improvement is achieved by the mixture that contains 15% of FA.

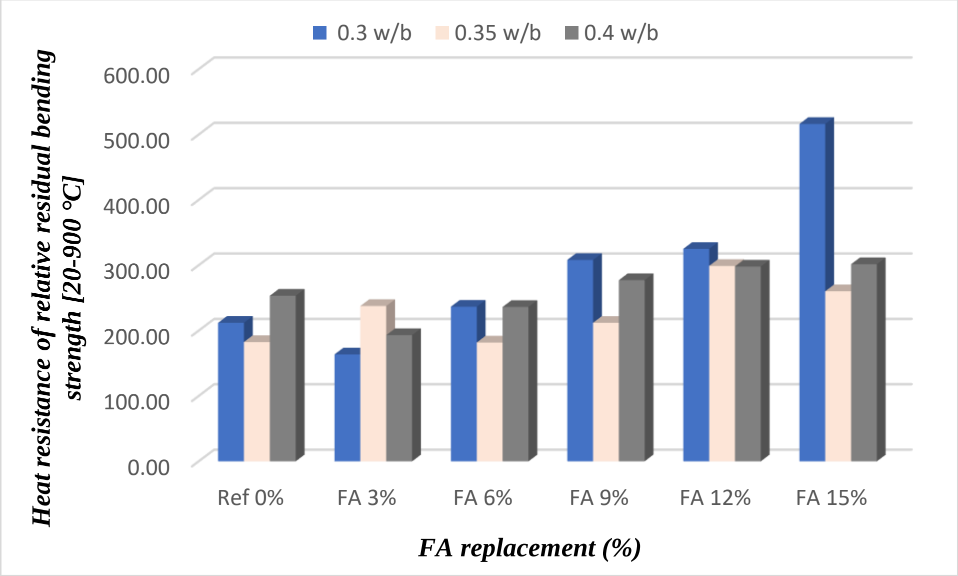

Figure 4.36 *Heat resistance of FA mixtures with the three w/b*

In conclusion, the findings of the abovementioned experimental study of the three SCM in case of 0.3 w/b ratio for compressive strength are summarized in **Table 4.1**. In general, using the optimum replacements for each of the three SCM; MK, SF or FA has advantages for the heat resistance of the HSCP. Furthermore, SF particularly showed higher heat resistance by 8% and 7% compared to MK and FA, respectively, as far as RRCS is concerned. This output could be related to the high content of SiO_2 on the composition of SF as well as due to the high fineness of particles. The highest replacement by cement was achieved by replacing 15% of FA, compared to the other pozzolanic materials. This could be due to the shape of FA particles, which is hollow and porous. The structure of FA particles enhances the resistance to the elevated temperature exposure with relatively high replacement allowing to use more than MK and SF. In the case of bending performance, the optimum replacement of MK has achieved higher heat resistance by 57% to 96 % compared to FA and SF optimum replacements, respectively. These results could be related to the elongated shapes of MK particles which works as micro-fibre.

This study highlights an important finding showing that the amount of the optimum replacement achieved for the compressive strength could differ from the amount of the optimum replacement achieved for the bending strength (**Table 4.1**). This could be attributed to the fact that each property is affected differently by the shape and morphology of each type of SCM. Furthermore, the hardened cement paste under bending loading is very sensitive to the microcracks more than under compression.

***Table 4.1** The optimum replacement values of the used SCM after exposure to elevated temperatures*

	MK	***SF***	***FA***
Compressive strength	9%	6%	15%
Bending strength	12%	3%	15%

The comparison has been conducted between CT results of samples of SF and FA. The patterns of the samples containing SF and FA after exposure to elevated temperature are not similar, even both samples showed positive enhancement. It could be explained by the difference in the porosity behaviour after exposure to elevated temperature that is mainly occur due to two main factors; (i) the very fine particles of SF, in which the densification in case of SF is higher than FA, and (ii) the hollow particles of FA with bigger spherical size, which work in some cases as micro-pores as shown in **Figure 3.4 b** and **Figure 4.31**.

The amounts of optimum replacements of the three SCM after exposure to elevated temperatures are higher than amounts of optimum replacements at ambient temperatures. The difference between the optimum replacements of ambient and elevated temperatures could be attributed to an important reason; at elevated temperatures the required amounts of SCM to decrease the amount of $Ca(OH)_2$ are higher than amounts of SCM needed at ambient temperature (**Figure 4.37**). All values confirmed the previous observation except the group of MK with 0.30 w/b ratio.

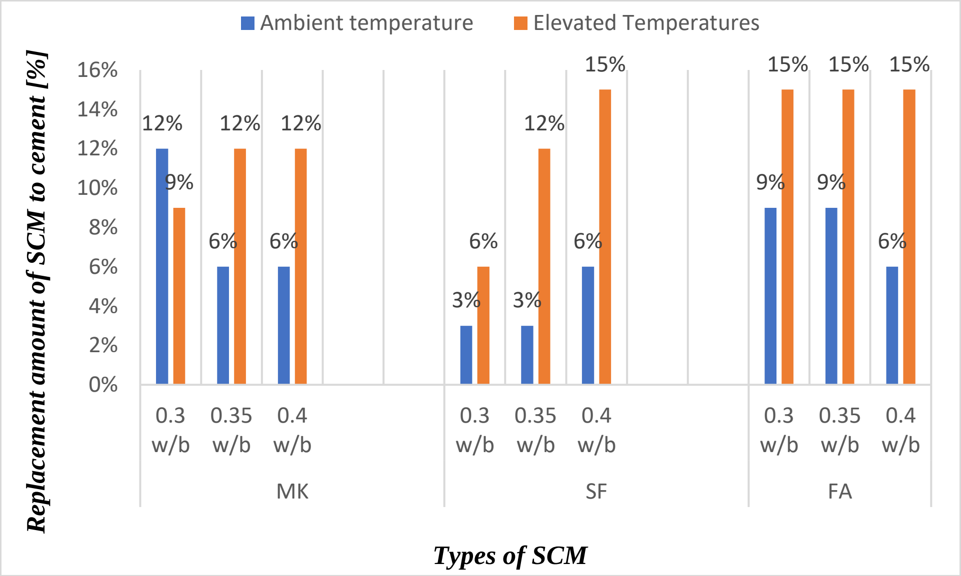

***Figure 4.37** The optimum replacement values of the used SCM (by cement replacement) at ambient and after exposure to elevated temperatures*

CHAPTER 5: EFFECT OF CHANGING CEMENT FINENESS ON THE BEHAVIOUR OF SCM AT ELEVATED TEMPERATURES

This chapter evaluates the changes occurred due to the cement fineness factor by investigating the optimum replacements of MK for two types of OPC, namely: CEM I 42.5 N and CEM I 52.5 N after exposure to different levels of temperatures. The mechanical, physical, and microstructural properties of HSCP are presented in this chapter. The mechanical properties were tested in three different w/b.

5.1 Influence of MK using CEM I 52.5 N

Fire resistance of HSCP is highly dependent on its constituents, inlcuding temperature level and duration of the exposure. Changes in OPC characteristics may change the behaviour of hardened cement paste after exposure to elevated temperatures. In this experimental study, the effect of cement fineness has been assessed on the selection of the optimum replacement of MK to cement.

Compressive strength values of HSCP are graphically represented as a function of MK replacements for the three w/b in **Figure 5.1**. The highest compressive strength values were obtained from the mixtures containing optimum 9%, 6%, and 6% for w/b ratio of 0.3, 0.35, and 0.4, respectively. The compressive strength values for the previous optimum mixtures are 119.68 MPa, 93.90 MPa, and 80.50 MPa, respectively. The difference in optimum replacement for the three w/b is attributed to the packing effect, which is more pronounced at low w/b and achieving the peak point with 0.3 w/b ratio.

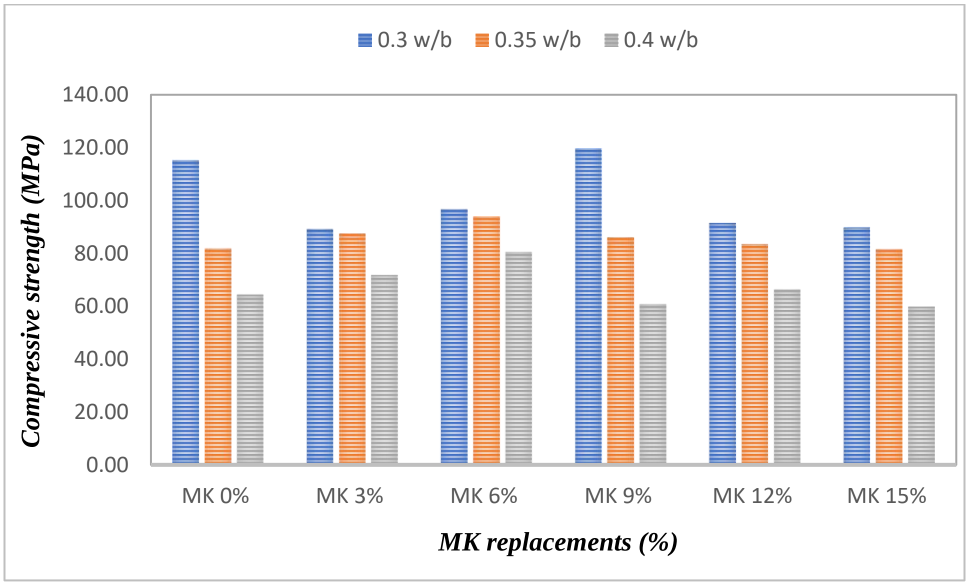

***Figure 5.1** Compressive strength of different MK replacements with respect to w/b ratio*

5.1.1 Relative residual compressive strength (RRCS)

The contribution of MK on the behaviour of HSCP is significant after exposure to elevated temperature. The reference mixture of 0% of MK exhibited the lowest RRCS up to 400 °C for 0.3 and 0.35 w/b, and to some extent for 0.4 w/b. After the increase of temperature exposure to 500 °C, the RRCS values are 65%, 55%, and 54% for the w/b ratio of 0.3, 0.35, and 0.4, respectively. By increasing the temperature up to 800 °C, the RRCS of the reference specimens are 51%, 39%, and 41% for the w/b ratio of 0.3, 0.35, and 0.4, respectively, as shown in **Figures 5.1**, **5.2**, and **5.3**.

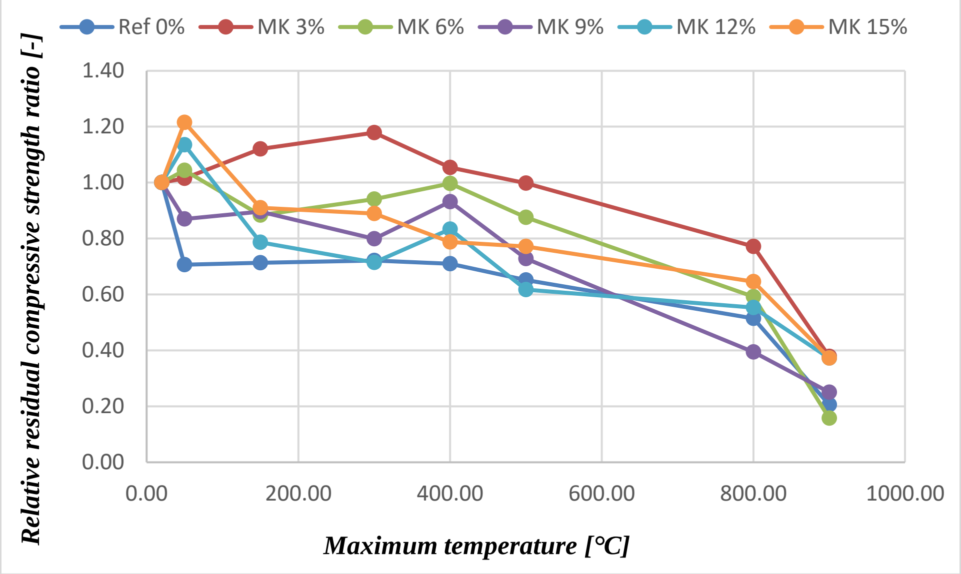

Figure 5.1 *Effect of the amount of MK on relative residual compressive strength of HSCP with 0.3 w/b*

Figure 5.1 shows the development of RRCS specimens of 0.3 w/b, in which the inclusion of MK is very efficient. Generally, RRCS increases in the presence of MK in all mixtures up to 500 °C. However, after 500 °C, the MK with low replacements (3% and 6%) show higher RRCS compared to the other replacements. This is mainly due to the potential of MK to densify the microstructure and decrease the large pore diameter due to the high specific surface area of MK; which led to the formation of internal stresses induced by the accumulation of vapour. Yet, it still shows relatively better behaviour than the reference mixture (0% MK). Comparing the various types of the studied mixtures, it can be observed that the mixture contains 3% of MK possess higher RRCS among the other five mixtures after exposure to elevated temperature exposure, achieving 100% and 77% after exposure to 500 and 800 °C, respectively. Other researchers observed that higher replacement of MK caused a higher loss in strength at higher temperatures exposure, concluding that relatively large pore area fraction is available in high MK mixtures after exposure to elevated temperature *(Poon et al., 2003)*.

In the case of mixtures prepared with 0.35 w/b ratio, **Figure 5.2** illustrates the RRCS values of the various mixtures. MK with 9% showed less loss RRCS (20%) than other mixtures after exposure to 500 °C. By increasing the heating up to 800 °C, 56% of RRCS remains.

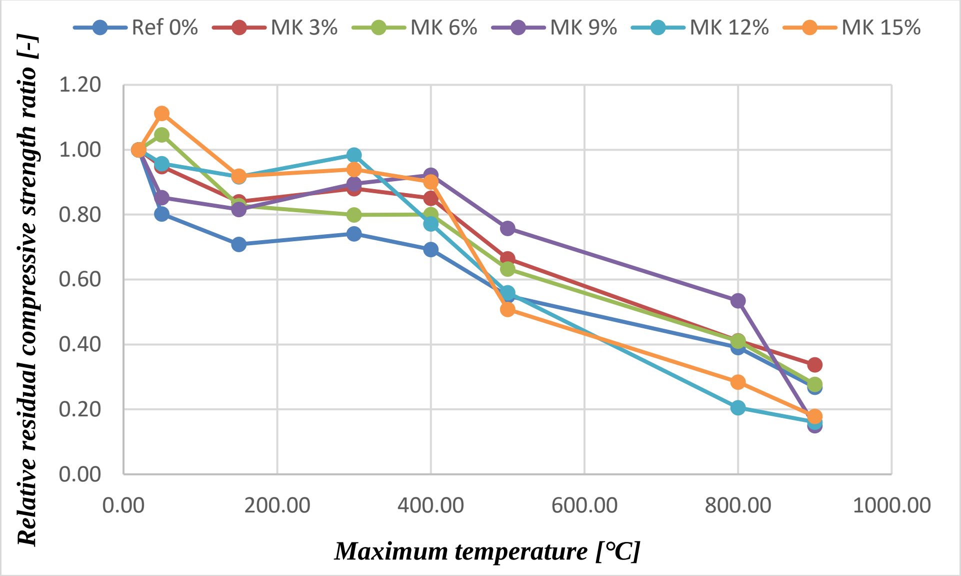

***Figure 5.2** Effect of the amount of MK on relative residual compressive strength of HSCP with w/b 0.35*

Mixtures of 0.4 w/b with different MK replacements after exposure to elevated temperatures are presented in **Figure 5.3**. Development of RRCS was observed for the mixtures containing 12% and 15% of MK. However, the RRCS of 12% MK were 83% and 63% for 500 and 800 °C, respectively.

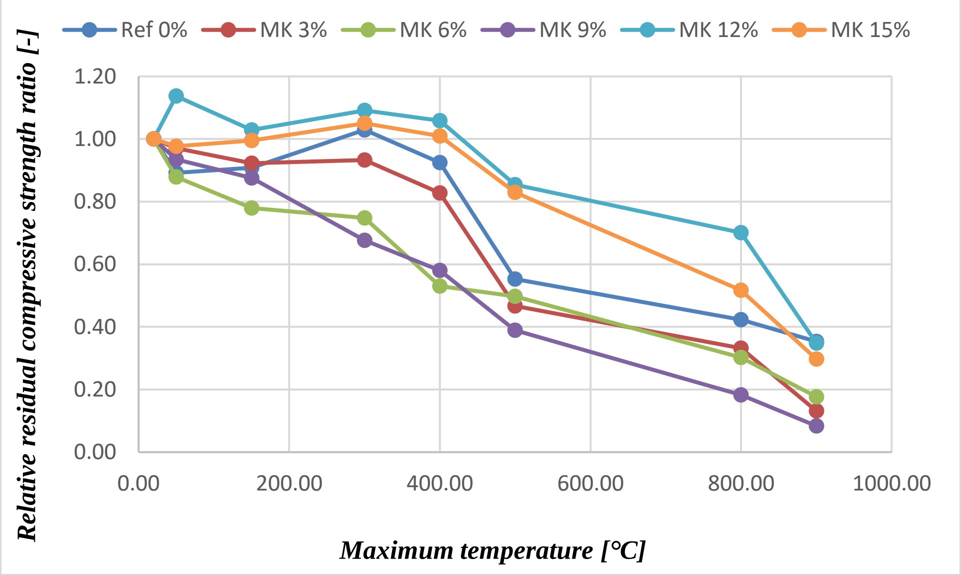

***Figure 5.3** Effect of the amount of MK on relative residual compressive strength of HSCP with 0.4 w/b*

The heat resistance of all MK replacements of the three w/b ratios are calculated and plotted in **Figure 5.4**. The mixtures containing 3%, 9%, and 12% of MK show the highest heat resistance for mixtures of 0.3, 0.35, and 0.4 w/b ratio, respectively. The results are similar to the previous results in **Figures 5.1**, **5.2**, and **5.3**.

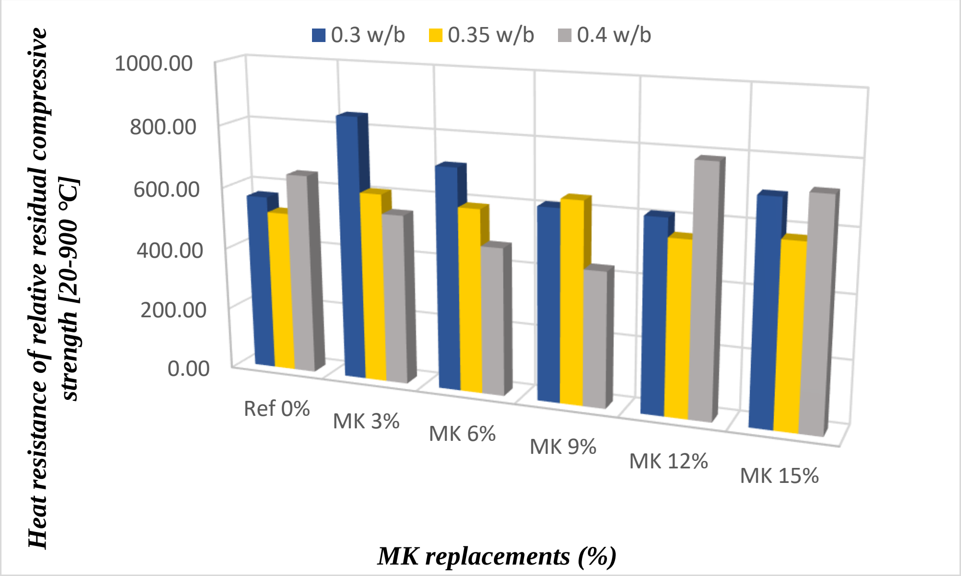

***Figure 5.4** Heat resistance of relative residual compressive strength [20–900 °C] for mixtures of the three w/b*

5.1.2 Relative residual bending strength (RRBS)

The effect of different MK replacements on the bending properties of hardened cement paste is investigated and presented herein. In general, the elevation of temperature affects the properties of hardened cement in terms of bending resistance, regardless of the type of mixture. The values of the RRBS of all mixtures blended with MK of 0.3 w/b ratio are plotted in **Figure 5.5**. The results show that the addition of MK relatively increases the RRBS of all specimens compared to that of the reference specimen. Besides, the highest RRBS is obtained in mixture with 3% of MK that showed 86% after exposure to 500 °C, whereas at 800 °C, RRBS was 63%. It is worth to mention that this mixture showed a significant improvement in all temperature levels while the reference mixture suffered after exposure to elevated temperatures maintaining only 33% and 13% after exposure to 500 °C and 800 °C, respectively.

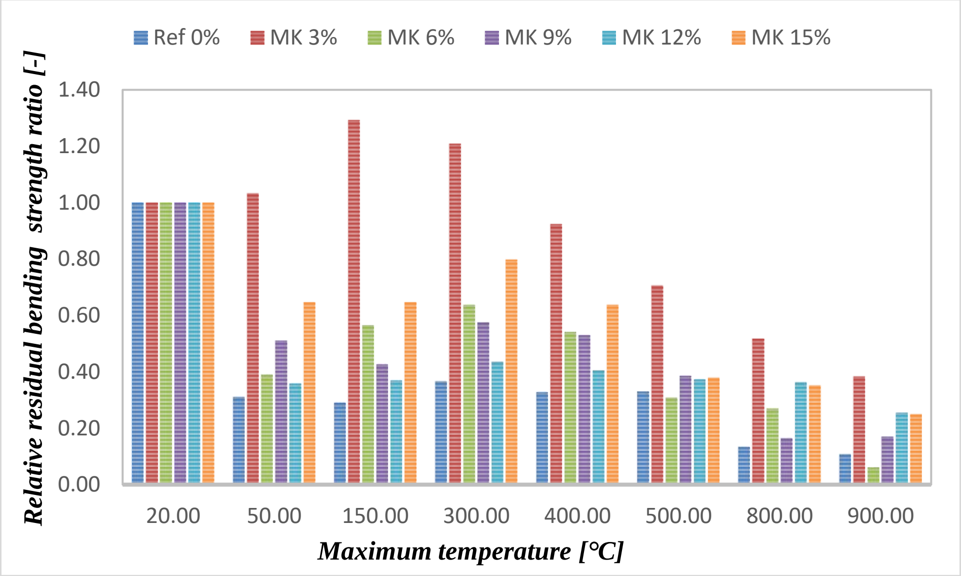

Figure 5.5 *Effect of the amount of MK on relative residual bending strength of HSCP with 0.3 w/b*

Figures 5.6 and **5.7** present the RRBS of all mixtures for mixtures of 0.35 and 0.4 w/b ratios, respectively. The development of strength due to MK is noticed in all the mixtures containing MK up to 400 °C. Afterwards, the RRBS decreases in all mixtures. However, the mixture containing 3% of MK has shown to be more valuable compared to the other replacements after 400 °C in terms of cracks occurring as well as strength properties.

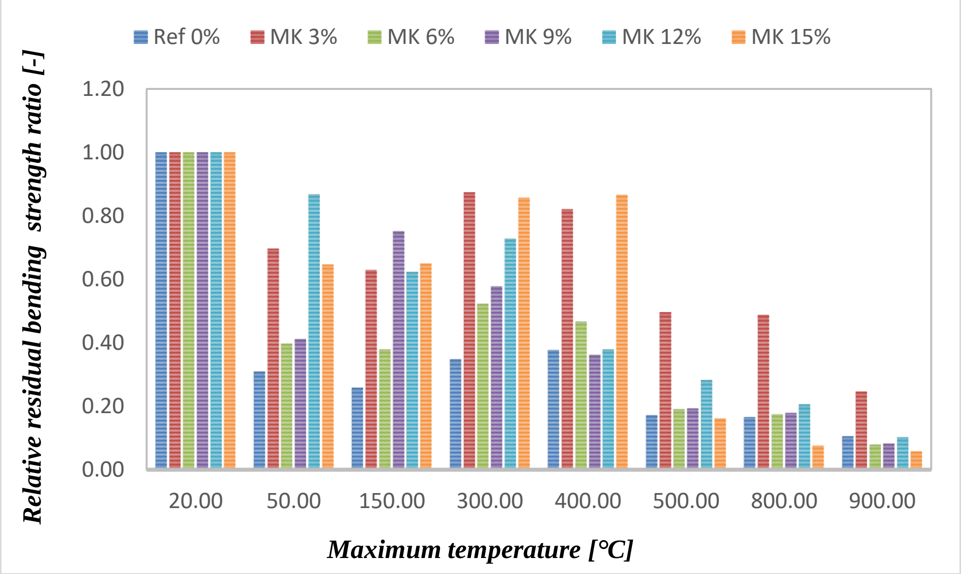

Figure 5.6 *Effect of the amount of MK on relative residual bending strength of HSCP with 0.35 w/b*

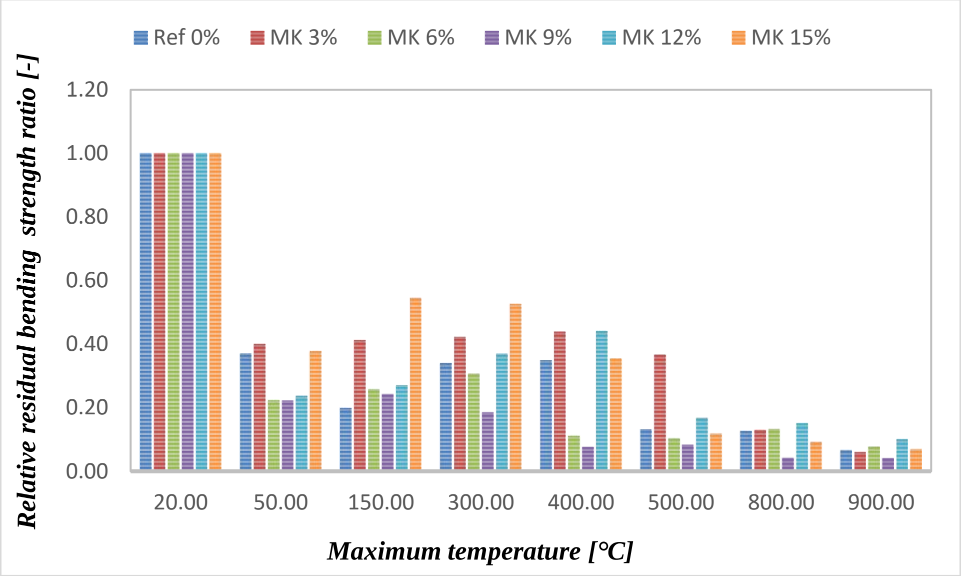

Figure 5.7 *Effect of the amount of MK on relative residual bending strength of HSCP with 0.4 w/b*

The heat resistance of all values of RRBS for all of the three w/b ratios is calculated and presented in **Figure 5.8**. The efficiency by adding MK on the RRBS with the elevation of temperatures has been observed up to 400 °C, after that the MK contribution decreases due to the high dense microstructure. Therefore, the maximum heat resistance has been obtained at very low MK replacement, in which 3% replacement of MK was the optimum replacement as far as RRBS is concerned.

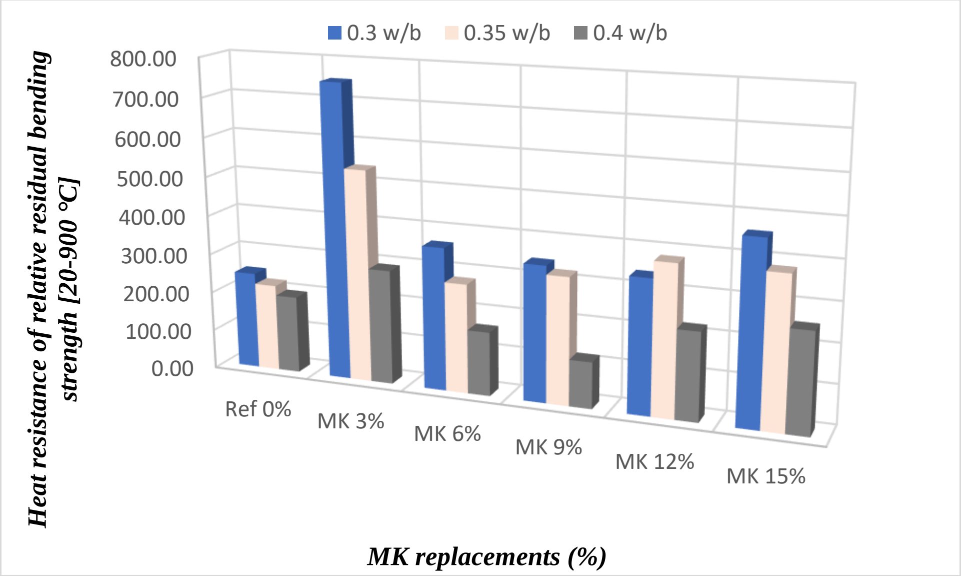

Figure 5.8 *Heat resistance of relative residual bending strength [20–900 °C] for mixtures of the three w/b*

5.2 Effect of changing cement fineness on the optimum replacements of MK on the compressive strength properties

The optimum replacements of MK in HSCP prepared with CEM I 42.5 N and CEM I 52.5 N after exposure to elevated temperatures are summarized in **Figure 5.9**. Based on the results, it was found that there is a significant effect of changing the fineness of cement on the behaviour of MK replacements on hardened cement paste after exposure to elevated temperature. In which, the optimum replacement obtained on compressive strength after the elevated temperature was 9% for MK based on CEM I 42.5 N, whereas by using CEM I 52.5 N, the optimum replacement is shifted below to be 3%. This conclusion could be interpreted by the high specific surface area of CEM I 52.5 N (4500 cm^2 g^{-1}) compared to CEM I 42.5 N. Fineness of CEM I 52.5 N allows to use limited amount of MK, especially at low w/b. Finally, the RRCS has shown that the increase in the fineness of cement decreases the amount of MK needed for the optimum value, as shown in **Figure 5.9**.

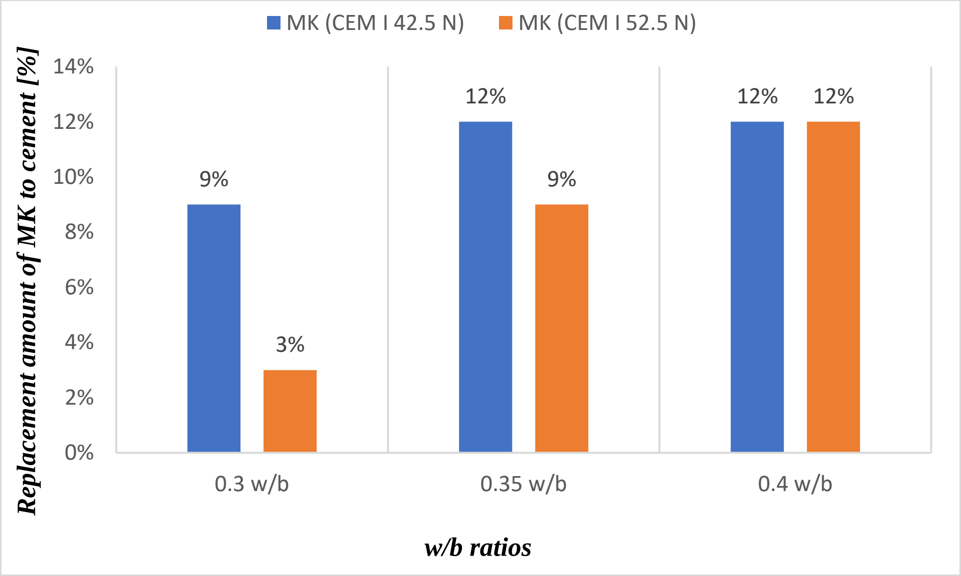

Figure 5.9 *The optimum replacements of MK with CEM I 42.5 N and CEM I 52.5 N in a function of w/b ratio*

In order to support the previous interpretations regarding the difference obtained by using two types of cement, the specimens have been investigated by SEM images. **Figure 5.10** shows the difference between cement pastes and their powders as long as cement fineness is concerned. In case of cement pastes, pastes prepared by CEM I 42.5 N are characterized by porous microstructure with different pores sizes (**Figure 5.10 a**), while specimens of cement pastes prepared by CEM I 52.5 N are characterized by less porous micro-structure than CEM I 42.5 N (**Figure 5.10 b**). Similarly, in case of powder particles, the images of CEM I 42.5 N and CEM I 52.5 N particles have been taken in the same magnifications. The nature of CEM I 42.5 N particles is coarser than CEM I 52.5 N powder particles (**Figures 5.10 c** and **d**).

Thus, the characteristics of CEM I 42.5 N could allow to use a relatively high amount of MK compared to CEM I 52.5 N particularly at low w/b. Therefore, the MK amount is more limited in case of CEM I 52.5 N due to the high dense microstructure, making it more susceptible to cracking after exposure to elevated temperatures.

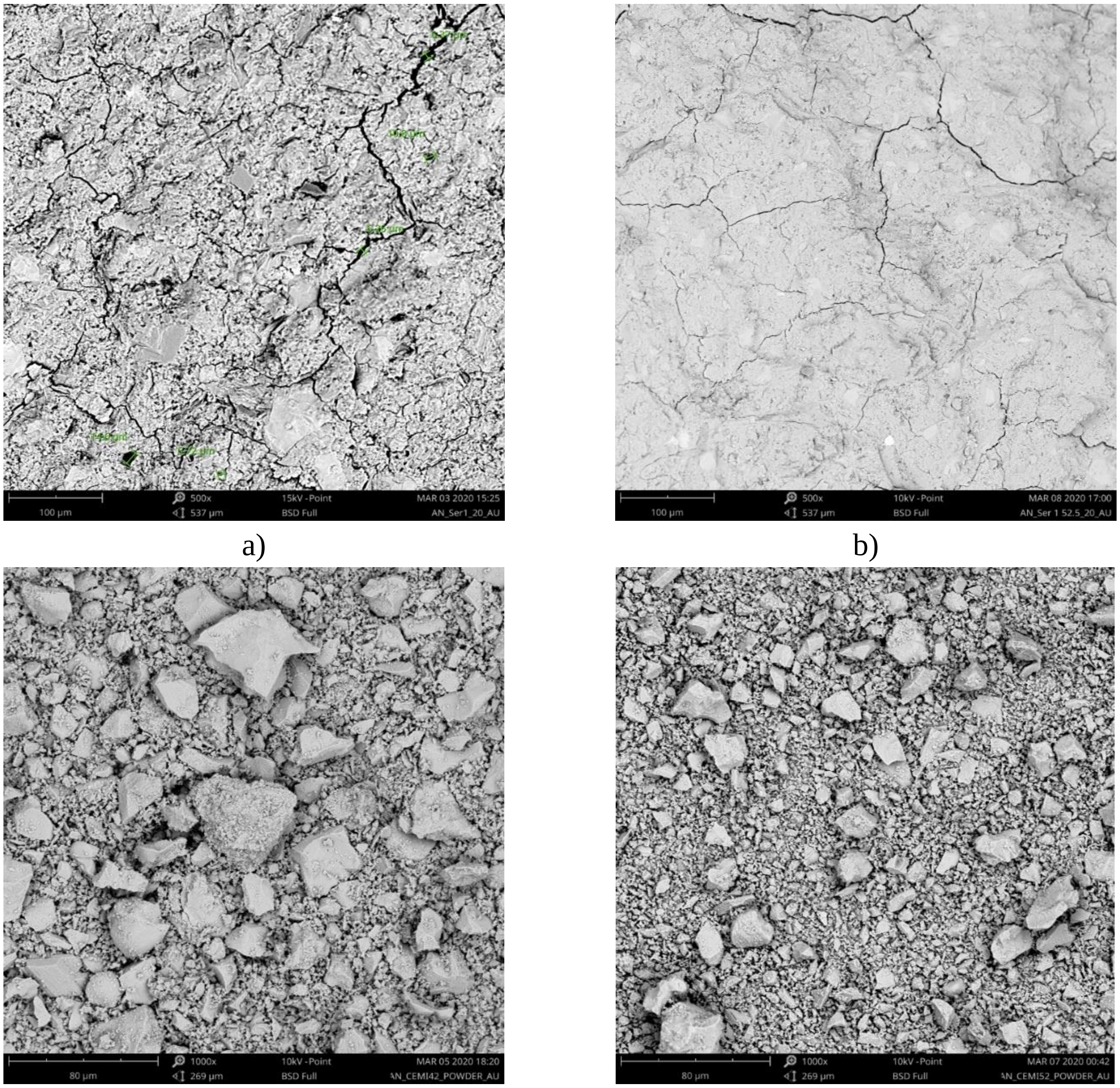

a) b)

c) d)

Figure 5.10 *Reference mixtures of 0.3 w/b at 20 ℃: a) Cement paste using CEM I 42.5 N, b) Cement paste using CEM I 52.5 N, c) Powder of CEM I 42.5 N, and d) Powder of CEM I 52.5 N*

Figure 5.11 shows the results of the heat resistance of the reference pastes at three w/b ratios prepared by different types of cement fineness (CEM I 42.5 N and CEM I 52.5 N). The value of the heat resistance of HSCP after exposure to elevated temperatures (up to 900 °C) increases as the cement fineness increases.

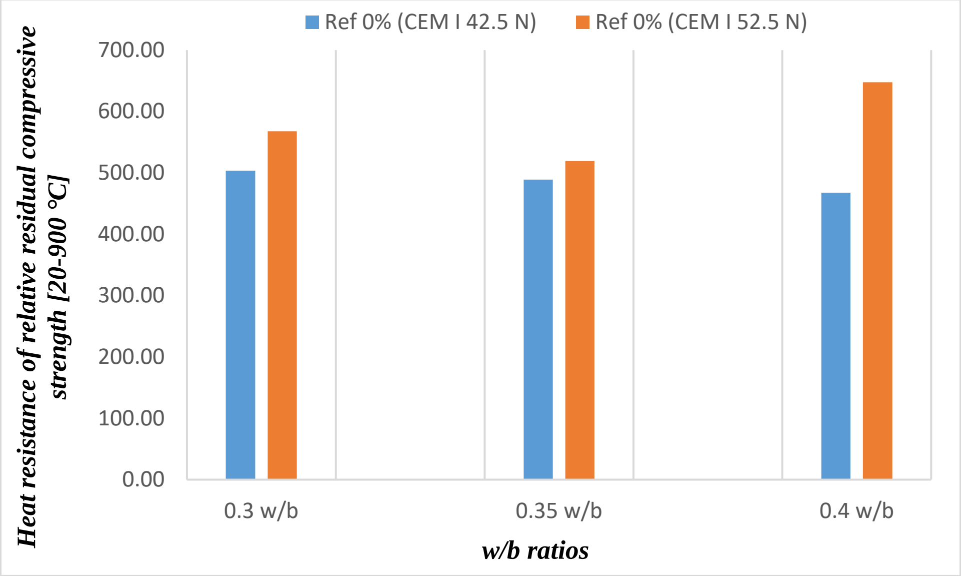

Figure 5.11 *Heat resistance results of reference mixtures with CEM I 42.5 N and CEM I 52.5 N [20–900 °C]*

5.3 High strength concrete

The optimum replacement of MK obtained on the RRCS of hardened cement paste prepared by 0.35 w/b using CEM I 52.5 N has been applied on concrete mixtures. The residual compressive strength results of the specimens are presented in **Figure 5.12.** Results show that the compressive strength values are 88.96 and 99.38 MPa for mixtures containing 0% and 9% of MK, respectively.

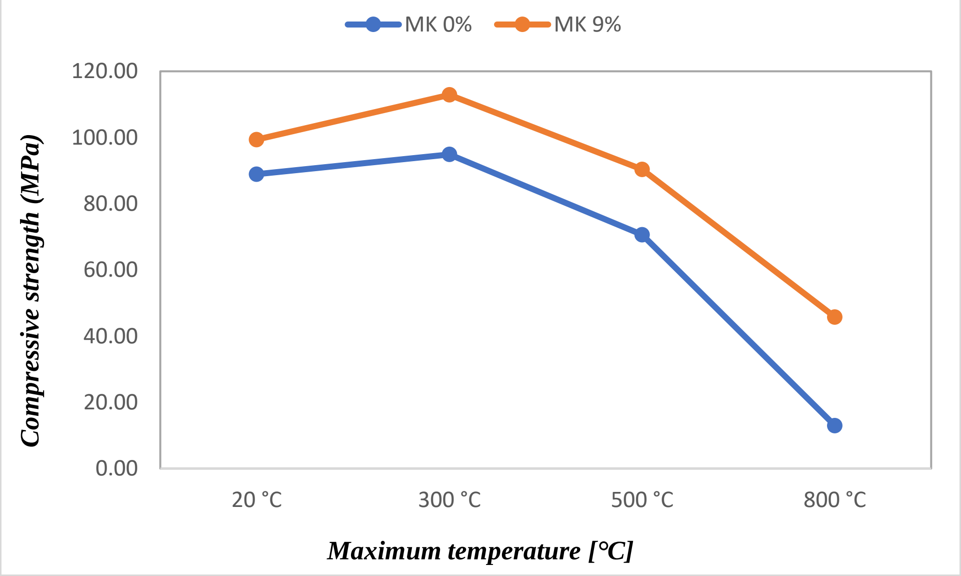

Figure 5.12 *Variation of compressive strength with respect to MK replacements and temperature ranges*

By including temperature parameter, from 20 ºC to 300 ºC, the compressive strength is increased by 6% and 14% for concrete mixtures of MK 0% and 9%, compared to their mixtures at 20 ºC, respectively. However, by increasing temperature up to 500 ºC, the compressive strength is slightly decreased by 21% and 9% for concrete mixtures of MK 0% and 9%, respectively. After exposure up to 800 ºC, the compressive strength is significantly decreased by 85% for concrete mixtures of MK 0%, and less significant for concrete mixtures of MK 9% decreasing the strength by 54%.

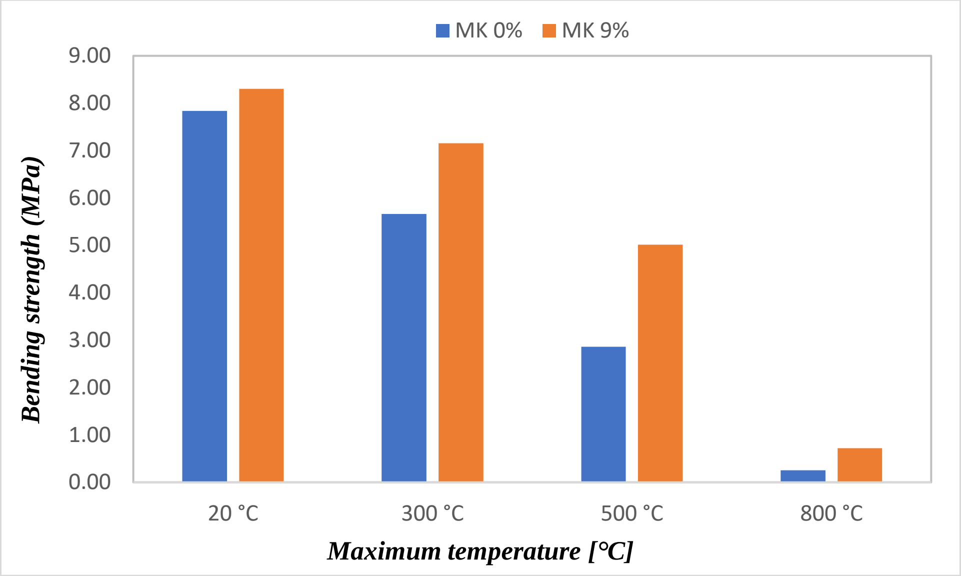

Figure 5.13 *Bending strength with respect to MK replacements at different temperatures exposure*

The residual bending strength results after different temperatures of exposure are presented in **Figure 5.13**. It can be observed that bending strength values are varied between 7 MPa to 8 MPa at ambient temperatures. The results showed that the bending strength is generally reduced by increasing the temperature. after exposure to 300 ºC, the RRBS values are 72% and 86% for the mixtures of 0% and 9% of MK, respectively, by increasing the temperature to 500 ºC, the RRBS are 37% and 60%, respectively. Exposing the specimens to 800 ºC, all mixtures show a significant loss, in which the RRBS values were 3% and 9% for the mixtures of 0% and 9% of MK, respectively. Incorporating MK seems to have advantages to enhance the bending strength at ambient temperature and mitigating loss on the residual bending strength in case of elevated temperatures.

5.3.1 Microstructure investigations results

A proposed mean of interpretation for the performance of HSC mixed with MK after exposure to elevated temperature is the SEM images. In addition to the changes made by the inclusion of MK on the level of cement paste, MK also can make a change on the Interfacial Transition Zone (ITZ). ITZ is considered as one of the weakest parts of ordinary concrete, particularly after exposure to elevated temperatures.

Figure 5.14 shows the ITZ between the mortar (M) and the aggregate (A) in which, wherein the HSC/MK is 0%, the ITZ has a porous layer and a clear separating line, and when HSC/MK is 9%, the ITZ is observed to be sewed by MK eliminating the separating line. The ITZ is primarily defined by the different chemical compositions in the mixtures. Therefore, three actions of MK, i.e., filling effect, pozzolanic reaction, and the consumption of $Ca(OH)_2$ affect the ITZ bond to be increased.

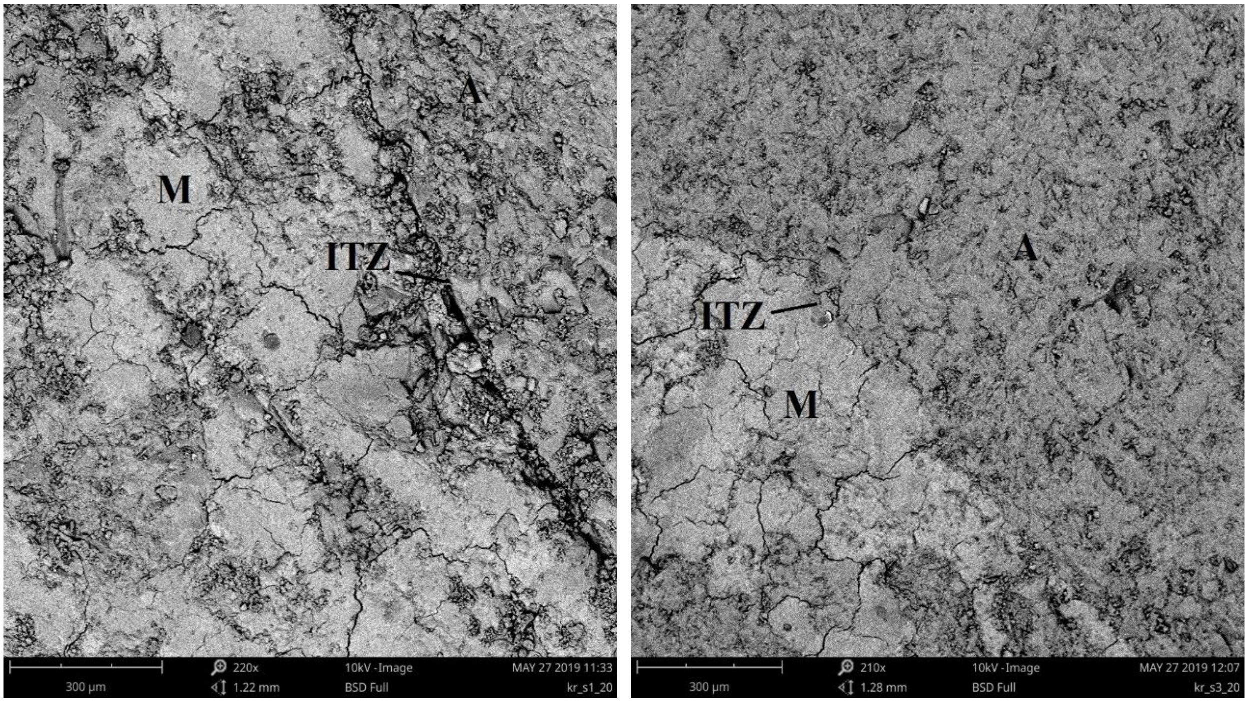

HSC/MK (0%) HSC/MK (9%)

***Figure 5.14** The ITZ between the mortar of HSC and the aggregate at the reference concrete (HSC/MK (0%)) and concrete with MK (HSC/MK (9%))*

5.4 Comparison between the behaviour of HSCP and HSC after exposure to elevated temperatures

Figure 5.15 shows the relationship between the behaviour of HSCP and HSC from ambient to elevated temperatures. Cement paste has unstable conditions in concrete during heating due to several chemical and physical changes, particularly from 60 °C to 800 °C *(Khoury, 1995)*. Thus, the heat resistance hardened cement pastes have chances to significantly enhance the heat resistance properties of concrete after exposure to elevated temperature. From our results, for mixtures of 0% MK (reference mixtures), the ratios of concrete mixtures (HSC) to the cement paste mixtures (HSCP) are 1.08 and 2.69 at temperatures 20 and 800 °C, respectively. For mixtures containing optimum MK replacement (9% of MK), the ratios of concrete to cement paste are 1.15 and 0.96 at temperatures 20 and 800 °C, respectively. This indicates the compatibility between concrete and cement paste obtained by the presence of MK at elevated temperatures by decreasing stresses due to the consumption of $Ca(OH)_2$.

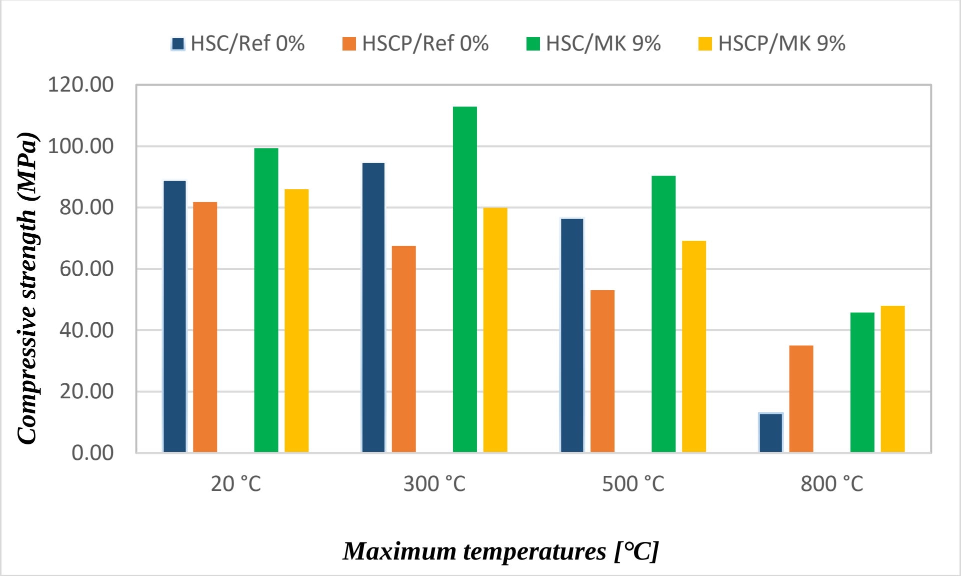

Figure 5.15 *Compressive strength values with respect to MK replacements and temperature levels for concrete (HSC) and cement paste (HSCP)*

CHAPTER 6: EFFECTS OF CHANGING W/B RATIO ON SCM OPTIMUM REPLACEMENTS

This chapter provides the results assessed due to changing w/b ratio in the mechanical properties of HSCP. The results below are limited to the optimum replacements of SCM obtained from compressive strength test results for CEM I 42.5 N only.

6.1 Effect of w/b ratio on the properties of the reference mixture (0% SCM)

The changing of w/b ratio on the hardened cement pastes significantly affects the mechanical properties behaviour. The amount of w/b ratio governs the porosity and heavily influences the behaviour *(Roy and Gouda, 1973; Ollivier and Buil, 1992; Chanvillard, 1999)*. **Figure 6.1** presents the compressive strength values of reference mixtures prepared with three different w/b ratios (0.3, 0.35, and 0.4) showing difference caused due to the changes in w/b ratio. The results are divided into two groups according to the main change in the strength in a function of temperatures. The first level is of the temperature range from 20 °C to 400 °C, where the second level is corresponding to the temperature above 400 °C to 900 °C. In the first group, the effect of w/b ratio is significant, in which the results obtained from 0.3 w/b ratio were significantly higher than results obtained by using 0.35 and 0.4 w/b ratios. In this group, the difference between results values due to changing w/b ratio is about 48 MPa at 400 °C. On the contrast, the results of the second group are completely different in which the strength loss is more pronounced particularly for the mixtures with 0.3 w/b ratio. This could be attributed to the high dense microstructure of mixtures with 0.3 w/b ratio, which is adversely affected the strength after exposure to elevated temperatures. In this group, the difference between results values due to changing w/b ratio is about 5 MPa at 900 °C.

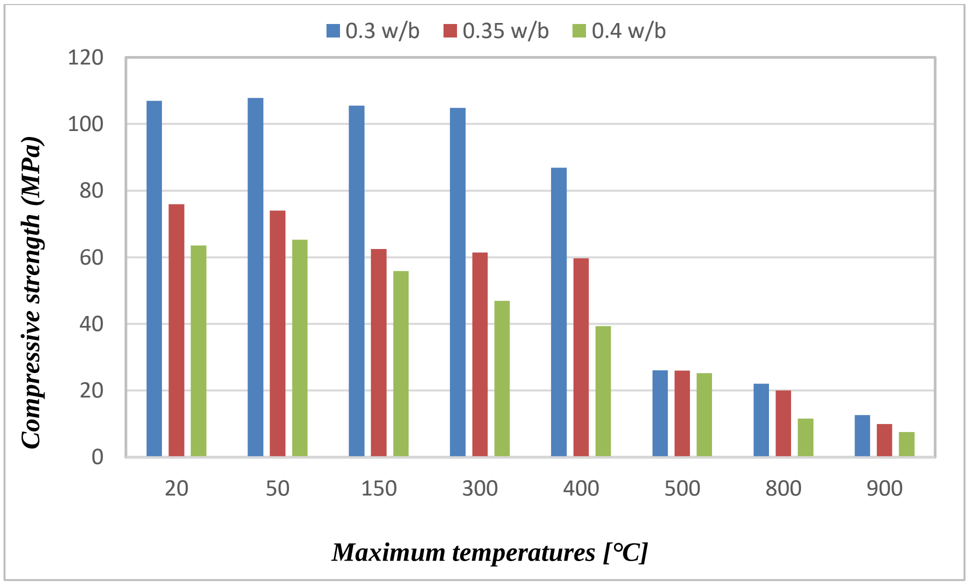

Figure 6.1 *Compressive strength of reference mixtures for the three w/b ratio as a function of temperature*

6.2 Effect of w/b ratio on the properties of the optimum replacements of MK

The optimum replacements of MK after exposure to elevated temperatures for the three w/b ratios are shown in **Figure 6.2**. In the case of mixtures prepared with 0.3 w/b ratio, the optimum replacement using MK was 9%. However, by changing the w/b to 0.35, the optimum replacement changes to become 12%. Then, increasing the w/b ratio to 0.4 the MK replacement still constant (12%) that could be due to the clinker dilution effect.

The content of water has an effect on the amount of optimum replacement of MK from a prespective of RRCS, in which as the w/b increases, pore size is enlarged and porosity is increased *(Cook and Hover, 1999)*. On the other hand, the presence of MK causes refinement in pore structure and increases the percentage of small pores *(Bredy et al., 1988; Khatib and Wild, 1996)*. Consequently, the likelihood of large cracks or spalling is increased with low w/b and low permeability *(Chowdhury, 2014)*. Thus, the optimum amount is shifted with an increase in w/b ratio.

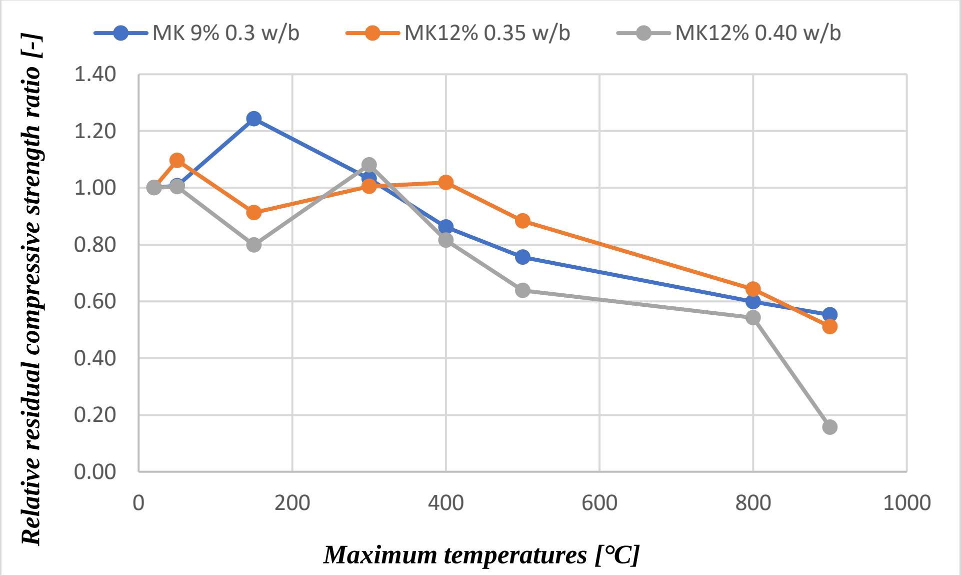

Figure 6.2 *Optimum replacements of MK with the three w/b*

6.3 Effect of w/b ratio on the properties of the optimum replacements of SF

The optimum mixtures of SF obtained in the three w/b are shown in **Figure 6.3**. The optimum replacements of SF are changed with changing w/b ratios, where it was 6% at 0.3 w/b, then shifted to 12% and 15% for 0.35 and 0.40 w/b, respectively. In conclusion, the use of SF is restricted by w/b ratio, in which at law w/b ratio (0.3 w/b), the allowed amount of SF is limited because of the strong densification of SF particles. Furthermore, as permeability decreases, the high replacement of SF induces cracking at elevated temperatures which adversely affect the mechanical properties that could lead to spalling. In contrast, as the w/b ratio increases, the amount of SF is allowed to increase.

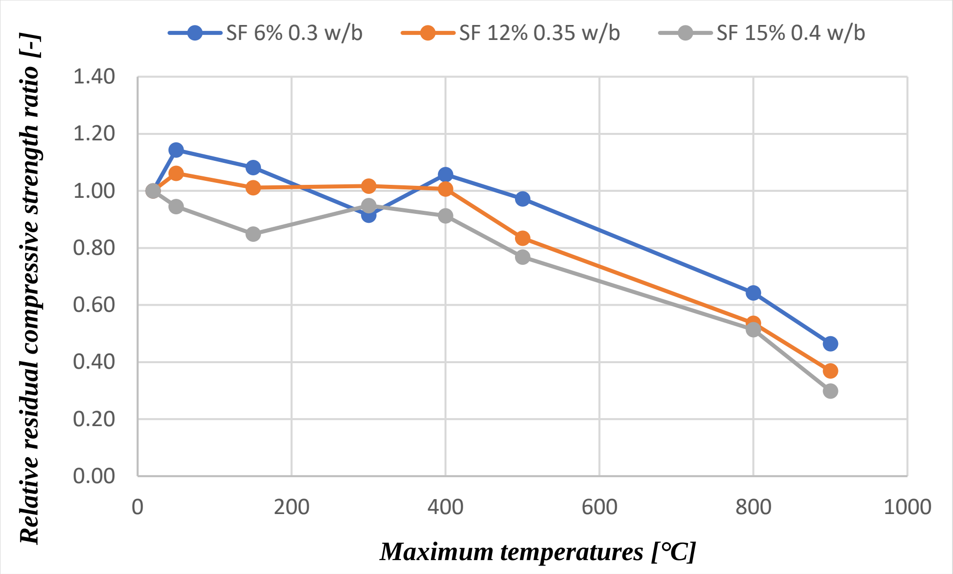

Figure 6.3 *Optimum replacements of SF in the three w/b*

6.4 Porosity development

In order to evaluate the effect of w/b ratio and porosity development in the HSCP, an example of SEM images have been provided. **Figure 6.4** shows the microstructure of cement paste of the three w/b ratios at constant SF replacement amount 6%. As illustrated in the figure, the increase of the porosity and pore size are significantly related to the w/b ratio, in which the porosity and the large size of pores increase by increasing w/b ratio. Thus, this observation could be an interpretation of the changes in the optimum amounts of SF with changing w/b ratio.

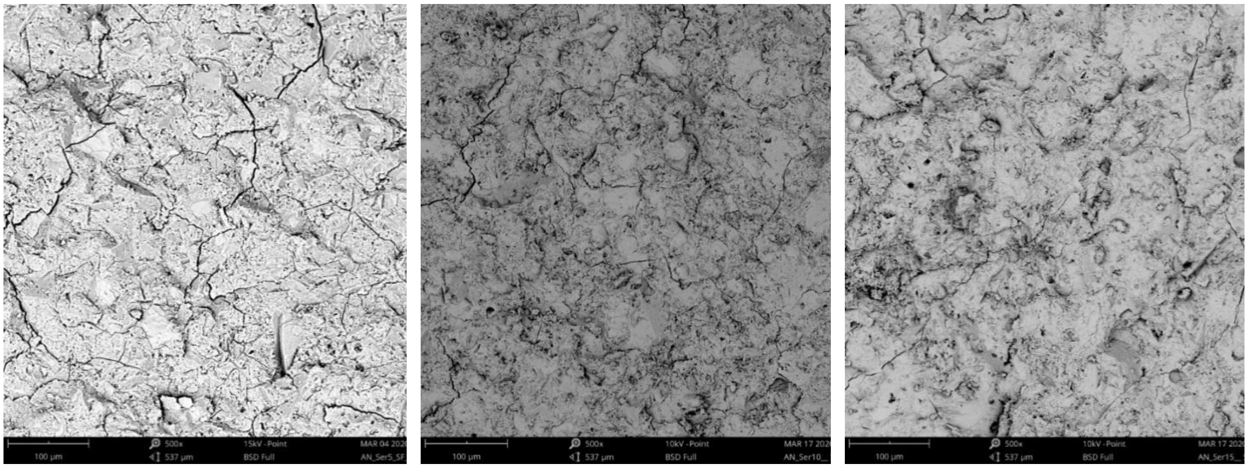

a) b) c)

Figure 6.4 *SEM images showing porosity development in HSCP at a fixed SF replacement (6%) as a function of w/b ratio: a) 0.3 w/b, b) 0.35 w/b, c) 0.4 w/b*

The porosity and pores content due to the changing of w/b ratio are also calculated by using CT measurement. The comparison has been conducted between mixture prepared with 0.3 w/b ratio and mixture prepared with 0.35 w/b ratio at fixed SF replacement (6%), as presented in **Figure 6.5**. Results show an increase in the porosity of hardened cement paste as the w/b ratio increases.

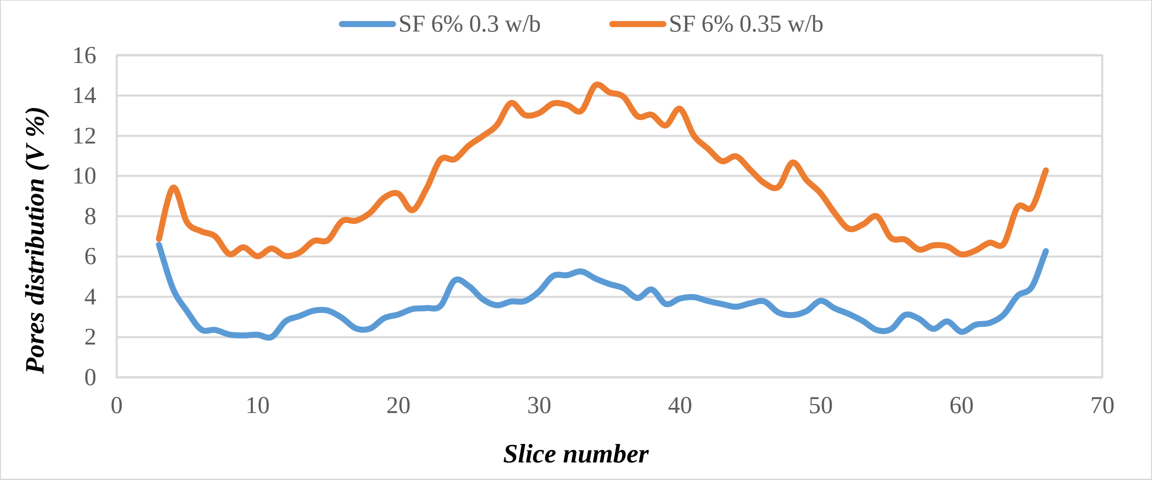

Figure 6.5 *The CT pores results of sample contains 6% of SF of 0.35 w/b ratio at 20 °C*

The effect of changing w/b ratio on the compressive strength of HSCP using CEM I 42.5 N incorporated with MK or SF is investigated herein. In addition, the effect of changing w/b ratio is also investigated on the compressive strength of HSCP using CEM I 52.5 N incorporated with MK only. Results, shown in **Figure 6.6,** show that value of the optimum replacement amount of MK or SF increases as the w/b ratio increases. This result has been justified by the high porosity of the mixes due to high w/b ratio, in which the higher the porosity of the mixture is the higher the value of the fine material is required.

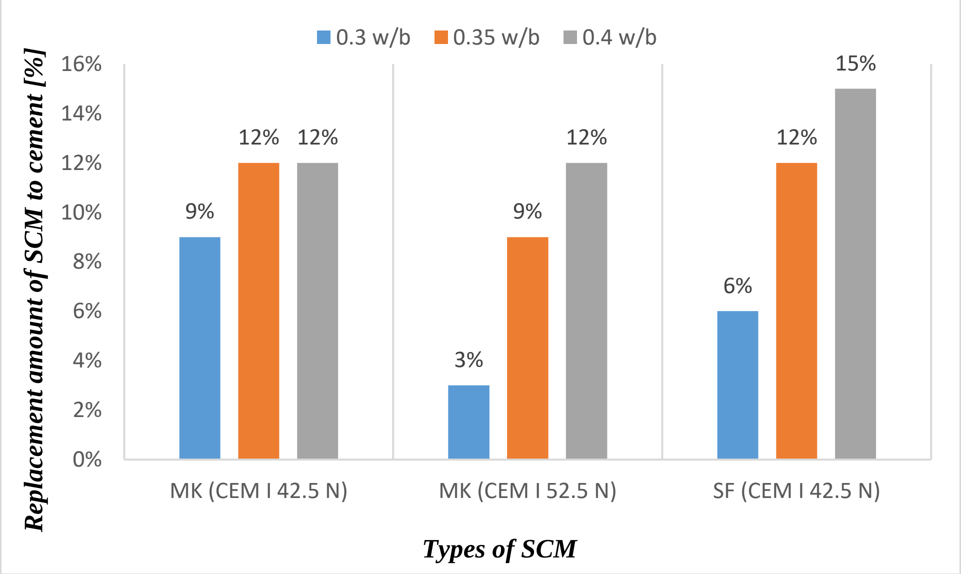

Figure 6.6 *The optimum replacements of MK and SF in function of w/b ratio*

CHAPTER 7: CONCLUSIONS

More than 3200 specimens of HSCP partially incorporated by amounts of SCM have been tested at the current study. Several research papers and books' chapters have been studied and served as useful documents in achieving all chapters of the Thesis. The constituent materials and the components of the cement paste were thoroughly investigated after being exposed to elevated temperatures. Three SCM were investigated, namely: metakaolin (MK), silica fume (SF), and fly ash (FA). The variable parameters that were tested at the current study included: Six different replacements of SCM (0%, 3%, 6%, 9%, 12%, and 15%), two types of cement fineness (CEM I 42.5 N and CEM I 52.5 N), eight temperature levels (20, 50, 150, 300, 400, 500, 800, and 900 °C), three water to binder ratio (0.3, 0.35, and 0.4), and type of mechanical properties (compressive and bending strength). The main research findings are given below:

Results of MK mixtures based on CEM I 42.5 N

- By studying the physical properties at the current study, MK has a significant influence on the surface cracking due to elevated temperatures. The more the paste contains MK the less the cracks have occurred.
- At ambient temperature, optimum replacements of MK were 12%, 6% and 6% for cement paste of the w/b ratio of 0.3, 0.35 and 0.4, respectively. Values of compressive strength tests have ranges from 55 MPa to 118 MPa depending on the difference of w/b ratio and the SCM content.
- RRCS of the reference mixtures showed weak performance at elevated temperatures, in which RRCS were 24% and 21% after exposure to 500 and 800 °C, respectively.
- Regarding w/b ratio 0.3, RRCS for the mixture containing 9% of MK has shown the highest value compared to other replacements after exposure to elevated temperatures.
- Regarding w/b ratios 0.35 and 0.4, RRCS for the mixtures containing 12% of MK have shown the highest values compared to other ratios after exposure to elevated temperatures.
- RRBS for the mixtures containing 12% of MK have shown the highest values compared to other replacements after exposure to elevated temperatures for all w/b ratios.
- RRBS of the reference mixtures showed weak performance after exposure to elevated temperatures, in which RRBS were 8% and 4% after exposure to 500 and 800 °C, respectively.
- Changing the value of w/b ratio has a significant effect on the optimum replacement of MK at both ambient and elevated temperatures.
- The amount of $Ca(OH)_2$ and the amount of $CaCO_3$ were captured to be responsible for the residual compressive strength deterioration using measurements of TG/DTA. In addition, the loss of mass caused by the decomposition of $Ca(OH)_2$ and $CaCO_3$ compounds is decreased in the presence of MK.
- Presence of MK increases the strength and protects the structure of the paste after exposure to elevated temperature, by decreasing the amount of $Ca(OH)_2$ and forming CSH and CASH by the pozzolanic reaction. This result is confirmed by SEM images.

Results of MK mixtures based on CEM I 52.5 N

- Changing the cement fineness affects the performance of hardened cement paste at ambient and elevated temperatures. Meanwhile, the behaviour of mixtures of MK is affected by the fineness of the cement.
- At ambient temperature, MK inclusion has insignificant influence on the compressive strength results particularly at low w/b ratio. However, the optimum replacements of MK at ambient temperature were 9%, 6%, and 6% in cement paste with w/b a ratio of 0.3, 0.35, and 0.4, respectively.
- Regarding w/b ratio 0.3, RRCS for the mixture containing 3% of MK has shown the highest value compared to other ratios after exposure to elevated temperatures.
- Regarding w/b ratio 0.35, RRCS for the mixture containing 9% of MK has shown the highest value compared to other ratios after exposure to elevated temperatures.
- Regarding w/b ratio 0.4, RRCS for the mixture containing 12% of MK has shown the highest value compared to other ratios after exposure to elevated temperatures.
- For bending results at elevated temperature, the mixtures containing a high amount of MK is susceptible to elevated temperatures. Mixture with 3% of MK significantly improved the RRBS. likewise, the optimum replacement of MK does not change with changing the w/b ratio to 0.35 and 0.4 w/b.

SF group results

- At ambient temperature, compressive strength of mixtures containing SF have generally higher values in mixes containing high w/b amount compared to mixtures with low w/b. The optimum replacements were 3%, 3%, and 6% for 0.3, 0.35, and 0.4 w/b ratio respectively. Values of compressive strength tests have ranges from 55 MPa to 113 MPa depending on the difference of w/b ratio and the SF content.
- For mixtures of 0.30 w/b, cement paste specimens that contain 6% SF possess the highest RRCS after exposure to elevated temperatures. Results show that values of RRCS are 97% and 64% after exposure to temperatures 500 °C and 800 °C, respectively.
- For mixtures of 0.35 w/b, cement paste specimens that contain 12% SF possess the highest RRCS after exposure to elevated temperatures. Results show that values of RRCS are 84% and 53% after exposure to temperatures 500 °C and 800 °C, respectively.
- For mixtures of 0.40 w/b, cement paste specimens that contain 15% SF possess the highest RRCS after exposure to elevated temperatures. Results show that values of RRCS are 77% and 51% after exposure to temperatures 500 °C and 800 °C, respectively.
- The optimum dosages are limited by the w/b ratio, in which at low w/b the specimens showed cracks as a result of dense microstructure. Furthermore, the amount of optimum SF is increased with the increase of w/b due to the increase of porosity.
- RRBS for the the optimum replacements were 3%, 3%, 6% for 0.3, 0.35, and 0.4 w/b, respectively.

FA group results

- At ambient temperature, compressive strength of mixtures containing FA have generally higher values in mixes containing high amount of w/b compared to mixtures with low amount of w/b. Values of compressive strength tests have ranges from 55 MPa to 123 MPa depending on the difference of w/b ratio and the FA content. The optimum replacements were 9%, 9%, and 6% for 0.3, 0.35, and 0.4 w/b ratios respectively.
- For mixtures of 0.30 w/b, cement paste specimens that contain 15% FA possess the highest RRCS after exposure to elevated temperatures. Results show that values of RRCS are 95% and 57% after exposure to temperatures 500 °C and 800 °C, respectively.
- For mixtures of 0.35 w/b, cement paste specimens that contain 15% FA possess the highest RRCS after exposure to elevated temperatures. Results show that values of RRCS are 67% and 46% after exposure to temperatures 500 °C and 800 °C, respectively.
- For mixtures of 0.40 w/b, cement paste specimens that contain 15% FA possess the highest RRCS after exposure to elevated temperatures. Results show that values of RRCS are 69% and 51% after exposure to temperatures 500 °C and 800 °C, respectively.
- For bending results at elevated temperature, mixtures containing 15% of FA significantly improved the RRBS regardless changing in the w/b ratio.

General conclusions

- The comparison of the used SCM from the perspective of heat resistance has been considered. SF cement paste specimens have shown higher heat resistance values than of MK or FA by approximately 8 and 7%, respectively.
- The effect of changing the fineness of cement is significant. The optimum value of the RRCS for MK mixtures using CEM I 42.5 N is shifted from 9% to 3% when using CEM I 52.5 N.
- Reference mixture using CEM I 52.5 N showed higher heat resistance than the reference mixture with CEM I 42.5 N. The increase in the heat resistance was higher by about 120%.
- Changing the w/b ratio has resulted in changing the optimum SCM replacements at elevated temperatures.
- The morphology of powder particles has an effect on the optimum replacement amounts as well as on the heat resistance. As SF is finer than the other SCM, optimum values of RRCS for SF has higher values than optimum values of RRCS for MK or FA.

CHAPTER 8: NEW SCIENTIFIC RESULTS

Several parameters have been investigated on the residual mechanical properties of HSCP after exposure to elevated temperature. These parameters include different types and ratios of SCM, cement fineness, level of elevated temperature, and different w/b ratios. All tests are carried out at the age of 90 days in a cold state in terms of compressive and bending strength tests. The relative residual compressive strength (RRCS) is expressed by the division of the residual strength for each level of temperature to residual strength of the same mixture at 20 °C. The following NSR are related to the main objectives of the study.

NSR 1: Influence of SCM on the mechanical properties of HSCP after exposure to elevated temperatures

A total of 48 mixtures of HSCP made of CEM I 42.5 N have been investigated at the current study. Results of the following NSR are corresponded to compressive strength tests for three types of SCM, i.e., MK, SF, and FA. Since the factor of w/b ratio has a separate section in the NSR (NSR 2.3), only the results of w/b of 0.30 have been considered herein.

The optimum replacement of SCM is considered to be the highest value of the relative residual strength at temperatures of 500 and 800 °C. In addition, the heat resistance method (area under the curve) is used to support the results of the optimum replacements.

1.1: I experimentally proved that incorporating MK material as a partial replacement of cement mass enhances the mechanical properties of cement paste after exposure to elevated temperatures. As a result, 9% of MK replacement to cement has been considered to be the optimum value, increasing the strength by about 52% and 39%, compared to the reference samples exposed to the same temperatures, in terms of RRCS after exposure to 500 and 800 °C, respectively [1, 3, 5, 16, 17].

Figures 4.3 and **4.6** show the results of the compressive strength tests and the measured heat resistance, respectively. Results are supported by physical and chemical investigations. The physical observations have shown that the presence of MK decreases the size and number of cracks keeping the body of HSCP coherent compared to the reference mixture that showed several disintegrations **Figures 4.2**. The chemical investigations have been conducted by different means of TG/DTA (**Figures 4.7**) and SEM (**Figures 4.8**) on the optimum replacement of MK (9%) and the reference mixture (0%). Results showed that the presence of MK decreases the harmful effect of $Ca(OH)_2$ decomposition after exposure to elevated temperature. The replacements amount of MK above the optimum replacement (12% and 15%) showed less RRCS compared to the optimum replacement (9%) after exposure to elevated temperature. This could be attributed to the high dense structure provided at high MK replacements which induce internal cracking.

1.2: I experimentally proved that incorporating SF material as a partial replacement of cement mass enhances the mechanical properties of cement paste after exposure to elevated temperatures. As a result, 6% of SF replacement to cement has been considered to be the optimum value, increasing the strength by about 73% and 43%, compared to the reference samples exposed to the same temperature, in terms of RRCS after exposure to 500 and 800 °C, respectively [12, 14, 16, 17].

Figures 4.14 and **4.17** show the results of the compressive strength tests and the measured heat resistance, respectively. Results are supported by physical, and chemical investigations. The physical properties have been conducted using CT measurements on the optimum and reference mixtures (**Figure 4.20**). Results have shown that the presence of SF decreases the porosity compared to the reference mixture which showed several disintegrations after exposure to elevated temperatures. The chemical investigations conducted by TG/DTA (**Figure 4.18**) and SEM (**Figure 4.19**) have shown that the presence of SF decreases the harmful effect of $Ca(OH)_2$ decomposition after exposure to elevated temperature.

From another hand, results showed that the highest value of the RRCS at temperature 500 °C is related to 6% replacement of SF whereas at temperature 800 °C, 9% replacement of SF has been observed to be slightly higher than 6% replacement as shown **Figures 4.14**. However, by measuring the heat resistance for all mixtures, 6% replacement of SF has been found to be the optimum value **Figures 4.17**.

1.3: I experimentally proved that incorporating FA material as a partial replacement of cement mass enhances the mechanical properties of cement paste after exposure to elevated temperatures. As a result, 15% of FA replacement to cement has been considered to be the optimum value, increasing the strength by about 71% and 36%, compared to the reference samples exposed to the same temperature, in terms of RRCS after exposure to 500 and 800 °C, respectively [16, 17].

Figures 4.26 and **4.29** show the results of the compressive strength tests and the measured heat resistance, respectively. Results are supported by physical, and chemical investigations. The physical properties have been conducted using CT measurements on the optimum and reference mixtures (**Figure 4.32**). Results have shown that the presence of FA decreases the porosity compared to the reference mixture which showed several disintegrations after exposure to elevated temperatures. The chemical investigations conducted by TG/DTA (**Figure 4.30**) and SEM (**Figure 4.31**) have shown that the presence of FA decreases the harmful effect of $Ca(OH)_2$ decomposition after exposure to elevated temperature. Results showed that the highest values of the RRCS and heat resistance for all mixtures are related to 15% replacement of FA.

1.4: I experimentally proved that elevating temperatures up to 800 °C has changed the optimum replacements of SCM compared to the optimum replacements at ambient temperatures. This result is valid for MK, SF, and FA as long as compressive strength is concerned [1, 14].

The amounts of optimum replacements of the three SCM after exposure to elevated temperatures are higher than amounts of optimum replacements at ambient temperatures. The difference between the optimum replacements of ambient and elevated temperatures could be attributed to an important reason; at elevated temperatures the required amounts of SCM to decrease the amount of $Ca(OH)_2$ are higher than amounts of SCM needed at ambient temperature (**Figure 4.37**). All values confirmed the previous observation except the group of MK with 0.30 w/b ratio.

NSR 2: Parameters affecting the behaviour of SCM on the HSCP after exposure to elevated temperatures.

Two parameters were considered regarding the behaviour of SCM during the tests; cement fineness represented by testing two grades of cement (CEM I 42.5 N and CEM I 52.5 N), and three ratios of w/b (0.30, 0.35 and 0.40).

2.1: By studying two different grading fineness of ordinary Portland cement (CEM I 42.5 N and CEM I 52.5 N), I have demonstrated that the value of the optimum replacement of MK after exposure to elevated temperatures decreases as the cement fineness increases. This result is valid at w/b ratios 0.30 and 0.35 as long as compressive strength is concerned [1, 7, 8, 13, 17].

The RRCS has shown that the increase in the fineness of cement decreases the amount of MK needed for the optimum value. This observation is confirmed for both 0.30 and 0.35 of the w/b ratios. Using MK as a fine material blended with fine cement (CEM I 52.5 N) have limitations due to the vulnerability to disintegration of the mix induced by the high densification. This result is more pronounced at low w/b ratio and high elevated temperatures yet, insignificant at relatively high w/b ratio (0.40), as shown in **Figure 5.9**.

2.2: By studying two different grading fineness of ordinary Portland cement (CEM I 42.5 N and CEM I 52.5 N) on reference mixtures, I have demonstrated that the value of the heat resistance of HSCP after exposure to elevated temperatures (up to 900 °C) increases as the cement fineness increases. This result is valid for w/b ratios of 0.30, 0.35, and 0.40 as long as compressive strength is concerned [1, 13, 17].

See results in **Figure 5.11**.

2.3: By studying three different w/b ratios (0.30, 0.35, and 0.40) on the compressive strength of the HSCP incorporated with SCM, I have demonstrated that the value of the optimum replacement amount of SCM after exposure to elevated temperatures increases as the w/b ratio increases. This result is valid for MK and SF as SCM [1, 12, 13, 14].

I have experimentally investigated the effect of changing w/b ratio on the compressive strength of HSCP using CEM I 42.5 N incorporated with MK or SF. In addition, the effect of changing w/b ratio is also investigated on the compressive strength of HSCP using CEM I 52.5 N incorporated with MK only. Results, shown in **Figure 6.6**, showed that value of the optimum replacement amount of MK or SF increases as the w/b ratio increases. This result has been justified by the high porosity of the mixes due to high w/b ratio, in which the higher the porosity of the mixture is the higher the value of the fine material is required.

NSR 3: A comparison between the behaviour of HSCP and high strength concrete after exposure to elevated temperatures.

The finding in this section provides a link between the results obtained from the studies of hardened cement paste and the results obtained from concrete. The relationship is obtained by applying the optimum replacement of MK in hardened cement paste to produce HSC. Production of heat-resistant hardened cement paste is of a great chance to enhance the heat-resistance of HSC.

3.1 By applying the obtained optimum replacement of MK of cement paste (9%) in concrete mixture, I have experimentally proved that the values of compressive strength of concrete are in a good agreement with the values of compressive strength of hardened cement paste. This result is limited to one type of cement (CEM I 52.5 N), one w/b (0.35), and one type of aggregate (normal river aggregate) [18].

Cement paste has unstable conditions in concrete during heating due to several chemical and physical changes, particularly from 60 °C to 800 °C *(Khoury, 1995)*. Thus, the heat-resistance hardened cement pastes have chances to significantly enhance the heat-resistance properties of concrete. From our results, for mixtures of 0% MK, the ratios of concrete mixtures (HSC) to the cement paste mixtures (HSCP) are 1.08 and 2.69 at 20 and 800 °C, respectively. For mixtures containing optimum MK replacement (9% of MK), the ratios of concrete to cement paste are 1.15 and 0.96 at 20 and 800 °C, respectively. This indicates the compatibility between concrete and cement paste obtained by the presence of MK at elevated temperatures, as shown in **Figure 5.15**.

3.2: By using scanning electron microscope, I proved that presence of MK significantly enhances the interfacial transition zone between mortar and aggregate for the high strength concrete. This result is limited to one type of cement (CEM I 52.5 N), one w/b (0.35), and one type of aggregate (normal river aggregate) [18].

The results are obtained by testing two types of concrete mixes (reference mixture and mixture containing 9% of MK). Using MK enhances the compressive and bending strength results at all levels of temperatures, as shown in **Figures 5.12** and **5.13**. Besides, the conducted tests for the mechanical properties are supported by SEM images as shown in **Figures 5.14**. Images clearly showed that presence of MK has mitigated the borderline between the mortar and the aggregate, enhancing the ITZ. This could be as a result of the filler effect and pozzolanic reaction provided by MK.

CHAPTER 9: FUTURE PERSPECTIVES

This Thesis has used different by-product waste powder materials to produce “green version” of high strength blended cement paste. This work can be used as a basis for further research regarding the following:

- Study the durability of high strength concrete containing MK, SF, and FA such as freeze/thaw resistance and providing additional relationships between its properties.
- Analytical studies on the life cycle of the Green HSC based on SCM with sustainability and economic values in mind.
- Additional investigations for other by-product materials which are available in different countries.
- Application of the same obtained optimum SCM mixtures on structural elements and study of the behaviour from the bond, and fracture perspective.
- Using the studied by-product material on recycled aggregate concrete and improving its performance.

LIST OF PUBLICATION

1. **Abdelmelek, N**. and Lubloy, E., 2020. “Evaluation of the mechanical properties of high-strength cement paste at elevated temperatures using metakaolin”. Journal of Thermal Analysis and Calorimetry, pp.1-15.
2. Balázs, G.L., Kopecskó, K., Alimrani, N., **Abdelmelek, N**. and Lublóy, É., 2018. “Fire Resistance of Concretes with Blended Cements”. In High Tech Concrete: Where Technology and Engineering Meet (pp. 1420-1427). Springer, Cham.
3. **Abdelmelek, N**. and Lublóy, É., 2017. “Improved fire resistance by using different dosages of metakaolin”. 12 th Central European Congress on Concrete Engineering. 31 August to 1st September 2017. 675p. Conference location, time: Tokaj, Hungary, FIB Magyar Tagozata, 2017. pp. 240-246. http://fib.bme.hu/konyvek/ccc2017.pdf
4. Balázs, G.L., Kopecskó, K., Alimrani, N., **Abdelmelek, N**., Lublóy, É. 2017. “Fire Resistance of Concretes with Blended Cements”. Proceedings, “High Tech Concrete: Where Technology and Engineering Meet” (Eds. Hordijk, D.A., Lukovic, M.), fib Symposium 12-14 June 2017 Maastricht, The Netherlands, Springer, pp. 1420-1427. www.springer.com
5. **Abdelmelek, N**., Lublóy, É. 2018. “Effect of Metakaolin on Mechanical Properties Of Cement Paste Exposed To Elevated Temperatures”. Proceeding of the 12th fib International PhD Symposium. PP 3-11, 2018, Czech Technical University in Prague, Prague, Czech Republic. http://phdsymp2018.eu/dwn/Proceedings
6. Éva, Lublóy., György, Baláz.s, Salem, G. Nehme., Katalin, Kopecskó., **Nabil Abdelmelek**., Viktor, Hlavicka. 2018. “A Betonfelület Leválásának Hatása A Szerkezet Tűzállóságára”. EPKO 2018, 22nd International Conference on Civil Engineering and Architecture. pp 141-146.
7. **Abdelmelek, N**. and Lublóy, É. 2019. “Evaluating compressive strength of cement paste at elevated temperatures using metakaolin”. Third international fire safety symposium 2019, in 5-7 June, Canada, PP 311-319.
8. **Abdelmelek, N**. and Lublóy, É. 2019. “Behaviour of high strength paste prepared with metakaolin at elevated temperature”. *fib* Symposium 2019, May 27-29, Krakow, Poland, PP. 663-665.
9. Alimrani, N., **Abdelmelek, N**., Balázs, G.L. Lublóy, É. 2017. “Fire behaviour of concrete – influencing parameters”, Journal Concrete Structures, 2017, Vol 18, pp. 36- 44. http://fib.bme.hu/folyoirat/cs/cs
10. **Abdelmelek, N**. and Lublóy, É. 2018. “Different properties of steel fibres reinforced concrete-review article”. Journal Concrete Structures 2018. Vol 19, PP 8-13. http://www.fib.bme.hu/folyoirat/cs/cs2018/cs2018-2.pdf

11. Balázs, L.G., Lublóy, É., Kopecskó, K., Nehme, S.G., Nemes, R., Kausay, T., Józsa, Zsuzsanna., Hlavička, V., Kakasy, G., Tóth, P., Nyíri, Sz., Lizakovszky, G., Molnár, T., Czirják, J., Földes, T., **Abdelmelek, N**., Abed, M., Alimrani ,N. 2017. "Influence of fire on the structure of concrete – State-of-the-Art Report". (Tűz hatásai a beton szerkezetére - helyzetfelmérő jelentés"), Journal Vasbetonépítés, 2017, Vol 2, pp. 26-32. http://fib.bme.hu/folyoirat/vb/vb2017_3/Vb2017_3_pp46-59.pdf
12. **Abdelmelek, N**. and Lublóy, É. "Properties of high strength paste mixed with silica fume at high temperatures". *fib* Symposium 2020**,** 22-24 November 2020, Shanghai, China. (Proceeding under process)
13. **Abdelmelek, N**. and Lublóy, É. "Heat resistant high strength cement paste". Journal of Construction and Building Materials**, (S**ubmitted)
14. **Abdelmelek, N**. and Lublóy, É. "Effects of Elevated Temperatures on the Properties of High Strength Cement Paste Containing Silica Fume". Journal of Periodica Polytechnica Civil Engineering Journal, (Submitted)
15. Tufail, R.F., Feng, X., Farooq, D., **Abdelmelek, N**. and Lublóy, É. "Behavior and strength predictions for CFRP confined rubberized concrete under axial compression". Journal of Periodica Polytechnica Civil Engineering Journal, (Accepted)
16. **Abdelmelek, N**. and Lublóy, É. "Flexural Strength of Silica Fume, Fly Ash or Metakaolin of Hardened Cement Paste after Exposure to Elevated Temperatures". Journal of Thermal Analysis and Calorimetry, (Submitted)
17. **Abdelmelek, N**. and Lublóy, É. "The impact of metakaolin, silica fume and fly ash on the heat resistance of high strength cement paste". Journal of Thermal Analysis and Calorimetry, (Submitted)
18. **Abdelmelek, N**., Alimrani, N., Krelias, N., Lublóy, É. "High Strength Concrete Based-Metakaolin Exposed to Elevated Temperatures". Journal of King Saud University - Engineering Sciences, (Submitted)

References

Abdelrazaq, A., 2012. Validating the structural behavior and response of Burj Khalifa: Synopsis of the full scale structural health monitoring programs. International Journal of High-Rise Buildings, 1(1), pp.37-51.

Abdulmatin, A., Khongpermgoson, P., Jaturapitakkul, C. and Tangchirapat, W. 2018. Use of eco-friendly cementing material in concrete made from bottom ash and calcium carbide residue. Arabian Journal for Science and Engineering, 43(4), pp.1617-1626.

Abrams, M.S., 1971. Compressive strength of concrete at temperatures to 1600F. Temperature and concrete, 25, pp.33-58.

ACI Committee 234, 2006. Guide for the Use of Silica Fume in Concrete. April 13, 2006.

ACI committee., 363. Guide for the use of silica fume in concrete. American Concrete Institute, Detroit, 1994.

Agenda June 1992. the Rio Declaration on Environment and Development, the Statement of Forest Principles, the United Nations Framework Convention on Climate Change and the United Nations Convention on Biological Diversity. United Nations Conference on Environment and Development (UNCED). Rio de Janeiro.

Ahmad, M.R. and Chen, B. 2020. Microstructural characterization of basalt fiber reinforced magnesium phosphate cement supplemented by silica fume. Construction and Building Materials, 237, p.117795.

Ahmaruzzaman, M. 2010. A review on the utilization of fly ash. Progress in energy and combustion science, 36(3), pp.327-363.

Aïtcin, P.C., 1998. High performance concrete. CRC press.

Alcamand, H.A., Borges, P.H., Silva, F.A. and Trindade, A.C.C. 2018. The effect of matrix composition and calcium content on the sulfate durability of metakaolin and metakaolin/slag alkali-activated mortars. Ceramics International, 44(5), pp.5037-5044.

Alimrani, N., Abdelmelek, N., György, L.B., Lublóy, E. (2017). Fire Behaviour of Concrete – Influencing Parameters. Concrete Structures, Hungarian Group of fib, Vol (18), pp. 30-35. http://fib.bme.hu/folyoirat/cs/cs2017.pdf

American Concrete Institute (ACI) Committee 363. 2005. State-of-the-art report on high-strength concrete. ACI 363R-92. In: ACI manual of concrete practice part I; 2005.

Aslani, F. and Bastami, M. 2011. Constitutive relationships for normal-and high-strength concrete at elevated temperatures. ACI Materials Journal, 108(4), p.355.

ASTM - C618–8a. 2009. Standard Specification for Coal Fly Ash and Raw or Calcined Natural Pozzolan for Use in Concrete. ASTM International, USA.

ASTM (2003). Standard specification for coal fly ash and raw or calcined natural pozzolan for use in concrete. ASTM C 618-03, Philadelphia.

ASTM E1868. 2010. Standard Test Method for Loss-On-Drying by Thermogravimetry. ASTM International, West Conshohocken, PA.

Aydın, S. 2008. Development of a high-temperature-resistant mortar by using slag and pumice. Fire safety journal, 43(8), pp.610-617.

Aydın, S. and Baradan, B. 2007. Effect of pumice and fly ash incorporation on high temperature resistance of cement based mortars. Cement and Concrete Research, 37(6), pp.988-995.

Baker, B. and Pawlikowski, J. 2015. The Design and Construction of the World's Tallest Building: The Burj Khalifa, Dubai. Structural Engineering International, 25(4), pp.389-394.

Balázs, G.L., Czoboly, O., Lublóy, É., Kapitány, K. and Barsi, Á. 2017. Observation of steel fibres in concrete with Computed Tomography. Construction and Building Materials, 140, pp.534-541. https://doi.org/10.1016/j.conbuildmat.2017.02.114

Balázs, G.L., Kopecskó, K., Alimrani, N., Abdelmelek, N. and Lublóy, É. 2018. Fire Resistance of Concretes with Blended Cements. In High Tech Concrete: Where Technology and Engineering Meet. Springer, Cham, pp. 1420-1427.

Bangi, M.R. and Horiguchi, T. 2011. Pore pressure development in hybrid fibre-reinforced high strength concrete at elevated temperatures. Cement and Concrete Research, 41(11), pp.1150-1156.

Bastami, M., Chaboki-Khiabani, A., Baghbadrani, M. and Kordi, M. 2011. Performance of high strength concretes at elevated temperatures. Scientia Iranica, 18(5), pp.1028-1036.

Bažant, Z.P., Kaplan, M.F. and Bazant, Z.P. 1996. Concrete at high temperatures: material properties and mathematical models.

Behnood, A. and Ghandehari, M. 2009. Comparison of compressive and splitting tensile strength of high-strength concrete with and without polypropylene fibers heated to high temperatures. Fire Safety Journal, 44(8), pp.1015-1022.

Behnood, A. and Ziari, H. 2008. Effects of silica fume addition and water to cement ratio on the properties of high-strength concrete after exposure to high temperatures. Cement and Concrete Composites, 30(2), pp.106-112.

Belkacem, T., Hocine, C., Hacene, H., and Resheidat, M. 2008. Effects of Cooling Condition on Residuals Properties of High- Performance Concrete at High Temperature. Proc. of Inter. Conf. on Construction and Building Materials (ICCBT - 2008) A-11 135-142.

Berodier, E.S.K.S.G. and Scrivener, K. 2014. Understanding the Filler Effect on the Nucleation and Growth of C-S-H. Journal of the American Ceramic Society, 97(12), pp.3764-3773.

Bettelini, M., Neuenschwander, H., Henke, A., Gagliardi, M. and Steiner, W. 2004. The fire in the St Gotthard tunnel of October 24, 2001. SP RAPPORT-STATENS PROVNINGSANSTALT, pp.49-68.

Bhanja, S. and Sengupta, B. 2005. Influence of silica fume on the tensile strength of concrete. Cement and concrete research, 35(4), pp.743-747.

Birchall, J.D., Howard, A.J. and Kendall, K. 1981. Flexural strength and porosity of cements. Nature, 289(5796), pp.388-390.

Bredy, P., Chabannet, M. and Pera, J. 1988. Microstructure and porosity of metakaolin blended cements. MRS Online Proceedings Library Archive, 136, 431 – 436.

BS 476, 1987. Fire tests on building materials and structures. BS476 Parts 20 to 22, British Standards Institution, UK.

BS EN 12620:2002+A1:2008. 2008. Aggregates for Concrete. BSI, British Standards Institution.

Caldarone, M.A. 2008. High-strength concrete: a practical guide. CRC Press; Combridge.

Cassagnabere, F., Diederich, P., Mouret, M., Escadeillas, G. and Lachemi, M. 2013. Impact of metakaolin characteristics on the rheological properties of mortar in the fresh state. Cement and Concrete Composites, 37, pp.95-107.

Castellote, M., Alonso, C., Andrade, C., Turrillas, X. and Campo, J. 2004. Composition and microstructural changes of cement pastes upon heating, as studied by neutron diffraction. Cement and concrete research, 34(9), pp.1633-1644.

Chan, S.Y., Peng, G.F. and Chan, J.K. 1996. Comparison between high strength concrete and normal strength concrete subjected to high temperature. Materials and Structures, 29(10), p.616.

Chan, S.Y.N., Luo, X. and Sun, W. 2000. Effect of high temperature and cooling regimes on the compressive strength and pore properties of high performance concrete. Construction and Building Materials, 14(5), pp.261-266.

Chan, S.Y.N., Peng, G.F. and Anson, M. 1999b. Fire behavior of high-performance concrete made with silica fume at various moisture contents. Materials Journal, 96(3), pp.405-409.

Chan, Y.N., Peng, G.F. and Anson, M. 1999a. Residual strength and pore structure of high-strength concrete and normal strength concrete after exposure to high temperatures. Cement and concrete composites, 21(1), pp.23-27.

Chanvillard, G. 1999. The concrete material: General knowledge. Aĺeas.115–39.

Chen, B. and Liu, J. 2004. Effect of aggregate on the fracture behavior of high strength concrete. Construction and Building Materials, 18(8), pp.585-590.

Chowdhury, S. H. 2014. Effect of elevated temperature on mechanical properties of high strength concrete. in ST Smith (ed.), 23rd Australasian Conference on the Mechanics of Structures and Materials (ACMSM23), vol. II, Byron Bay, NSW, 9-12 December, Southern Cross University, Lismore, NSW, pp. 1077-1082. ISBN: 9780994152008.

Cohen, M.D., Olek, J. and Dolch, W.L. 1990. Mechanism of plastic shrinkage cracking in portland cement and portland cement-silica fume paste and mortar. Cement and Concrete Research, 20(1), pp.103-119.

Colombo, M. and Felicetti, R. 2007. New NDT techniques for the assessment of fire-damaged concrete structures. Fire Safety Journal, 42(6-7), pp.461-472.

Cook, R.A. and Hover, K.C. 1999. Mercury porosimetry of hardened cement pastes. Cement and Concrete research, 29(6), pp.933-943.

Cwirzen, A. and Penttala, V. 2005. Aggregate–cement paste transition zone properties affecting the salt–frost damage of high-performance concretes. Cement and Concrete Research, 35(4), pp.671-679.

Cyr, M., Lawrence, P. and Ringot, E. 2005. Mineral admixtures in mortars: quantification of the physical effects of inert materials on short-term hydration. Cement and Concrete Research, 35(4), pp.719-730.

Delhomme, F., Ambroise, J. and Limam, A. 2012. Effects of high temperatures on mortar specimens containing Portland cement and GGBFS. Materials and structures, 45(11), pp.1685-1692.

Dinakar, P., Sahoo, P.K. and Sriram, G. 2013. Effect of metakaolin content on the properties of high strength concrete. International Journal of Concrete Structures and Materials, 7(3), pp.215-223.

Duggal, S. k. 2003. building materials, New Delhi: New Age International (P) Ltd., Publishers, 2003.

El Mir, A., Nehme, S.G. 2017. Utilization of industrial waste perlite powder in self-compacting concrete. Journal of Cleaner Production, 156, pp.507-517.

Elahi, A., Basheer, P.A.M., Nanukuttan, S.V. and Khan, Q.U.Z. 2010. Mechanical and durability properties of high performance concretes containing supplementary cementitious materials. Construction and Building Materials, 24(3), pp.292-299.

El-Diadamony, H., Amer, A.A., Sokkary, T.M. and El-Hoseny, S. 2018. Hydration and characteristics of metakaolin pozzolanic cement pastes. HBRC journal, 14(2), pp.150-158.

EN 1008. 2002. Mixing water for concrete-Specification for sampling, testing and assessing the suitability of water, including water recovered from processes in the concrete industry, as mixing water for concrete.

EN 1992-1-2. 2004. Eurocode 2: Design of concrete structures-Part 1-2: General rules-structural fire design. European Committee for Standardization.

European Cement Association. 2011. Activity Report 2011. Bruxelles: CEMBUREAU. Retrieved July, 28, p.2013.

Fehérvári, S. and Nehme, S.G. 2008. Residual Properties of Hardened Cements after Thermal Shock. Radić, J, pp.02-03.

Fehérvári, S. and Nehme, S.G. 2009a. Effect of the concrete´ s component on the heat shock bearing capacity of tunnel linings. Periodica Polytechnica Civil Engineering, 53(1), pp.15-23.

Fehérvári, S. and Nehme, S.G. 2009b. Effect of Concrete Components on the Temperature Endurance of Tunnel Linings (Doctoral dissertation, Ph. D. Thesis, Budapest University of Technology and Economics, Budapest).

Felicetti, R., Gambarova, P.G., Rosati, G., Corsi, F. and Giannuzzi, G. 1996. Residual mechanical properties of high-strength concretes subjected to high-temperature cycles. In 4th International Symposium on Utilization of High-Strength/High-Prformance Concrete, , Paris, France, 1996, pp.579-588.

fib Bulletin 38. 2007. Fire design of concrete structures materials, structures and modeling. State of art report.

fib. Bulletin 46. 2008. Fire design of concrete structures structural behaviour and assessment. State-of-art report prepared by. Task Group 4.3, Document Competence Center Siegmar Kästl e.K., Germany.

Fredonia World Construction Aggregates to 2011– Demand and Sales Forecasts. 2011. Market Share, Market Size, Market leaders, Industry.

Fu, Y.F., Wong, Y.L., Poon, C.S. and Tang, C.A. 2005. Stress–strain behaviour of high-strength concrete at elevated temperatures. Magazine of Concrete Research, 57(9), pp.535-544.

Fu, Y.F., Wong, Y.L., Poon, C.S., Tang, C.A. and Lin, P. 2004. Experimental study of micro/macro crack development and stress–strain relations of cement-based composite materials at elevated temperatures. Cement and Concrete Research, 34(5), pp.789-797.

Furumura, F., Abe, T., Shinohara, Y. 1995. Mechanical Properties of High Strength Concrete at High Temperatures. Proceedings of the Fourth Weimar Workshop on High Performance Concrete: Material Properties and Design, held at Hochschule far Architektur and Bauwesen (HAB), Weimar, Germany, October 4th and 5th, 1995, pp. 237 - 254.

Gao, D., Li, X., Yang, S. 2012a. Flexural properties of fiber reinforced slag concrete after high temperature treatment. China Concrete Cement Production, 5, pp. 42-47

Gao, D., Zhao, L. and Yang, S. 2012b. Splitting Tensile Properties of Fiber Reinforced Ground Granulated Blast Furnace Slag Concrete at High Temperatures. Journal of the Chinese Ceramic Society, 40(5), pp.677-684.

Ghandehari, M., Behnood, A. and Khanzadi, M. 2010. Residual mechanical properties of high-strength concretes after exposure to elevated temperatures. Journal of materials in Civil Engineering, 22(1), pp.59-64.

Gómez-Zamorano, L.Y. and Escalante-García, J.I. 2010. Effect of curing temperature on the nonevaporable water in portland cement blended with geothermal silica waste. Cement and Concrete Composites, 32(8), pp.603-610.

Gutteridge, W.A. and Dalziel, J.A. 1990. Filler cement: the effect of the secondary component on the hydration of Portland cement: part I. A fine non-hydraulic filler. Cement and Concrete Research, 20(5), pp.778-782.

Hager, I. 2004. Comportement à haute température des bétons à haute performance: évolution des principales propriétés mécaniques (Doctoral dissertation, École nationale des ponts et chaussées (France)).

Hager, I. 2013. Behaviour of cement concrete at high temperature. Bulletin of the Polish Academy of Sciences: Technical Sciences, 61(1), pp.145-154.

Halse, Y., Goult, D.J. and Pratt, P.L. 1984. Calorimetry and microscopy of fly ash and silica fume cement blends. In Proc. Br. Ceram. Soc. (No. 35, p. 403).

Hammer, T.A. 1995. High Strength Concrete Phase 3: Report 6.1. Compressive strength and E-modulus at elevated temperatures. (SP6 fire resistance, report 6.1). SINTEF Structures and Concrete.

Hansen, P.A. and Jensen, J.J. 1995. High-strength concrete phase 3, fire resistance and spalling behaviour of LWA beams. SP6–Fire Resistance, report, 6.

Harmathy, T.Z. 1970. Thermal properties of concrete at elevated temperatures. Journal of Materials.

Heikal, M., El-Didamony, H., Sokkary, T.M. and Ahmed, I.A. 2013. Behavior of composite cement pastes containing microsilica and fly ash at elevated temperature. Construction and building materials, 38, pp.1180-1190.

Hertz, K. 1984. Heat-induced explosion of dense concretes. Technical University of Denmark, Institute of Building Design.

Hertz, K.D. 1992. Danish investigations on silica fume concretes at elevated temperatures. Materials Journal, 89(4), pp.345-347.

Hoff, G.C., Bilodeau, A. and Malhotra, V.M. 2000. Elevated temperature effects on HSC residual strength. Concrete International, 22(4), pp.41-48.

Hooton, R.D. 1993. Influence of silica fume replacement of cement on physical properties and resistance to sulfate attack, freezing and thawing, and alkali-silica reactivity. materials Journal, 90(2), pp.143-151.

Husem, M. 2006. The effects of high temperature on compressive and flexural strengths of ordinary and high-performance concrete. Fire Safety Journal, 41(2), pp.155-163.

Ibrahim, R.K., Hamid, R. and Taha, M.R. 2012. Fire resistance of high-volume fly ash mortars with nanosilica addition. Construction and Building Materials, 36, pp.779-786.

Ismail, K.N., Hussin, K. and Idris, M.S. 2007. Physical, chemical and mineralogical properties of fly ash. Journal of Nuclear and Related Technology, 4, pp.47-51.

Ismail, M., Ismail, M.E. and Muhammad, B. 2011. Influence of elevated temperatures on physical and compressive strength properties of concrete containing palm oil fuel ash. Construction and Building Materials, 25(5), pp.2358-2364.

ISO-834. 1975. Fire resistance test-elements of building construction. International Standard ISO384, Geneva, Switzerland, 1975.

Jala, S. and Goyal, D. 2006. Fly ash as a soil ameliorant for improving crop production—a review. Bioresource Technology, 97(9), pp.1136-1147.

Janotka, I., and Bagel, L. 2003. Pore Structures Permeabilities and Compressive Strengths of Concrete at Temperatures up to 8000C. ACI Materials Journal, 99(1) 196–200.

Jia, W., Baoyuan, L., Songshan, X. and Zhongwei, W. 1986. Improvement of paste-aggregate interface by adding silica fume. In Proceedings of the 8th International Congress on the Chemistry of Cement (Vol. 3, pp. 460-465).

Juenger, M.C. and Siddique, R. 2015. Recent advances in understanding the role of supplementary cementitious materials in concrete. Cement and Concrete Research, 78, pp.71-80.

Karakurt, C. and Topçu, İ.B. 2012. Effect of blended cements with natural zeolite and industrial by-products on rebar corrosion and high temperature resistance of concrete. Construction and Building Materials, 35, pp.906-911.

KAWAI, T. 2005. State-of-the-art report on high-strength concrete in Japan–Recent developments and applications. In JSCE/VIFCEA Joint Seminar on Concrete Engineering (pp. 8-9).

Khaliq, W. 2012. Performance characterization of high performance concretes under fire conditions (Vol. 73, No. 09).

Khaliq, W. and Khan, H.A. 2015. High temperature material properties of calcium aluminate cement concrete. Construction and Building Materials, 94, pp.475-487.

Khan, M.I. 2003. Isoresponses for strength, permeability and porosity of high performance mortar. Building and Environment, 38(8), pp.1051-1056.

Khatib, J.M. 2008. Metakaolin concrete at a low water to binder ratio. Construction and Building Materials, 22(8), pp.1691-1700.

Khatib, J.M. and Wild, S. 1996. Pore size distribution of metakaolin paste. Cement and Concrete Research, 26(10), pp.1545-1553.

Khatib, J.M., Clay, R.M. 2004. Absorption characteristics of metakaolin concrete. Cement Concrete Research. 34, (1), pp. 19–29.

Khoury, G.A. 1992. Compressive strength of concrete at high temperatures: a reassessment. Magazine of concrete Research, 44(161), pp.291-309.

Khoury, G.A. 1995. Effect of heat on concrete material. Imperial college report, pp. 73.

Khoury, G.A. 2000. Effect of fire on concrete and concrete structures. Progress in Structural Engineering and Materials, 2(4), pp.429-447.

Khoury, G.A. Anderberg, Y., Both, K., Fellinger, J., Høj, N. and Majorana, C. 2007. Fib bulletin 38: Fire design of concrete structures—materials, structures and modelling, state-of-the art report. Federation internationale du beton, Lausanne, Switzerland.

Khoury, G.A., Grainger, B.N. and Sullivan, P.J. 1985. Transient thermal strain of concrete: literature review, conditions within specimen and behaviour of individual constituents. Magazine of concrete research, 37(132), pp.131-144.

Khoury, G.A., Majorana, C.E., Pesavento, F. and Schrefler, B.A. 2002. Modelling of heated concrete. Magazine of concrete research, 54(2), pp.77-101.

Khoury, G.A., Sarshar, R., Sulivan, P.J.E., Grainer, B.N. 1990. Factors affecting the compressive strength of unsealed cement paste and concrete at elevated temperatures up to 600°C. In: Proceedings of 2nd international workshop on mechanical behaviour of concrete under extreme thermal and hygral conditions. ISSN 0863-0720, pp. 89–92, Weimar.

Kim, H.S., Lee, S.H. and Moon, H.Y. 2007. Strength properties and durability aspects of high strength concrete using Korean metakaolin. Construction and building materials, 21(6), pp.1229-1237.

Kodur, V.K.R. 2000. Spalling in high strength concrete exposed to fire: concerns, causes, critical parameters and cures. In Advanced Technology in Structural Engineering (pp. 1-9).

Kodur, V.K.R. and Phan, L. 2007. Critical factors governing the fire performance of high strength concrete systems. Fire Safety Journal, 42(6-7), pp.482-488.

Kodur, V.K.R. and Sultan, M.A. 2003. Effect of temperature on thermal properties of high-strength concrete. Journal of materials in civil engineering, 15(2), pp.101-107.

Koksal, F., Gencel, O. and Kaya, M. 2015. Combined effect of silica fume and expanded vermiculite on properties of lightweight mortars at ambient and elevated temperatures. Construction and Building Materials, 88, pp.175-187.

Kosmatka, S.H. and Wilson, M.L. 2011. Design And Control Of Concrete Mix. (15th ed.), Portland. Cement. Association, Skokie, Illinois, pdf.

Kosmatka, S.H., Kerkhoff, B. and Panarese, W.C. 2002a. Fly ash, slag, silica fume, and natural pozzolans. Design and control of concrete mixtures, 13, pp.57-72.

Kosmatka, S.H., Kerkhoff, B. and Panarese, W.C. 2002b. Design and control of concrete mixtures (Vol. 5420, pp. 60077-1083). Skokie, IL: Portland Cement Association.

Kostuch, J.A., Walters, G.V. and Jones, T.R. 2000. High performance concretes incorporating metakaolin: a review. Concrete, 2(1993), pp.1799-811.

Krishna, B.V., Hussain, S.A.M. and Kumar, V.R. 2014. Ceraplast and Ceraproof Admixtures Behaviour on High Strength Concrete. International Journal of Scientific Engineering and Research (IJSER), 2(5), pp.15-19.

Kulkarni, K.S., Yaragal, S.C. and Narayan, K.B. 2011. An overview of high performance concrete at elevated temperatures. International Journal of Applied Engineering and Technology, 1(1), pp.48-60.

Kumagai, H., Saito, H., and Morita, T. 1992. Residual Mechanical Properties of High Strength Concrete Members Exposed to High Temperature - Part 3. Test on Reinforced Concrete Columns. Summaries of Technical Papers of Annual Meeting, Architectural Institute of Japan, Niigata, August (in Japanese).

Kuroda, M., Watanabe, T. and Terashi, N. 2000. Increase of bond strength at interfacial transition zone by the use of fly ash. Cement and Concrete Research, 30(2), pp.253-258.

Lau, A. and Anson, M. 2006. Effect of high temperatures on high performance steel fibre reinforced concrete. Cement and concrete research, 36(9), pp.1698-1707.

Li, Q., Li, Z. and Yuan, G. 2012. Effects of elevated temperatures on properties of concrete containing ground granulated blast furnace slag as cementitious material. Construction and Building Materials, 35, pp.687-692.

Li, Z., Ding, Z. and Zhang, Y. 2004, May. Development of sustainable cementitious materials. In Proceedings of international workshop on sustainable development and concrete technology, Beijing, China (pp. 55-76).

Liao, K.Y., Chang, P.K., Peng, Y.N. and Yang, C.C. 2004. A study on characteristics of interfacial transition zone in concrete. Cement and Concrete Research, 34(6), pp.977-989.

Lootens, D. and Bentz, D.P. 2016. On the relation of setting and early-age strength development to porosity and hydration in cement-based materials. Cement and Concrete Composites, 68, pp.9-14.

Lothenbach, B., Scrivener, K. and Hooton, R.D. 2011. Supplementary cementitious materials. Cement and concrete research, 41(12), pp.1244-1256.

Lublóy, É., Ambrus, D., Kapitány, K. and Barsi, Á. 2015. Air void distribution of asphalts determined by computed tomography. Periodica Polytechnica Civil Engineering, 59(4), pp.503-510.

Lublóy, É., Kapitány, K., Balázs, G.L., Földes, T., Hlavicka, V. and Hlavicka-Laczák, L. 2019. CT and laboratory test of the wall panels after fire load. Construction and Building Materials, 211, pp.1105-1116. https://doi.org/10.1016/j.conbuildmat.2019.03.148

Lublóy, É., Kopecskó, K., Balázs, G.L., Restás, Á. and Szilágyi, I.M. 2017. Improved fire resistance by using Portland-pozzolana or Portland-fly ash cements. Journal of Thermal Analysis and Calorimetry, 129(2), pp.925-936.

Lublóy, É., Kopecskó, K., Balázs, G.L., Szilágyi, I.M. and Madarász, J. 2016. Improved fire resistance by using slag cements. Journal of thermal analysis and calorimetry, 125(1), pp.271-279.

Luo, X., Sun, W. and Chan, S.Y.N. 2000. Effect of heating and cooling regimes on residual strength and microstructure of normal strength and high-performance concrete. Cement and Concrete Research, 30(3), pp.379-383.

Ma, Q., Guo, R., Zhao, Z., Lin, Z. and He, K. 2015. Mechanical properties of concrete at high temperature—A review. Construction and Building Materials, 93, pp.371-383.

Malhotra, V., Mehta, P. 2005. High performance, high volume fly ash concrete. materials, mixture, proportioning, properties, construction practice, and case histories. Supplementary cementing materials for sustainable development incorporated, Ottawa.

Martin, J.C., Delémont, O. and Calisti, C. 2005. Tunnel fire investigation II: The St Gotthard Tunnel fire, 24 October 2001 (pp. 53-76). Thomas Telford.

Memon, S.A., Shah, S.F.A., Khushnood, R.A. and Baloch, W.L. 2019. Durability of sustainable concrete subjected to elevated temperature–A review. Construction and Building Materials, 199, pp.435-455.

Mendes, A., Sanjayan, J. and Collins, F. 2008. Phase transformations and mechanical strength of OPC/Slag pastes submitted to high temperatures. Materials and structures, 41(2), p.345.

Mendes, A., Sanjayan, J.G., Gates, W.P. and Collins, F. 2012. The influence of water absorption and porosity on the deterioration of cement paste and concrete exposed to elevated temperatures, as in a fire event. Cement and concrete composites, 34(9), pp.1067-1074.

Merida, A. and Kharchi, F. 2015. Pozzolan concrete durability on sulphate attack. Procedia Engineering, 114, pp.832-837.

Model Code. 2010. *fib* Model Code for Concrete Structures. KGaA, Weinheim, Germany: Wiley-VCH Verlag GmbH & Co.

Morsy, M.S., Al-Salloum, Y.A., Abbas, H. and Alsayed, S.H. 2012. Behavior of blended cement mortars containing nano-metakaolin at elevated temperatures. Construction and Building materials, 35, pp.900-905.

Morsy, M.S., Alsayed, S.H. and Aqel, M. 2010. Effect of elevated temperature on mechanical properties and microstructure of silica flour concrete. International journal of civil & environmental engineering, 10(1), pp.1-6.

Morsy, M.S., Rashad, A.M. and El-Nouhy, H.A. 2009. Effect of elevated temperature on physico-mechanical properties of metakaolin blended cement mortar. Structural Engineering and Mechanics, 31(1), pp.1-10.

MSZ 4798. 2015. Hungarian standard of working community of concrete and cement manufacturers.

MSZ EN 12390-3. 2009. Testing hardened concrete. Part 3: Compressive strength of test specimens.

MSZ EN 12390-5. 2009. Testing hardened concrete. Part 5: Flexural strength of test specimens.

MSZ EN 196-2. 2013. Cement testing methods. Part 2: Chemical analysis of cement. Budapest: Magyar Szabvanyugyi Testulet, 2013.

MSZ EN 525-12. 2014. Chemical analysis of cement. Part 12: Determination of free lime content. Budapest: Magyar Szabvanyugyi Testulet.

Nadeem, A., Memon, S.A. and Lo, T.Y. 2013. Qualitative and quantitative analysis and identification of flaws in the microstructure of fly ash and metakaolin blended high performance concrete after exposure to elevated temperatures. Construction and Building Materials, 38, pp.731-741.

Nadeem, A., Memon, S.A. and Lo, T.Y. 2014. The performance of fly ash and metakaolin concrete at elevated temperatures. Construction and Building Materials, 62, pp.67-76.

Neville., and J. Brooks, J. 2010. concrete technology. Malaysia: British Libray cataloguing-in-publication data.

Nielsen, C.V. and Biéanić, N. 2003. Residual fracture energy of high-performance and normal concrete subject to high temperatures. Materials and Structures, 36(8), p.515.

Noumowe, A.N., Clastres, P., Debicki, G. and Costaz, J.L. 1996. Transient heating effect on high strength concrete. Nuclear engineering and design, 166(1), pp.99-108.

Noumowe, A.N., Siddique, R. and Debicki, G. 2009. Permeability of high-performance concrete subjected to elevated temperature (600 °C). Construction and Building Materials, 23(5), pp.1855-1861.

Ollivier, J. P., Buil, M. 1992. Concrete design: the porous structure, The durability of concrete. Presses of l'ENPC, Editors. Paris.

Ozawa, M., Uchida, S., Kamada, T. and Morimoto, H. 2012. Study of mechanisms of explosive spalling in high-strength concrete at high temperatures using acoustic emission. Construction and Building Materials, 37, pp.621-628.

Parsa, J., Munson-McGee, S.H. and Steiner, R. 1996. Stabilization/solidification of hazardous wastes using fly ash. Journal of Environmental Engineering, 122(10), pp.935-940.

PCA. 1980. High Strength Concrete-Costs More in the Truck, Costs Less in the Structure. Concrete Technology Today, No. 4, December 1980, p. 3.

Peng, G.F., Bian, S.H., Guo, Z.Q., Zhao, J., Peng, X.L. and Jiang, Y.C. 2008. Effect of thermal shock due to rapid cooling on residual mechanical properties of fiber concrete exposed to high temperatures. Construction and Building Materials, 22(5), pp.948-955.

Peng, G.F., Yang, W.W., Zhao, J., Liu, Y.F., Bian, S.H. and Zhao, L.H. 2006. Explosive spalling and residual mechanical properties of fiber-toughened high-performance concrete subjected to high temperatures. Cement and Concrete Research, 36(4), pp.723-727.

Phan, L.T. 2008. Pore pressure and explosive spalling in concrete. Materials and structures, 41(10), pp.1623-1632.

Phan, L.T. and Carino, N.J. 1998. Review of mechanical properties of HSC at elevated temperature. Journal of Materials in Civil Engineering, 10(1), pp.58-65.

Phan, L.T. and Carino, N.J. 2001. Mechanical properties of high-strength concrete at elevated temperatures (No. NIST Interagency/Internal Report (NISTIR)-6726).

Phan, L.T. and Carino, N.J. 2002. Effects of test conditions and mixture proportions on behavior of high-strength concrete exposed to high temperatures. ACI Materials Journal, 99(1), pp.54-66.

Phan, L.T. and Phan, L.T. 1996. Fire performance of high-strength concrete: A report of the state-of-the art. US Department of Commerce, Technology Administration, National Institute of Standards and Technology, Office of Applied Economics, Building and Fire Research Laboratory.

Phan, L.T., Lawson, J.R. and Davis, F.L. 2001. Effects of elevated temperature exposure on heating characteristics, spalling, and residual properties of high performance concrete. Materials and structures, 34(2), pp.83-91.

Piasta, J. 1984. Heat deformations of cement paste phases and the microstructure of cement paste. Materials and Structures, 17(6), pp.415-420.

Poon, C.S., Azhar, S., Anson, M. and Wong, Y.L. 2001a. Comparison of the strength and durability performance of normal-and high-strength pozzolanic concretes at elevated temperatures. Cement and concrete research, 31(9), pp.1291-1300.

Poon, C.S., Azhar, S., Anson, M. and Wong, Y.L. 2003. Performance of metakaolin concrete at elevated temperatures. Cement and Concrete Composites, 25(1), pp.83-89.

Poon, C.S., Kou, S.C. and Lam, L. 2006. Compressive strength, chloride diffusivity and pore structure of high performance metakaolin and silica fume concrete. Construction and building materials, 20(10), pp.858-865.

Poon, C.S., Lam, L., Kou, S.C., Wong, Y.L. and Wong, R. 2001b. Rate of pozzolanic reaction of metakaolin in high-performance cement pastes. Cement and concrete research, 31(9), pp.1301-1306.

Poon, C.S., Shui, Z.H. and Lam, L. 2004. Compressive behavior of fiber reinforced high-performance concrete subjected to elevated temperatures. Cement and Concrete Research, 34(12), pp.2215-2222.

Portland Cement Association (PCA). 2019. Supplementary Cementing Materials. Available at: https://www.cement.org/cement-concrete-applications/concrete-materials/supplementary-cementing-materials, Accessed: 12 December 2020.

Rajora, D. and Yadav, B.P. 2018. Review on Fire Safety in Car Parking. Proceedings of National Conference: Advanced Structures, Materials and Methodology in Civil Engineering (ASMMCE – 2018), 03 - 04th November 2018.

Ramachandran, V.S. and Malhotra, V.M. 1996. Superplasticizers. Concrete admixtures handbook: properties, science and technology. (pp. 410-517). William Andrew Publishing.

Ramezanianpour, A.A. and Jovein, H.B. 2012. Influence of metakaolin as supplementary cementing material on strength and durability of concretes. Construction and Building materials, 30, pp.470-479.

Rashad, A.M. and Sadek, D.M. 2017. An investigation on Portland cement replaced by high-volume GGBS pastes modified with micro-sized metakaolin subjected to elevated temperatures. International Journal of Sustainable Built Environment, 6(1), pp.91-101.

Rashid, M.A. and Mansur, M.A. 2009. Considerations in producing high strength concrete. Journal of Civil Engineering (IEB), 37(1), pp.53-63.

Razak, H.A. and Wong, H.S. 2005. Strength estimation model for high-strength concrete incorporating metakaolin and silica fume. Cement and Concrete Research, 35(4), pp.688-695.

Reynolds, S. 2009. The Future of Ferrous Slag, Market Forecasts to 2020. Pira International Ltd., Cleeve Road, Surrey KT227RU, Leatherhead, UK.

RILEM 73-SBC Committee. 1988. Siliceous by-products for use in concrete. Mater. Struct., 69, 8, p.69.

RILEM Technical Committees 129-MHT. 1995. Test Methods for mechanical properties of concrete at high temperatures, Part 1: Introduction, Part 2: Stress-strain relation, Part 3: Compressive strength for service and accident conditions. Mater Struct. 28(181):410-14.

Robert, F. and Colina, H. 2009. The influence of aggregates on the mechanical characteristics of concrete exposed to fire. Magazine of concrete research, 61(5), pp.311-321.

Rossen, J.E. 2014. Composition and morphology of CASH in pastes of alite and cement blended with supplementary cementitious materials (No. THESIS). EPFL.

Rossen, J.E., Lothenbach, B. and Scrivener, K.L. 2015. Composition of C–S–H in pastes with increasing levels of silica fume addition. Cement and Concrete Research, 75, pp.14-22.

Rostasy, F.S., Weiβ, R. and Wiedemann, G. 1980. Changes of pore structure of cement mortars due to temperature. Cement and Concrete Research, 10(2), pp.157-164.

Roy, D.M. and Gouda, G.R. 1973. Porosity-strength relation in cementitious materials with very high strengths. Journal of the American Ceramic Society, 56(10), pp.549-550.

Saad, M.N., De Andrade, W.P. and Paulon, V.A. 1982. Properties of mass concrete con taining an active pozzolan made from clay. Concrete International, 4(7), pp.59-65.

Sabir, B.B., Wild, S. and Bai, J. 2001. Metakaolin and calcined clays as pozzolans for concrete: a review. Cement and concrete composites, 23(6), pp.441-454.

Safiuddin, M. 2008. Development of self-consolidating high performance concrete incorporating rice husk ash.

Saito, H., Kumagai, H. and Morita, T. 1992. Residual mechanical properties of high strength concrete members exposed to high temperature-Part 2. Test on reinforced concrete beams. In Summaries of Technical Papers of Annual Meeting, Architectural Institute of Japan, Niigata.

Sancak, E., Sari, Y.D. and Simsek, O. 2008. Effects of elevated temperature on compressive strength and weight loss of the light-weight concrete with silica fume and superplasticizer. Cement and Concrete Composites, 30(8), pp.715-721.

Sanjayan, G. and Stocks, L.J. 1993. Spalling of high-strength silica fume concrete in fire. Materials Journal, 90(2), pp.170-173.

Sanjayan, G., and Stocks, L. 1991. Spalling of High Strength Concrete in Fire. ACI Spring Convention, March 1991, Boston, MA.

Sarshar, R. and Khoury, G.A. 1993. Material and environmental factors influencing the compressive strength of unsealed cement paste and concrete at high temperatures. Magazine of concrete research, 45(162), pp.51-61.

Sata, V., Jaturapitakkul, C. and Kiattikomol, K. 2007. Influence of pozzolan from various by-product materials on mechanical properties of high-strength concrete. Construction and Building Materials, 21(7), pp.1589-1598.

Savva, A., Manita, P. and Sideris, K.K. 2005. Influence of elevated temperatures on the mechanical properties of blended cement concretes prepared with limestone and siliceous aggregates. Cement and Concrete Composites, 27(2), pp.239-248.

Schneider, M., Romer, M., Tschudin, M. and Bolio, H. 2011. Sustainable cement production—present and future. Cement and concrete research, 41(7), pp.642-650.

Scrivener, K. 2012. Issues in sustainability in cements and concrete. Am. Ceram. Soc. Bull, 91, pp.47-50.

Seleem, H.E.H., Rashad, A.M. and Elsokary, T. 2011. Effect of elevated temperature on physico-mechanical properties of blended cement concrete. Construction and building Materials, 25(2), pp.1009-1017.

Senapati, A.K., Bhatta, A., Mohanty, S., Mishra, P.C. and Routra, B.C. 2014. An extensive literature review on the usage of fly ash as a reinforcing agent for different matrices. Int J InnovSci Mod Eng, 2(3), pp.4-9.

Shah, S.N.R., Akashah, F.W. and Shafigh, P. 2019. Performance of High Strength Concrete Subjected to Elevated Temperatures: A Review. Fire Technology, 55(5), pp.1571-1597.

Shirley, S.T., Burg, R.G., and Fiorato, A.E. 1987. Fire Resistance of High-Strength Concrete Slabs. Task Force Report, Chicago Committee on High-Rise Buildings, Report No. 11, October 1987.

Short, N.R., Purkiss, J.A. and Guise, S.E. 2001. Assessment of fire damaged concrete using colour image analysis. Construction and building materials, 15(1), pp.9-15.

Siddique, R. 2011. Utilization of silica fume in concrete: Review of hardened properties. Resources, Conservation and Recycling, 55(11), pp.923-932.

Siddique, R. and Kaur, D. 2012. Properties of concrete containing ground granulated blast furnace slag (GGBFS) at elevated temperatures. Journal of Advanced Research, 3(1), pp.45-51.

Sideris, K.K., Manita, P. and Chaniotakis, E. 2009. Performance of thermally damaged fibre reinforced concretes. Construction and Building Materials, 23(3), pp.1232-1239.

Snellings, R., Mertens, G. and Elsen, J. 2012. Supplementary cementitious materials. Reviews in Mineralogy and Geochemistry, 74(1), pp.211-278.

Sobolev, K. 2004. The development of a new method for the proportioning of high-performance concrete mixtures. Cement and Concrete Composites, 26(7), pp.901-907.

Sudarshan, D.K. and Vyas, A.K. 2019. Impact of fire on mechanical properties of concrete containing marble waste. Journal of King Saud University-Engineering Sciences, 31(1), pp.42-51.

Suhendro, B. 2014. Toward green concrete for better sustainable environment. Procedia Engineering, 95(95), pp.305-320.

Tam, V.W., Butera, A. and Le, K.N. 2020. Microstructure and chemical properties for CO2 concrete. Construction and Building Materials, 262, p.120-584, 2020. https://doi.org/10.1016/j.conbuildmat.2020.120584

Tang, W.C. and Lo, T.Y., 2009. Mechanical and fracture properties of normal-and high-strength concretes with fly ash after exposure to high temperatures. Magazine of Concrete Research, 61(5), pp.323-330.

Tangchirapat, W., Jaturapitakkul, C. and Chindaprasirt, P. 2009. Use of palm oil fuel ash as a supplementary cementitious material for producing high-strength concrete. Construction and Building Materials, 23(7), pp.2641-2646.

Tanyildizi, H. and Coskun, A. 2008. The effect of high temperature on compressive strength and splitting tensile strength of structural lightweight concrete containing fly ash. Construction and building materials, 22(11), pp.2269-2275.

Targan, Ş., Olgun, A.S.İ.M., Erdogan, Y. and Sevinc, V. 2003. Influence of natural pozzolan, colemanite ore waste, bottom ash, and fly ash on the properties of Portland cement. Cement and Concrete Research, 33(8), pp.1175-1182.

Taylor, H.F. 1997. Cement chemistry (Vol. 2). London: Thomas Telford.

Verbeck, G. and Copeland, L.E. 1972. Some physical and chemical aspects of high pressure steam curing. Special Publication, 32, pp.1-14.

Vinayagam, P., 2012. Experimental investigation on high performance concrete using silica fume and superplasticizer. International Journal of Computer and Communication Engineering, 1(2), p.168.

Wang, H.Y. 2008. The effects of elevated temperature on cement paste containing GGBFS. Cement and Concrete Composites, 30(10), pp.992-999.

Wang, W., Liu, X., Guo, L. and Duan, P. 2019. Evaluation of properties and microstructure of cement paste blended with metakaolin subjected to high temperatures. Materials, 12(6), p.941.

Wang, X.S., Wu, B.S. and Wang, Q.Y. 2005. Online SEM investigation of microcrack characteristics of concretes at various temperatures. Cement and Concrete Research, 35(7), pp.1385-1390.

Wild, S. and Khatib, J.M. 1997. Portlandite consumption in metakaolin cement pastes and mortars. Cement and concrete research, 27(1), pp.137-146.

Wild, S., Khatib J.M., Jones, A. 1996. Relative strength, pozzolanic activity and cement hydration in superplasticised metakaolin concrete. Cement Concrete Research. 26, (10), pp. 1537–1544

Wong, H.S. and Razak, H.A. 2005. Efficiency of calcined kaolin and silica fume as cement replacement material for strength performance. Cement and Concrete Research, 35(4), pp.696-702.

Xiao, J. and Falkner, H. 2006. On residual strength of high-performance concrete with and without polypropylene fibres at elevated temperatures. Fire safety journal, 41(2), pp.115-121.

Xu, Y., Wong, Y.L., Poon, C.S. and Anson, M. 2001. Impact of high temperature on PFA concrete. Cement and concrete research, 31(7), pp.1065-1073.

Xu, Y., Wong, Y.L., Poon, C.S. and Anson, M. 2003. Influence of PFA on cracking of concrete and cement paste after exposure to high temperatures. Cement and Concrete Research, 33(12), pp.2009-2016.

Yan, X., Li, H. and Wong, Y.L. 2007. Assessment and repair of fire-damaged high-strength concrete: strength and durability. Journal of materials in civil engineering, 19(6), pp.462-469.

Yazıcı, Ş., Sezer, G.İ. and Şengül, H. 2012. The effect of high temperature on the compressive strength of mortars. Construction and Building Materials, 35, pp.97-100.